

2019

Analysis of PARylation and PTEN Mutation Effects on PARP and PARG Inhibition Treatment in Primary Brain Tumors

Henre Michael Hermanowski

Follow this and additional works at: <https://scholarworks.uvm.edu/hcoltheses>

Recommended Citation

Hermanowski, Henre Michael, "Analysis of PARylation and PTEN Mutation Effects on PARP and PARG Inhibition Treatment in Primary Brain Tumors" (2019). *UVM Honors College Senior Theses*. 321.
<https://scholarworks.uvm.edu/hcoltheses/321>

This Honors College Thesis is brought to you for free and open access by the Undergraduate Theses at ScholarWorks @ UVM. It has been accepted for inclusion in UVM Honors College Senior Theses by an authorized administrator of ScholarWorks @ UVM. For more information, please contact donna.omalley@uvm.edu.

Abstract:

Glioblastoma multiforme (GBM) is the most aggressive primary brain tumor, with a median survival of approximately 15 months. Standard care for GBM has remained the same for more than 10 years and has yet to produce remission. Phosphatase and tensin homolog (PTEN) is a common biomarker of GBM, whose mutation is associated with defects in homologous recombination (HR), making it a candidate for targeted therapy by synthetic lethality (SL). PARylation is a transient, post-translational modification that modulates DNA repair fidelity and genomic stability. Inhibitors of PARylation (PARP inhibitors, PARPi; PARG inhibitors, PARGi) have been developed for therapeutic use in HR-defective cancers, and their efficacy has been demonstrated in HR-deficient breast and ovarian cancers based on the concept of SL. My main goal was to identify the DNA double-strand break repair pathways activated and/or inhibited by PARPi and PARGi in function of PTEN status, and to support the concept of SL in GBM cell lines. This was accomplished by various methods including flow cytometry and immunofluorescence. Subsequently, by western blot and immunohistochemistry, I aimed to uncover the expression and localization of PARP-1 and PARG in human tissue to validate the potential of PARPi and PARGi as therapeutic agents. I revealed that inhibitor treatment caused the accumulation of GBM cells in G2 phase without the initiation of apoptosis or necrosis. Importantly, PTEN-wildtype cells displayed higher levels of DNA damage after PARPi treatment compared to PTEN-mutant cells. However, there was no indication of efficient DNA repair by NHEJ. These findings strengthen the case for PARP and PARG inhibition as inducers of DNA damage, but do not support the concept of SL between PARP inhibition and PTEN mutations in GBM cells, despite PARP-1 and PARG over-expression in GBM tissues. Further research must be done to understand the complex relationship between PARylation and PTEN, and to propose PARPi and/or PARGi for personalized therapeutic use in GBM patients.

Background:

Glioblastoma

Primary brain tumors are rare (~2% of all cancers), with an incidence rate of 7.23 cases out of 100,000 persons/year; by contrast, prostate cancer and breast cancer have incidence rates of 201.40 and 171.20 persons/year, respectively (Nayak, Lee, & Wen, 2012; Ostrom et al., 2014; Ostrom et al., 2015). Among these primary brain tumors, gliomas are one of the most common, comprising ~30% of all brain and central nervous system tumors (2008-2012 brain tumor incidence; (Nayak et al., 2012; Ostrom et al., 2014; Ostrom et al., 2015)). Gliomas are derived from glial cells, such as astrocytes, microglial cells, ependymal cells, and oligodendrocytes. The World Health Organization (WHO) has recently revised the classification of gliomas, including astrocytoma (grade II and III), oligodendroglioma (grade II and III) and glioblastoma (grade IV), also referred to as glioblastoma multiforme (GBM), based on morphological and molecular characteristics (Louis et al., 2016).

GBM is the most aggressive primary brain tumor, with a median survival of approximately 15 months (Adeberg et al., 2014), and accounts for more than half (55.1%) of all glioma subtypes (2008-2012 brain tumor incidence; (Nayak et al., 2012; Omuro & DeAngelis, 2013; Ostrom et al., 2014; Ostrom et al., 2015)) (**Figure 1**). GBM are divided into two subtypes distinguished by the presence or absence of mutations in isocitrate dehydrogenase (IDH) 1 and 2 genes (Louis et al., 2016). IDH1/2 mutations are frequently found in low grade gliomas (astrocytoma II and oligodendroglioma II), indicating that it is an early event in the mechanism of tumorigenesis. IDH1/2 are key metabolic enzymes involved in the tricarboxylic acid cycle, whose mutations lead to the synthesis of an oncometabolite named 2-hydroxyglutarate (2-HG) (Dang et al., 2009; Zhao et al., 2009). Accumulation of 2-HG dysregulates DNA methylation and gene transcription (Cohen, Holmen, & Colman, 2013). Thus, only secondary GBM (~10% of total GBM) resulting from astrocytoma II/III and oligodendroglioma II/III presents IDH1/2 mutations, while primary (or *de novo*) GBM (~90% of

total GBM) are IDH-wildtype. Primary GBM predominate in patients over 55 years of age (Louis et al., 2016). It is noteworthy that for some GBM the full IDH profile cannot be obtained, often due to the challenges of sample acquisition. Studies to further characterize the molecular events responsible for tumorigenesis in the brain may provide additional knowledge (Louis et al., 2016). My research solely focuses on primary GBM, thus the term “GBM” will refer to the IDH-wildtype tumor.

Despite inconclusive attempts to identify environmental and genetic factors (e.g., age, sex, gene variation) contributing to GBM, its prevalence is well recognized to vary amongst populations. Incidence of this brain tumor is higher within white demographics, for example. GBM is diagnosed in patients at a median age of 65 years, compared to oligodendrogliomas which affect patients in their 40’s (Nayak et al., 2012; Ostrom et al., 2014; Ostrom et al., 2015). GBM is also more common in males than in females (incidence rate of 3.99/100,000 and 2.53/100,000 individuals, respectively) (Nayak et al., 2012; Ostrom et al., 2014; Ostrom et al., 2015).

Standard care for GBM has remained the same for more than 10 years: surgical resection associated with radiation therapy (60 Gy) and temozolomide (TMZ) chemotherapy (up to 6 cycles) (Stupp et al., 2005). However, this therapeutic strategy has yet to produce remission, largely due to the acquisition of TMZ resistance (Hegi et al., 2005). Despite the high demand for effective therapies, few options exist, limited by the lack of knowledge on gliomagenesis and the modest selection of drugs that can cross the blood-brain barrier (Jain, 2018).

Major GBM Biomarkers

A biomarker is any measurable molecule within an organism whose presence is indicative of a physiological phenomenon, such as infection or disease. Biomarkers of cancer are often divided into four groups in function of their clinical application: diagnostic, predictive, prognostic, and therapeutic (Carlomagno et al., 2017). Diagnostic biomarkers allow the detection of a disease, and thus permit early treatment. Predictive biomarkers indicate a patient’s prospective response to targeted therapy and

may define patient subpopulations in function of treatment efficacy (Carlomagno et al., 2017). Prognostic biomarkers provide information on the outcome of a disease. Often, these biomarkers are indicative of a patient's quality of life, or life expectancy. Finally, therapeutic biomarkers are targets for therapy (Carlomagno et al., 2017).

Two major biomarkers of GBM are phosphatase and tensin homolog (PTEN), and O⁶-methylguanine–DNA methyltransferase (MGMT). The prognostic relevance of PTEN mutation or deletion, observed in 50-70% of GBM patients, remains debated. Several studies show that these genetic alterations may correlate with decreased survival, while others do not (Montano, D'Alessandris, Izzo, Fernandez, & Pallini, 2016). These conflicting reports result from the insufficient characterization of the mutations at the molecular level. This tumor suppressor has both phosphatase-dependent and phosphatase-independent activities that regulate myriad processes associated with metabolism, cellular proliferation, and genomic stability (Lee, Chen, & Pandolfi, 2018). PTEN also modulates DNA double strand break (DSB) repair via the homologous recombination (HR) pathway (Lee et al., 2018).

The *MGMT* gene is involved in the maintenance of genomic stability by encoding the DNA repair protein MGMT. This enzyme directly repairs the DNA lesion O⁶-methylguanine via a one-step alkyl transfer reaction (Kaina, Christmann, Naumann, & Roos, 2007). By restoring the appropriate structure of guanine, DNA replication and transcription errors are prevented (Kaina et al., 2007). The epigenetic silencing of *MGMT* most often results from the DNA methylation of its promoter (Kaina et al., 2007). *MGMT* silencing is strongly indicative of therapy response to the alkylating agent TMZ and is shown to increase overall survival (OS) by three months, making it a predictive biomarker of GBM (Stupp et al., 2005).

Brief overview of DNA repair mechanisms

It has been estimated that each human cell is subject to approximately 10,000 lesions per day (De Bont & van Larebeke, 2004; Jackson & Bartek, 2009). These damages vary from oxidative lesions to single-strand breaks (SSBs) and DSBs. This heterogeneity requests specialized activities for their correct repair, explaining the numerous DNA damage repair pathways utilized by the cell.

For instance, alkylated bases, resulting from alkylating agents (e.g., TMZ) or oxidative reactions of cellular metabolism can be directly repaired by enzymes like MGMT by an error-free mechanism. MGMT can remove the methyl group from O⁶-methylguanine and O⁴-methylthymine, restoring the proper DNA sequence. In absence of MGMT, other DNA repair pathways are activated, such as mismatch repair (MMR), base excision repair (BER) or nucleotide excision repair (NER). DSBs are the most cytotoxic form of DNA damage. Whether generated by endogenous (e.g., stalled DNA replication fork) or exogenous (e.g., irradiation) sources, DSBs will always be marked by the presence of the phosphorylated histone variant H2AX (on serine 139, named γ H2AX) (Chapman, Taylor, & Boulton, 2012). This DNA damage biomarker plays a major role in the signaling and recruitment of factors required for the repair of lesions.

DSBs may be repaired by two major pathways: non-homologous end joining (NHEJ) or HR (**Figure 2**). Due to the need of a sister chromatid template, HR is restricted to the S and G2 phases of the cell cycle, whereas NHEJ is activated in G1. Tumor suppressor p53-binding protein 1 (53BP1) has a pivotal role in the DSB repair pathway choice, made in function of the cell cycle phase (Chapman et al., 2012). Phosphorylation of 53BP1 and its recruitment to damage sites in G1 promotes the recruitment of NHEJ repair factors and prevents HR. In the NHEJ pathway, both ends of the DSB are bound by the heterodimer Ku70/Ku80, which in turn recruits DNA dependent protein kinase (DNA-PK) to initiate the repair (Mahaney, Meek, & Lees-Miller, 2009).

Conversely, the HR pathway begins with resection of the broken DNA ends to form 5'-end and 3'-end single-stranded DNA (ssDNA) molecules, the tails of which are coated by replication protein A subunits 1, 2 and 3 (RPA1/2/3) for the removal of secondary structure (Chapman et al., 2012). RPA

is subsequently replaced by the ssDNA binding protein RAD51, which then facilitates the homology search and initiates formation of the Holliday junction (HJ) (Zhang, 2013). The breast cancer type 1 (BRCA1) susceptibility protein, another mediator of HR, displays multiple functions in DSB repair (Pitroda et al., 2014). Most notably, BRCA1 promotes the removal of 53BP1 in S phase to allow DNA resection (Bunting et al., 2010). Furthermore, BRCA1 is required for the subnuclear assembly of RAD51, facilitating HR.

Upregulated repair pathways have been known to underpin chemotherapy resistance in certain cancers. In recurrent GBM, an acquired resistance to TMZ may be due to the loss of MMR and the re-expression of MGMT (Gil Del Alcazar, Todorova, Habib, Mukherjee, & Burma, 2016). Moreover, resistance can result from increased levels of TMZ-induced DSBs, which stimulate the upregulation of HR and desensitize the cell to alkylating agent therapies. Such cells are frequently cross-resistant to other HR-inducing agents (Gil Del Alcazar et al., 2016).

PARylation

PARylation is a transient, post-translational modification modulating numerous molecular mechanisms involved in the maintenance of genome stability, including DNA repair and transcription (Gupte, Liu, & Kraus, 2017). The polymer of poly(ADP-ribose) (PAR) is composed of ADP-ribose units covalently bound to target proteins by poly(ADP-ribose) polymerase-1 (PARP-1) and removed by poly(ADP-ribose) glycohydrolase (PARG) (**Figure 2**). In the context of DNA damage, PAR is a cellular signal that participates in DNA damage accessibility, regulation of protein-protein interaction, and recruitment of integral DNA repair factors, acting as a chief modulator of genome integrity. PAR degradation by PARG also contributes to the DNA damage response, facilitating the release of DNA repair machinery and helping to restore the functional structure of chromatin. Thus, in the epigenetic context, PARP-1 is defined as a writer and PARG an eraser of ADP-ribose (Lord & Ashworth, 2017).

Over the last 60 years, the enzymatic role of PARP-1, and to a lesser extent PARG, has been studied in response to DNA damage (Gupte et al., 2017). PARP-1 senses and binds to damaged DNA via its N-terminal zinc finger motifs, triggering conformational changes and stimulating PARP-1 activity in presence of its substrate NAD⁺ (**Figure 2**). The hydrolysis of NAD⁺ leads to the release of nicotinamide and the iterative transfer of an ADP-ribose unit (linked by an α (1 \rightarrow 2) O-glycosidic bond) in a linear or branched form onto the target protein. On the other hand, PARG degrades the PAR polymer by breaking the 2',1''-glycosidic ribose-ribose bonds and releasing free ADP-ribose moieties (Slade et al., 2011).

Common targets of PARylation include proteins involved in BER (e.g., XRCC1), NHEJ (e.g., DNA-PK) and PARP-1 itself (known as automodification) (Beck, Robert, Reina-San-Martin, Schreiber, & Dantzer, 2014). This large panel of targets suggests that PARP-1 is able to discern and act upon varying DNA damages, including alkylated adducts repaired by BER, or DSBs repaired by NHEJ and HR. For instance, in the presence of a DSB, PARP-1 promotes HR by competing with Ku70/Ku80 binding after break recognition, stimulating resection and RAD51 recruitment (Mahaney et al., 2009). Interestingly, if resection is limited or unable to occur, alternative-NHEJ (alt-NHEJ), a minor and mutagenic DSB repair pathway, will take place (Mahaney et al., 2009). Altogether, the activities of PARP-1 and PARG are involved in the recognition and signaling of DNA damage and the balance between the different DNA repair pathways highlighting the major role of PARylation in repair fidelity and genomic integrity (Beck et al., 2014) (**Figure 2**).

Therapeutic Candidates

Due to the function of PARylation in genome integrity and cellular survival, inhibitors (PARPi and PARGi) have been generated to further study the function of PARP-1 and PARG and to test their potential use as therapeutic agents. Most efforts have focused on PARPi, with the design of two types of inhibitors (type 1 and type 2) derived from the substrate NAD⁺ (Pommier, O'Connor, & de Bono,

2016). Type 1 inhibitors (e.g., veliparib) compete directly with the NAD⁺ substrate for PARP-1, inhibiting its enzymatic activity (Murai & Pommier, 2016; Murai et al., 2014). Type 2 inhibitors (e.g., olaparib) stabilize PARP-DNA complexes in a mechanism called “PARP-1 molecular trapping”. This induces additional damage by collision with transcription or replication machinery. Interestingly, type 2 inhibitors are significantly more cytotoxic than the genetic deletion of PARP-1 itself, indicating that inactivated and trapped PARP-1 produces direct DNA damage within the cell (Pommier et al., 2016).

In presence of DNA damage and the absence of PARPi, PARP-DNA complexes are dissociated by the automodification of PARP-1. This charge repulsion mechanism is required for the progress of DNA repair. Upon type 2 inhibition, in which PARP-1 is neither automodified nor released, the toxic PARP-DNA complexes impose severe consequences on the cell. Thus, PARPi works to stabilize these complexes and disable the process of automodification, ultimately proving more toxic than unrepaired SSBs (Pommier et al., 2016). The drugs olaparib and veliparib are two PARPi currently in advanced clinical trials. Today, the major interest is their use in HR-deficient tumors (McCabe et al., 2006). As such, several type 2 PARPi have recently been FDA-approved for the treatment of ovarian cancer mutated in the DNA repair factor BRCA (i.e., olaparib, rucaparib and niraparib) (Scott, Swisher, & Kaufmann, 2015).

Inhibiting PARG has also been considered for chemotherapeutic use. The potent PARGi PDD00017273 has recently been designed, though no therapeutic benefit has yet been explored (James et al., 2016). *In vitro* studies show that PARGi PDD00017273 appears to sensitize HR-deficient cells (e.g., BRCA1 mutated cells) following a different and poorly characterized molecular pathway than PARPi olaparib (Gravells, Grant, Smith, James, & Bryant, 2017; Gravells et al., 2018). PARGi treatment leads to the accumulation of aberrant mitotic cells, likely a result of unrepaired DNA damage and stalled replication forks.

While PARP-1 and PARG inhibition dysregulates the same post translational modification (i.e., PARylation), the downstream consequences of each are different, likely due to their specific roles

in DNA repair and genome stability (James et al., 2016). Still, both PARPi and PARGi are postulated to sensitize DNA damage-response deficient cells following the concept of synthetic lethality (SL).

The Concept of Synthetic Lethality

PARPi improves the efficacy of radiotherapy and/or chemotherapy according to the SL model (Lord & Ashworth, 2017). SL arises when a combination of deficiencies in the expression of two or more genes (or gene products) leads to cell death, whereas a defect in only one does not (Ashworth & Lord, 2018) (**Figure 3**). This concept is best described by the synthetically lethal relationship observed between PARPi and BRCA mutations. BRCA1/2 proteins are tumor suppressors whose mutations are associated with familial breast and ovarian cancer (Curtin & Szabo, 2013). These tumors display deficiencies in HR and are more sensitive to DNA damage, like those induced by PARPi (Cruz et al., 2018). Based on effective clinical trials demonstrating SL, PARPi olaparib, rucaparib and niraparib have recently been FDA-approved for the treatment of BRCA-mutated ovarian cancer (Scott et al., 2015). This success has launched the pursuit of new therapeutic candidates, driving the research of genes or gene products whose defects display “BRCAness” phenotype upon PARP inhibition (Turner, Tutt, & Ashworth, 2004). The high frequency of PTEN mutations in GBM associated with its role in the DNA damage response is an intriguing model to test the efficacy of SL in GBM with PARPi and PARGi. However, little has been done to examine this relationship.

Overview

GBM is a lethal form of brain cancer whose heterogeneity and localization have rendered treatment difficult and too often unsuccessful. Chemical resistance, blood-brain barrier penetrance, and inadequate knowledge on gliomagenesis are only some of the challenges for effective therapies. SL with PARPi is a promising approach for the treatment of GBM, but little has been done to demonstrate its potential. My goal is to distinguish the DNA DSB repair pathways activated and/or

inhibited by PARPi and PARGi in function of PTEN status and validate the concept of SL in GBM. I predict that PTEN mutations will sensitize cells to DNA damage by PARP and PARG inhibition, and that PARPi olaparib will prove more effective than PARPi veliparib due to PARP-1 molecular trapping.

To test this hypothesis, I will analyze the biology of PARylation and DNA damage response upon PARPi and PARGi in GBM using molecular and cellular approaches including immunofluorescence (IF), flow cytometry, western blot and immunohistochemistry (IHC). By validating SL in GBM, I will be able to better understand the functional relationship between PARP-1, PARG and PTEN, and propose treatment options that may increase patient OS and quality of life.

Methods:

Cell Culture and Treatment

Three established GBM cell lines, LN-229 (PTEN-wildtype), U-87MG and U-118MG (PTEN mutated with the substitution mutation c.209+1G>T and c.1026+1G>T, respectively), were cultured in Dulbecco's Modified Eagle's Medium complemented with 10% fetal bovine serum and 1% penicillin streptomycin in a 5% CO₂ tissue culture incubator at 37°C.

For cell harvest, the medium was removed, and the cells were washed twice with 10 mL 1X PBS. The cells were trypsinized with 0.025% trypsin, whose enzymatic activity was later inhibited by addition of 9 mL of complemented medium. Cellular concentration (cells/mL) was determined by counting living cells diluted in trypan blue (1:1 dilution) on a Neubauer hemacytometer.

For treatment, GBM cells were either untreated (NT, DMSO), or treated with PARPi veliparib (IC₅₀ concentration: 250 µM for LN-229 and 500 µM for U-87MG and U-118MG), PARPi olaparib (IC₅₀ concentration: 10 µM for LN-229 and 100 µM for U-87MG and U-118MG), or PARGi PDD00017273 (IC₅₀ concentration: 350 µM for LN-229 and 150 µM for U-87MG and U-118MG) for 24 hours at 37°C, 5% CO₂ incubator (IC₅₀ determined previously in Quenet lab, Aldrighetti *et al.* unpublished). As a positive DNA damage control, cells were treated with 10 µM doxorubicin for 30 min to induce cell death in γ H2AX and 53BP1 experiments and 4 hrs in Ku80 experiments; cells were treated with 5 µM etoposide for 4 hrs in BRCA1 and RAD51 experiments, and 2 mM hydroxyurea for 24 hrs in FANCD2 experiments. As an apoptotic control, cells were treated with 30 µg/mL digitonin for 30 min at 37°C, 5% CO₂ incubator.

Flow Cytometry Analysis

To study cell cycle distribution, cells were harvested and seeded on a P100 plate (100,000 cells). Two days later, cells were treated with digitonin to induce apoptosis, doxorubicin to generate DNA damage, TMZ, PARPi veliparib, PARPi olaparib, or PARGi at IC₅₀ for 24h. After incubation,

cells were washed twice with 1X PBS, trypsinized, and collected in 15 mL tubes. Then, they were centrifuged at 1,000 rpm for 10 min at 4°C. Pellets were washed in ice-cold 1X PBS and centrifuged at 1,000 rpm for 10 min at 4°C. Cells were fixed in 1% paraformaldehyde (PFA) diluted in 1X PBS for 15 min on ice, and permeabilized in ice-cold 70% ethanol for overnight to 1 week at -20°C. On the day of flow cytometry analysis, cells were centrifuged at 1,000 rpm for 10 min at 4°C, and pellets were washed in ice-cold 1X PBS, prior being resuspended in propidium iodide (PI) staining solution (50 µg/mL PI; 0.1% Triton X-100; 1X PBS). Samples were then analyzed by flow cytometry on the BD LSRII equipment available at the Harry Hood Bassett Flow Cytometry and Cell Sorting Facility (UVM). PI fluorescence emission was measured at 530 nm, and based on the cellular DNA content, cells were categorized between Sub-G1, G1, S, G2 and polyploid using FlowJo software.

To study cell death, cells were harvested and seeded on a P100 plate (100,000 cells). Two days later, cells were treated with digitonin to induce apoptosis, PARPi veliparib, PARPi olaparib, or PARGi at IC₅₀ for 24h. Then, cells were harvested, washed with cold 1X PBS, and prepared for analysis using the PI/Annexin V staining kit (#V13241, ThermoFisher), following manufacturer instructions. Briefly, cells were resuspended at ~10⁶ cells/mL in 1X annexin-binding buffer and stained with FITC-annexin V and PI (5 µL and 1 µL, respectively, per 100 µL of cell suspension). After 15 min of incubation on ice, 400 µL of 1X annexin-binding buffer were added and samples were immediately analyzed by flow cytometry via BD LSRII equipment. PI and FITC-annexin V fluorescence emissions were measured at 530 nm and 575 nm, respectively. Cell population was expected to separate into three groups: living cells (annexin V⁻/PI⁻), necrotic and apoptotic cells (annexin V⁺/PI⁺), and early apoptotic cells (annexin V⁺/PI⁻).

Two and three biological replicates were performed for the cell cycle and cell death assays, respectively, with 10,000 cells counted per condition. Data were acquired and analyzed using FlowJo software. Standard deviations were determined and two-way ANOVA tests were performed to assess the significance of the results using Prism 8.

γ H2AX, 53BP1, and FANCD2 Immunofluorescence

To study γ H2AX, 53BP1, FANCD2 markers, cells were seeded on coverslips (60,000 cells) in 12-well plates 24 hrs prior treatment. Then, cells were washed twice with ice-cold 1X PBS and fixed in ice-cold 4% PFA, 2% sucrose, 1X PBS for 10 min. After two washes with 1X PBS for 5 min at room temperature, cells were permeabilized in 0.5% Triton X-100, 20 mM Hepes pH7.4, 50 mM NaCl, 3 mM MgCl₂, 300 mM sucrose, 1X PBS for 5 min at room temperature. Cells were washed two times in 0.1% Triton X-100, 1X PBS for 5 min at room temperature, and then incubated with primary antibody (**Table 1**) diluted in 2% BSA, 1X PBS at 4°C overnight in humidified chamber. Cells were washed twice in 0.1% Triton X-100, 1X PBS for 5 min at room temperature, and incubated with secondary antibody (goat anti-rabbit #A11008 labelled with Alexa⁴⁸⁸ fluorochrome, Life Technologies) diluted 1/1,000 in 2% BSA, 1X PBS for 1 hr at room temperature in a dark humidified chamber. Cells were then washed in the dark at room temperature three times in 0.1% Triton X-100, 1X PBS for 5 min, once in 0.1% Triton X-100, 1X PBS complemented with DAPI (0.1 μ g/mL) for 10 min, and finally in 1X PBS for 5 min. Cells were rinsed in distilled water and mounted with Prolong Gold antifade medium.

Ku80 Immunofluorescence

To study Ku80 marker, cells were seeded on coverslips (60,000 cells) in 12-well plates 24 hrs prior treatment. Then, cells were washed once with ice-cold 1X PBS, incubated twice in CSK buffer (10 mM PIPES pH6.8, 100 mM NaCl, 300 mM sucrose, 3 mM MgCl₂, 1 mM EGTA) complemented with 0.7% Triton X-100 and 0.3 mg/mL RNase A for 3 min, and then rinsed with 1X PBS at room temperature. Cells were fixed with 2% PFA in 1X PBS for 15 min, rinsed in 1X PBS, blocked with 1X PBS complemented with 0.1% Tween 20 and 5% BSA for 1 hr at room temperature, and incubated with the primary antibody (**Table 1**) diluted in 1X PBS complemented with 0.1% Tween 20 and 5%

BSA at 4°C overnight in a humidified chamber. After three washes with 0.1% Tween 20, 1X PBS for 5 min each, cells were incubated with secondary antibody (goat anti-rabbit #A11008 labelled with Alexa⁴⁸⁸ fluorochrome, Life Technologies) diluted 1/1,000 in 0.1% Tween 20, 5% BSA, 1X PBS, for 1 hr in the dark at room temperature. Cells were washed in the dark at room temperature two times with 0.1% Tween 20, 1X PBS for 5 min, and once with 1X PBS complemented with DAPI (0.1 µg/mL) for 10 min. After two washes with 1X PBS for 5 min, cells were rinsed in distilled water and mounted on slides with Prolong Gold antifade medium.

RAD51 Immunofluorescence

To study Rad51 marker, cells were seeded on coverslips (60,000 cells) in 12-well plates 24 hrs prior treatment. Then, cells were washed once with ice-cold 1X PBS and fixed with 100% methanol (refrigerated at -20°C) for 20 min at 4°C. Cells were permeabilized with ice-cold 0.5% Triton, 1X PBS, and washed with ice-cold 1X PBS for 5 on ice. Cells were blocked with 0.1% BSA, 1X PBS (blocking buffer) for 1 hr on ice, and then, incubated overnight at 4°C in a humidified chamber with the primary antibody (**Table 1**) diluted in blocking buffer. Cells were washed three times for 5 min with 1X PBS and incubated with secondary antibody (goat anti-mouse #A1129 labelled with Alexa⁴⁸⁸ fluorochrome, Life Technologies) diluted in blocking buffer (1/1,000) for 1 hr in a dark humidified chamber at room temperature. Cells were washed at room temperature in the dark with 1X PBS for 5 min and once with 1X PBS complemented with DAPI (0.1 µg/mL) for 10 min. Cells were washed with 1X PBS for 10 min in the dark at room temperature, rinsed in distilled water, and mounted on slides with Prolong Gold antifade medium.

BRCA1 Immunofluorescence

All previously described immunofluorescent protocols have been tested to immunostain BRCA1 (**Table 1**) which has been revealed with goat anti-mouse secondary antibody labelled with Alexa⁴⁸⁸ fluorochrome (#A1129, Life Technologies).

Immunofluorescence Analysis

Slides were observed under a Nikon Ti-E inverted microscope (objective 40X for counting and 60X for picture acquisition) using NIS-Elements microscope imaging software. Three biological replicates were performed for each tested marker, with at least 100 cells counted per condition. Pictures were prepared on the open source image processing program Fiji (<https://imagej.net/>).

For γ H2AX and 53BP1, cells were manually counted and categorized as followed: ≤ 1 focus, 2-5 foci and ≥ 6 foci, while for FANCD2, cells were either classified with or without foci. Percentages of cells of each category were graphed on a 100% stacked column chart.

Ku80 signal intensity in the nucleus was measured automatically by the NIS-Elements microscope imaging software, using the DAPI signal to identify the region of interest and quantify Alexa⁴⁸⁸ fluorescent signal. For each biological replicate, these values were normalized to the not-treated condition and graphed.

Rad51 foci number (Alexa⁴⁸⁸ fluorescent signal) in the nucleus was measured automatically by the NIS-Elements microscope imaging software, using the DAPI signal to identify the region of interest. For each biological replicate, these values were tabulated and graphed on a box plot chart where the average, median, minimum, maximum, and first and third quartiles are indicated.

Numerical data were tabulated in an Excel document. Two-way ANOVA was performed to assess statistical variance between cell lines and/or treatment using PRISM 8.

Tissue Bank

Dr. Jaworski (Department of Neurological Sciences, UVM) accepted to share tissues that she collected between 2008-2015 (IRB #16-556). Dr. Jaworski's tumor bank is comprised of 48 primary brain and metastatic tumor samples obtained from newly-diagnosed patients at the time of surgery and normal post-mortem brain samples. Twenty-four of these tissues are GBM surgical tumor samples. Their classification is based on the 2016 WHO classification of tumors of the central nervous system (Louis et al., 2016). The samples were flash-frozen within 15 minutes of resection and are of high quality for our molecular study.

Protein Extraction, SDS-PAGE, and Western Blot

Flash frozen tissues collected from patients were resuspended in triton lysis buffer (20 mM Tris pH7.4, 137 mM NaCl, 25 mM β -glycerolphosphate pH7.4, 2 mM sodium pyrophosphate, 2 mM EDTA pH7.4, 1% Triton X-100, 10% glycerol) complemented with protease inhibitor complex (1:200 ratio, #11873580001, Roche). For consistency, the same ratio of tissue sample to triton lysis buffer was added (0.2g/0.5ml). The tissues were homogenized, centrifuged at 14,000 rpm for 15 min at 4°C, and transferred to pre-cooled 1.5 mL tubes. By Bradford assay, protein concentration was determined.

Equal quantities of proteins were diluted in Laemmli Buffer and denatured for 5 min at 100°C. Then, proteins were separated on a 10% SDS-PAGE. After transfer on a nitrocellulose membrane at 50 mA at 4°C overnight, the membrane was blocked in 1% BSA, 1X PBS for 60 min at room temperature under gentle agitation. Then, the membrane was incubated with the primary antibody (**Table 1**) diluted in hybridization buffer (1X PBS, 0.5% BSA, 0.1% Tween 20) overnight at 4°C under gentle agitation. Following three washes in 0.01% Tween 20, 1X PBS for 5 min at room temperature under gentle agitation, the membrane was incubated with the secondary antibody (donkey anti-mouse IRDye[®] 800CW or donkey anti-rabbit IRDye[®] 680RD, #926-32212 or #926-68073, LI-COR) for 1 hr at room temperature under gentle agitation. After three washes in 0.01% Tween 20, 1X PBS for 5

min at room temperature under gentle agitation, the membrane was scanned on a LI-COR Imaging System (available at the Neuroscience Center of Biomedical Research, UVM).

Pictures were prepared on the open source image processing program Fiji (<https://imagej.net/>). Signals of protein of interest (K counts) were quantified on Image Studio software (LI-COR). Background was subtracted and ratios to the loading control (β -actin) were determined and graphed. Two technical replicates were performed.

Immunohistochemistry

Paraffin-embedded sections were provided by the Department of Pathology and Laboratory Medicine (UVM). Tissue sections were baked for 3 days at 37°C and 1 hr at 60°C. After deparaffinization of tissue sections with xylene and decreasing concentrations of ethanol (from 100% to 50%), slides were incubated in 1X DAKO Antigen Retrieval Buffer (#S1699, Agilent) diluted in 50% glycerol for 15 min at 95°C, followed by three washes in water for 5 min at room temperature. To quench endogenous peroxidase, tissue sections were incubated with 3% H₂O₂ diluted in 100% methanol for 10 min on a rocking platform. After three rinses in water, tissue sections were immersed in blocking buffer (#MP-7401 or #MP-7452, ImmPRESS Reagents) for 20 min at room temperature, incubated with primary antibody (diluted in 1X PBS, **Table 1**) for 60 min, and washed three times in 1X PBS for 5 min at room temperature. Then, tissue sections were incubated with the secondary antibody coupled with peroxidase (#MP-7401 for anti-rabbit IgG, and #MP-7452 for anti-mouse IgG, Vector laboratories) for 30 min at room temperature, and rinsed three times for 5 min in 1X PBS. Sections were incubated with peroxidase substrate (AEC Substrate kit, #SK-74200, Vector laboratories) for 10 min, rinsed in water for 5 min, and counterstained with Mayer's Hematoxylin and Lithium Carbonate for 1-2 min. After a final rinse in water, coverslips were mounted with Mounting medium (#H5501, Vector). Slides were scanned with a Leica-Aperio Versa 8 whole slide scanner (Objective 40X, available at the Microscopy Core Center, UVM).

To immunostain another marker of interest, tissue sections were destained and destripped after the scan with washes in increasing concentrations of ethanol (from 50% to 100%). When no signal was observed, tissue sections were washed in decreasing concentrations of ethanol (from 100% to 50%) and the protocol restarted at the antigen retrieval step (incubation in 1X DAKO Antigen Retrieval Buffer).

Pictures were analyzed on Photoshop CS6.

Results:

Preferential accumulation of GBM cells in G2 phase was observed after treatment with PARPi in LN-229 cells and PARGi in U-87MG and U-118MG cells.

To analyze the overall cellular effect of PARP-1 and PARG inhibition in GBM established cell lines, the cell cycle progression of unsynchronized LN-229, U-87MG and U-118MG cells upon PARPi and PARGi (24 hrs treatment at IC₅₀) were studied by flow cytometry (**Figure 4**, Supplemental Table 1). LN-229 NT cells were mainly in G1 phase (~56%), while ~23% and ~15% of cells were in S and G2 phases, respectively (**Figure 4**, Supplemental Table 1, Supplemental Table 2). Few LN-229 cells were in sub-G1 or displayed polyploidy (<5% each). This same pattern was observed upon treatment with digitonin (apoptotic-inducing agent), doxorubicin (DNA-damaging agent) and TMZ (DNA-damaging agent). In contrast, LN-229 cells treated with PARPi veliparib or olaparib were accumulated in G2 phase (P<0.0001 compared to NT), while PARG inhibition led to the accumulation of LN-229 cells in G1 (P=0.0012 compared to NT).

U-87MG NT cells displayed high levels of polyploidy (~30%), moderate proportions of cells in G1 and G2 phases (~26% and ~37%, respectively), and a low proportion of cells in S phase and sub-G1 (<6% each) (**Figure 4**, Supplemental Table 1, Supplemental Table 3). Digitonin, doxorubicin and TMZ treatments did not significantly change this pattern. Intriguingly, PARPi veliparib was associated with an increased polyploid (P<0.0001 compared to NT) and decreased G1-cell (P<0.0001 compared to NT) population, and PARPi olaparib with a decreased polyploid (P<0.0001 compared to NT) and increased G1-cell (P<0.0001 compared to NT) population. Moreover, there was a significant increase in the proportion of U87-MG G2-cells after PARGi treatment (P<0.0001 compared to NT).

As with U-87MG, U-118MG NT cells displayed high levels of polyploidy (~16%) (**Figure 4**, Supplemental Table 1, Supplemental Table 4). These cells distributed as followed over the other phases of the cell cycle: ~3% in sub-G1, ~40% in G1, ~10% in S and ~31% in G2, with a similar pattern after doxorubicin, TMZ and PARPi treatment. In contrast, treatment with digitonin caused a

significant increase of the sub-G1 population as compared to the NT group ($P < 0.0001$). Finally, PARGi was associated with an accumulation of cells in G2 ($P < 0.0001$ compared to NT).

Overall, these data showed that LN-229 PTEN-wildtype cells preferentially accumulate in G2 phase upon PARP inhibition, and U-87MG and U-118MG PTEN-mutant cells after PARGi treatment (**Figure 4.C**). These results reflect the difference of sensitivity previously observed by clonogenic assay in the lab (Aldrighetti et al., unpublished), with LN-229 cells being more sensitive to PARPi and U-87MG and U-118MG cells more sensitive to PARGi.

24-hour PARPi and PARGi treatment at IC_{50} did not induce GBM cell death.

To determine whether PARPi- and/or PARGi-associated G2 arrest triggered cell death activation in GBM cell lines, markers of apoptosis and necrosis were analyzed by flow cytometry (**Figure 5**, Supplemental Table 5). As expected, GBM cells treated with digitonin (apoptotic/necrotic-inducing agent) were positive for both annexin V and PI, indicating that they were dead. In contrast, cells treated with DNA damaging agent doxorubicin presented similarly to the non-treated cells, suggesting that the treatment was not toxic enough to induce cell death or that the analysis was performed too soon. As with doxorubicin treatment, GBM cells did not activate a cell death pathway (apoptosis or necrosis) upon PARP or PARG inhibition, suggesting that 24 hr treatment at IC_{50} was not sufficient to induce cell death.

PARPi triggered the accumulation of $\gamma H2AX$ foci in PTEN-wildtype GBM cells, while PTEN-mutant cells were less prone to DNA damage upon PARPi and PARGi.

The accumulation of cells in G2 phase can result from activation of the G2/M DNA damage checkpoint. This control mechanism examines cells for the presence of DNA damage or incomplete DNA replication, preventing compromised cells from entering mitosis (Dillon, Good, & Harrington,

2014). To determine whether PARP-1 or PARG inhibition induces an accumulation of DNA damage, a series of IF focusing on specific and key markers of DNA repair was performed.

First, to reveal the degree of DNA damage within the GBM cells, the level of γ H2AX foci was analyzed (**Figure 6**, Supplemental Table 6). The majority (~60%) of LN-229 NT cells displayed one or fewer γ H2AX foci, while ~10% and ~25% exhibited 2-5 foci and ≥ 6 foci, respectively (**Figure 6**, Supplemental Table 6). As expected, doxorubicin treatment was associated with a significant increase in the expression of γ H2AX foci (~80% of cells with ≥ 6 foci, $P < 0.0001$ compared to NT). The same was observed after PARP-1 inhibition with veliparib and olaparib ($P < 0.0001$ compared to NT), but not PARG inhibition, suggesting that DNA damage is generated by PARPi in PTEN-wildtype cells.

In comparison to LN-229 cells, a lower percentage of U-87MG NT cells presented γ H2AX foci (~5% of cells with ≥ 6 foci, **Figure 6**, Supplemental Table 6). However, γ H2AX-positive cells increased after doxorubicin treatment to ~60% ($P < 0.0001$ compared to NT). To a lower extent, PARPi and PARGi caused an increase of γ H2AX foci (~40% for PARPi veliparib, ~30% for PARPi olaparib and ~30% for PARGi for cells with ≥ 6 foci) which was not statistically significant compared to NT.

Similarly, U-118MG NT cells presented few γ H2AX foci (~10% of cells with ≥ 6 foci, **Figure 6**, Supplemental Table 6), while doxorubicin treatment was associated with a significant increase of γ H2AX foci (~50% of cells with ≥ 6 foci, $P < 0.0001$ compared to NT). The mild percent increase in γ H2AX-positive cells after PARP or PARG inhibition was not significant (PARPi veliparib: ~15%, PARPi olaparib: ~25%, PARGi: ~20%). Altogether these data suggest that PARP inhibition triggers the accumulation of DNA damage in PTEN-wildtype GBM cells, while PTEN-mutant cells are less sensitive to PARPi and PARGi treatment.

PARP inhibition was associated with 53BP1 foci formation in PTEN-wildtype but not PTEN-mutant GBM cells.

Next, the ability of GBM cells to decide between HR and NHEJ was analyzed by measuring the level of 53BP1 foci formed upon PARPi or PARGi treatment using an IF approach (**Figure 7**, Supplemental Table 7).

Only ~20% of NT LN-229 cells displayed ≥ 6 53BP1 foci (**Figure 7**, Supplemental Table 7). However, doxorubicin treatment increased this percentage (~80% of cells with ≥ 6 foci, $P < 0.0001$ compared to NT). Interestingly, more 53BP1-positive cells were counted after PARPi olaparib than PARPi veliparib (~90% vs. ~60% of cells with ≥ 6 foci, $P < 0.0001$ for olaparib and $P = 0.0066$ for veliparib compared to NT). PARGi did not induce the formation of 53BP1 foci.

In U-87MG NT cells, 53BP1 foci were observed in ~15% of cells in the non-treated condition, and ~90% of cells in response to doxorubicin ($P < 0.0001$ compared to NT) (**Figure 7**, Supplemental Table 7). While PARP-1 inhibition moderately increased the level of 53BP1 foci (~25% for veliparib and ~40% for olaparib for cells with ≥ 6 foci), these changes were not statistically significant. As observed for LN-229, PARGi did not induce the formation of 53BP1 foci in U-87MG (~10% of cells with more than 6 foci).

While only ~10% of U-118MG NT cells displayed ≥ 6 53BP1 foci compared to ~40% of U-118MG doxorubicin-treated cells, this difference was not considered statistically significant (**Figure 7**, Supplemental Table 7). Similarly, neither PARPi nor PARGi treatment provoked an increase of 53BP1 foci (~10% for veliparib, ~20% for olaparib and ~5% for PARGi of cells with ≥ 6 foci).

Thus, these data indicate that upon PARPi treatment, the NHEJ marker 53BP1 forms foci in PTEN-wildtype GBM cells, but not in PTEN-mutant GBM cells. In contrast, PARGi does not contribute to 53BP1 foci formation in GBM cells.

PARP and PARG inhibition did not significantly alter nuclear localization of Ku80 in GBM cells.

53BP1 promotes DSB repair by NHEJ (Chapman et al., 2012). To validate the potential activation of this DNA repair pathway in PTEN-wildtype cells after PARP-1 inhibition, the nuclear localization of Ku80, a NHEJ mediator, was quantified by IF (**Figure 8**, Supplemental Table 8).

In contrast to γ H2AX and 53BP1, Ku80 does not form foci, but accumulates in the nucleus upon DNA damage. Thus, nuclear Ku80 signals were quantified following treatment and compared to the NT condition (ratio: nuclear Ku80 signal “Treated” / nuclear Ku80 signal “Not Treated”). As expected, this ratio increased upon doxorubicin treatment in the three tested GBM cell lines, indicating that DNA damage can be repaired by a Ku80-dependent pathway in these experimental conditions ($P < 0.0001$ compared to NT, **Figure 8**, Supplemental Table 8). However, PARPi and PARGi treatment did not significantly change the nuclear signal of Ku80, suggesting that NHEJ is not the prime pathway to repair PARPi- or PARGi-induced damage in GBM cells.

BCRA1 immunostaining failed to reveal foci after etoposide, doxorubicin, or camptothecin treatment.

To confirm that NHEJ is not efficiently stimulated in response to PARPi and PARGi treatment in GBM cells, the major signaling factor of HR, BRCA1, was studied. Like γ H2AX and 53BP1, BRCA1 recruitment at DNA damage sites leads to the observation of foci (Zhang, 2013). We tested three different protocols published in the literature to visualize the formation of these foci upon etoposide. Etoposide (a topoisomerase II inhibitor) prevents DNA synthesis by forming a topoisomerase II-DNA complex. The trapping of topoisomerase II leads to DSBs that cannot be properly repaired. Unfortunately, all attempted immunostaining protocols for BRCA1 were unsuccessful (**Figure 9**). BRCA1 foci were not observed upon etoposide (**Figure 9**), doxorubicin, or camptothecin treatment (DNA damaging agents, data not shown).

RAD51 foci were accumulated in PTEN-wildtype GBM cells after PARP inhibition, and in PTEN-mutant GBM cells after PARPi olaparib and PARGi treatment.

After unsuccessful BRCA1 immunostaining, the potential activation of HR in response to PARPi and PARGi in GBM cells was analyzed by RAD51 IF (**Figure 10**, Supplemental Table 9, 10).

The number of RAD51 foci ranged from 0 to >120 in function of the treatment, and thus foci number per cell was determined and plotted. NT LN-229 cells displayed few RAD51 foci in comparison to cells treated with etoposide ($P<0.0001$) (mean ~2 vs. ~13 RAD51 foci, respectively, **Figure 10**, Supplemental Table 9, 10). Both PARPi veliparib and olaparib treatment led to an overall increase of RAD51 foci, as observed upon etoposide ($P<0.0001$ compared to NT). By contrast, PARGi-treated cells displayed a similar level of expression to those in the NT group. These data suggest that PARPi, but not PARGi, activate the HR pathway in LN-229 cells.

As in cell line LN-229, few RAD51 foci were counted in U-87MG cells (mean ~2, **Figure 10**, Supplemental Table 9, 10). As expected, this mean increased after etoposide treatment ($P<0.0001$ compared to NT) (mean ~14 RAD51 foci). While PARPi veliparib was not associated with an overall increase of RAD51 foci, PARPi olaparib was ($P<0.0001$ compared to NT) (mean ~3 vs. ~16 RAD51 foci, respectively). PARGi also increased the mean of RAD51 foci, but to a lesser extent ($P=0.0078$ compared to NT) (mean ~6).

Finally, U-118MG cells did not display RAD51 foci at the basal level, but etoposide treatment increased the mean ($P<0.0001$ compared to NT) (mean ~8, **Figure 10**, Supplemental Table 9, 10). Upon PARPi and PARGi treatment, the number of RAD51 foci barely increased (mean ~2 vs. ~4 vs. ~3, for PARPi veliparib, PARPi olaparib, and PARGi, respectively) and was not found to be statistically significant.

Altogether these data show that in response to PARPi PTEN-wildtype cells activate the HR pathway, whereas PTEN-mutant cells have a partial activation of that pathway after PARPi olaparib and PARGi treatment.

PARPi and PARGi treatment do not induce FANCD2 foci accumulation in GBM cells.

PARylation plays a role in the response of replication stress by participating in the repair of DNA damage (SSBs and DSBs) and the resolution of stalled replication forks (Gupte et al., 2017; Thompson et al., 2017). Because the G2/M arrest observed in **Figure 1** could have resulted from unreplicated DNA, the marker of stalled replication forks, FANCD2, was analyzed by IF (**Figure 11**, Supplemental Table 11).

Foci were too small and often too numerous to count, therefore cells were categorized as “positive” when FANCD2 foci were observed and “negative” when no foci were detected. Few LN-229 NT cells displayed FANCD2 foci (~2% of positive cells, **Figure 11**, Supplemental Table 11). By contrast, treatment with hydroxyurea (a drug that unbalances the ratio of nucleotides, triggering replication stress) increased positive FANCD2 cells to ~30%. Upon PARPi olaparib, a similar increase was observed, though it was not found to be statistically significant. Neither PARPi veliparib nor PARGi lead to the formation of FANCD2 foci.

In the non-treated condition, ~7% of U-87MG NT cells were found positive, while hydroxyurea treatment increase that percentage to ~45% ($P=0.0011$, **Figure 11**, Supplemental Table 11). No statistically significant differences were measured between NT and PARPi (~15% positive cells for veliparib and ~30% positive cells for olaparib) or PARGi (~18% positive cells) treatment groups, suggesting that none of these drugs induces the accumulation of FANCD2 foci.

Finally, the same pattern as seen in U-87MG cells was observed for U-118MG cells, with a basal level of ~9% of cells displaying FANCD2 foci, and ~55% in response to hydroxyurea ($P<0.0001$, **Figure 11**, Supplemental Table 11). Again PARPi (~9% positive cells for veliparib and ~30% positive cells for olaparib) and PARGi (~30% positive cells) treatment did not significantly change FANCD2 foci number compared to NT.

These data suggest that neither PARP nor PARG inhibition induces replication stress in GBM cells. Thus, the DNA damage (**Figure 3**) and the G2/M arrest (**Figure 1**) observed do not likely result from DNA replication error.

PARP-1, and PARG are differently expressed in brain tumors.

To determine the levels of PARP-1, PARG, and PTEN expression in multiple brain tumors, a western blot was performed. Solid tissue samples from 49 brain tumors and normal tissue (e.g., normal, malignant, and benign tumors, grade II-IV) were analyzed (two technical replicates). PARP-1 was found highly expressed in GBM compared to low-grade brain tumors, whereas PARG was potentially revealed in meningioma (**Figure 12**). However, no correlation was observed between tumor type and PARP-1, PARG, and PTEN expression.

PAR, PARP-1, and PARG were over-expressed in GBM tissue sections.

To identify the cellular subtypes expressing PAR, PARP-1 and PARG, IHC was performed on human tissue sections from normal and GBM-diagnosed patients by co-staining these factors with specific cellular markers. Over the summer of 2018, colleague Ashley Coleman validated the required antibodies and established the immunostaining protocol. Preliminary data identified the over-expression of PAR, PARP-1, and PARG in GBM tissue sections (**Figure 13**). In addition, PARP-1 was demonstrated to co-localize with GBM stem cells, which are believed to be responsible for GBM relapse. These data show promise for future IHC tissue microarray studies. I will analyze the expression of PAR, PARP-1, and PARG in function of cellular subtype across all 49 tissues previously examined by western blotting.

Discussion:

In this thesis I report that PARP and PARG inhibition treatment in GBM affect the process of DNA DSB repair in function of PTEN status. Still, there is insufficient evidence to validate the concept of SL (**Figure 14**).

This novel finding arose from the initial observation that PTEN-wildtype GBM cells were arrested in G2 phase after PARP inhibition, and PTEN-mutant cells after PARG inhibition. However, no apoptosis or necrosis was observed after 24 hrs of treatment. This result does not reject entirely the cytotoxicity effect of these inhibitors, as cell death may be a late event of these treatments. Thus, by analyzing the GBM cell death response to PARPi and PARGi after longer treatments, such as 36 and 48 hrs, or after a period of rest, the deadly phenotype may be observed. It is noteworthy that longer treatment will require pharmacological studies to confirm the stability of PARPi and PARGi to maintain the IC₅₀ constant. For instance, PARPi olaparib has a stability of 12 hrs and must be administered twice to sustain 48 hrs of effective treatment.

The observed G2 arrest may have resulted from the accumulation of DNA damage, preventing cells from completing aberrant chromosome segregation during mitosis. Analysis of the DNA damage biomarker γ H2AX revealed an overall increase of DNA lesions upon PARPi and PARGi. It was hypothesized that PTEN mutations may be associated with an HR-defective phenotype, as observed in BRCA1/2-mutated breast and ovarian cancers. Thus, the increase of γ H2AX foci may be explained by either the direct generation of DNA damage by PARPi and PARGi or defective DSB repair pathways. Following the concept of SL, greater levels of γ H2AX foci should be observed in the absence of PTEN activity. Surprisingly, PTEN-wildtype LN-229 cells displayed the highest accumulation of γ H2AX foci as compared to U-87MG and U-118MG cells after PARPi treatment. It is possible that unidentified genetic variances could impact the DNA damage response to inhibitor

treatment, such as BRCA1. Unpublished RNA sequencing (RNA-seq) data from Trevor Wolf (graduate student, Wolf et al., unpublished) indicates no difference in the levels of BRCA1 mRNA between LN-229 and U-87MG cells. Still, further analysis of protein expression (*e.g.*, mass spectrometry) with a focus on proteins involved in the DNA repair response is required for an adequate comparison of the cell lines. To mitigate any confounding genetic differences, I also propose the establishment of an LN-229 PTEN knockdown cell line. Analyzing the outcomes of PARP and PARG inhibition in a genetically identical cell line will provide a direct link between PTEN status and treatment response.

DNA damage accumulation does not signify sensitivity to a drug, particularly if the damage may be efficiently repaired. 53BP1 foci formation was analyzed to specify the repair pathway choice made by GBM cells in response to inhibitor-induced DNA damage. 53BP1 has no known enzymatic activity, yet by restricting end resection of DNA DSBs in G1 phase it promotes NHEJ. 53BP1 foci accumulation was associated with PARPi treatment in LN-229, but not in U-87MG or U-118MG cells, indicating that a PTEN mutation is not inevitably associated with HR-defective phenotype and NHEJ activation. No 53BP1 foci were observed upon PARGi treatment which suggests DNA damage generated by PARGi is not likely repaired by NHEJ. Importantly, despite G2 arrest, PTEN-wildtype LN-229 cells displayed high levels of 53BP1 foci, demonstrating an uncharacteristic activation of NHEJ in G2 phase during which HR is typically preferred.

To validate effective NHEJ stimulation after PARP inhibition in LN-229 cells, the nuclear accumulation of Ku80 was evaluated. The absence of significant Ku80 translocation in response to PARPi in LN-229 was unexpected, and may suggest NHEJ inactivity. If Ku80 results are accurate, they indicate the cellular inability to effectively perform NHEJ repair despite its activation. An alternative explanation is the inappropriate method of analysis. Ku80 is a ubiquitous protein whose nuclear localization is partially dependent on its dimerization with Ku70, making the quantification of distinct foci challenging. Our efforts to automatize this analysis may or may not be powerful to discern

active versus inactive Ku80 signals. Investigating another biomarker of the NHEJ pathway can provide valuable information on its functionality. The nuclease Artemis is exclusively involved in the classical NHEJ (C-NHEJ) pathway, and thus is a strong candidate for this purpose. Targeting Artemis in future experiments may validate NHEJ activation or inhibition upon PARPi treatment.

To study HR repair pathway activation, RAD51 foci formation was examined. The results demonstrate HR activation in PTEN-wildtype GBM cells after PARP inhibition, but not PARG inhibition, suggesting DNA damage generated by PARPi is resolved by HR. In contrast, RAD51 foci levels increased after PARPi olaparib in U-87MG and partially after PARGi in both U-87MG and U-118MG cells. These observations suggest that the localization of PTEN mutations could modulate HR efficiency in GBM. For instance, the U-87MG PTEN mutation, localized at the N-terminus of the protein, may disrupt its phosphatase activity, an effect not likely present in U-118MG cells with a C-terminal mutation. The characterization of PTEN mutations that affect DSB repair by HR and contribute to BRCAness phenotype is essential for future research on GBM. My data suggest the decreased efficiency of HR repair in PTEN deficient cells, supporting BRCAness phenotype in U-87MG and U-118MG cells. Moreover, HR activation in PTEN-mutant cells after PARPi olaparib, but not PARPi veliparib, suggests the greater ability of PARP-1 trapping as compared to enzymatic competition to initiate HR repair in GBM. While PARG inhibition mechanisms are currently unknown, its small effect on PTEN-mutant cells suggests that it is unlikely to function by molecular trapping. It also suggests that PARG inhibition is less sensitive to PTEN mutation differences. These data support the previously proposed hypothesis that PARPi and PARGi do not utilize the same mechanism.

The observation of G2 arrest without evidence for a cell death response may also result from replication stress in S phase. Thus, FANCD2 was assessed to investigate replication fork stalling. No significant changes in FANCD2 foci formation were observed between NT and inhibitor treatments, indicating that the DNA damage accumulation and cycle arrest is not due to errors in DNA replication. The observed DNA damage is more likely the direct result of inhibitor effects.

Cell lines are a useful tool to establish the molecular mechanisms behind DNA damage repair; however, as homogenous cultures they are not perfect representations of tumor tissue. GBM are largely heterogenous tumors that contain many cellular subtypes which may respond differently to the inhibitor treatments. PAR, PARP-1 and PARG expression in GBM tissue sections was investigated. These factors were found to be differently expressed within the 49 tissue samples, with no indication of correlation with tumor type or grade. Preliminary data acquired by Ashley Coleman (Coleman et al., unpublished) demonstrates the over-expression of PAR, PARP-1 and PARG in GBM compared to normal brain samples, and the cellular co-localization of PARP-1 with GBM stem cells. Further TMA assays are currently ongoing to assess these cellular subtypes and their expression of PARylation factors for all 49 tissues analyzed by western blot. Future studies with a larger tissue bank will provide valuable information on the relationship between tumor type/grade and factors of PARylation.

Collectively, these results support the treatment of PTEN-wildtype GBM with PARPi veliparib, as it has shown to induce substantial G2 arrest and DNA damage without effective initiation of NHEJ or complete activation of HR for repair. Inhibitor efficacy has been found to vary in PTEN-mutant GBM, likely in function of mutation localization. In an attempt to personalize GBM treatment, I propose that GBM displaying mutations in the N-terminus of PTEN (U-87MG) will benefit from PARPi veliparib, while GBM with C-terminal mutations (U-118MG) will profit from both PARPi and PARGi treatment. Testing this new hypothesis in combination with current treatment will further characterize the molecular mechanism of SL in GBM for the long-term interest of patient survival.

Acknowledgements:

I am profoundly grateful for the support of my advisor and principal investigator, Dr. Delphine Quénet, who has supplied endless guidance and encouragement throughout the last year. I extend my further gratitude toward past and present colleagues Trevor Wolf, Piotr Sowulewski, Mary Liesenberg, Riona O'Donnell, Jenna Hurley, and Ashley Coleman for the immense sense of community, and Dr. Diane Jaworski for generous access to her personal bank of tissue samples.

References

- Adeberg, S., Bostel, T., Konig, L., Welzel, T., Debus, J., & Combs, S. E. (2014). A comparison of long-term survivors and short-term survivors with glioblastoma, subventricular zone involvement: a predictive factor for survival? *Radiat Oncol*, *9*, 95. doi:10.1186/1748-717X-9-95
- Ashworth, A., & Lord, C. J. (2018). Synthetic lethal therapies for cancer: what's next after PARP inhibitors? *Nat Rev Clin Oncol*, *15*(9), 564-576. doi:10.1038/s41571-018-0055-6
- Beck, C., Robert, I., Reina-San-Martin, B., Schreiber, V., & Dantzer, F. (2014). Poly(ADP-ribose) polymerases in double-strand break repair: focus on PARP1, PARP2 and PARP3. *Exp Cell Res*, *329*(1), 18-25. doi:10.1016/j.yexcr.2014.07.003
- Bunting, S. F., Callen, E., Wong, N., Chen, H. T., Polato, F., Gunn, A., . . . Nussenzweig, A. (2010). 53BP1 inhibits homologous recombination in Brca1-deficient cells by blocking resection of DNA breaks. *Cell*, *141*(2), 243-254. doi:10.1016/j.cell.2010.03.012
- Carlomagno, N., Incollingo, P., Tamaro, V., Peluso, G., Rupealta, N., Chiacchio, G., . . . Santangelo, M. (2017). Diagnostic, Predictive, Prognostic, and Therapeutic Molecular Biomarkers in Third Millennium: A Breakthrough in Gastric Cancer. *Biomed Res Int*, *2017*, 7869802. doi:10.1155/2017/7869802
- Chapman, J. R., Taylor, M. R., & Boulton, S. J. (2012). Playing the end game: DNA double-strand break repair pathway choice. *Mol Cell*, *47*(4), 497-510. doi:10.1016/j.molcel.2012.07.029
- Cohen, A. L., Holmen, S. L., & Colman, H. (2013). IDH1 and IDH2 mutations in gliomas. *Curr Neurol Neurosci Rep*, *13*(5), 345. doi:10.1007/s11910-013-0345-4
- Cruz, C., Castroviejo-Bermejo, M., Gutierrez-Enriquez, S., Llop-Guevara, A., Ibrahim, Y. H., Gris-Oliver, A., . . . Serra, V. (2018). RAD51 foci as a functional biomarker of homologous recombination repair and PARP inhibitor resistance in germline BRCA-mutated breast cancer. *Ann Oncol*, *29*(5), 1203-1210. doi:10.1093/annonc/mdy099
- Curtin, N. J., & Szabo, C. (2013). Therapeutic applications of PARP inhibitors: anticancer therapy and beyond. *Mol Aspects Med*, *34*(6), 1217-1256. doi:10.1016/j.mam.2013.01.006
- Dang, L., White, D. W., Gross, S., Bennett, B. D., Bittinger, M. A., Driggers, E. M., . . . Su, S. M. (2009). Cancer-associated IDH1 mutations produce 2-hydroxyglutarate. *Nature*, *462*(7274), 739-744. doi:10.1038/nature08617
- De Bont, R., & van Larebeke, N. (2004). Endogenous DNA damage in humans: a review of quantitative data. *Mutagenesis*, *19*(3), 169-185.
- Dillon, M. T., Good, J. S., & Harrington, K. J. (2014). Selective targeting of the G2/M cell cycle checkpoint to improve the therapeutic index of radiotherapy. *Clin Oncol (R Coll Radiol)*, *26*(5), 257-265. doi:10.1016/j.clon.2014.01.009
- Gil Del Alcazar, C. R., Todorova, P. K., Habib, A. A., Mukherjee, B., & Burma, S. (2016). Augmented HR Repair Mediates Acquired Temozolomide Resistance in Glioblastoma. *Mol Cancer Res*, *14*(10), 928-940. doi:10.1158/1541-7786.MCR-16-0125
- Gravells, P., Grant, E., Smith, K. M., James, D. I., & Bryant, H. E. (2017). Specific killing of DNA damage-response deficient cells with inhibitors of poly(ADP-ribose) glycohydrolase. *DNA Repair (Amst)*, *52*, 81-91. doi:10.1016/j.dnarep.2017.02.010
- Gravells, P., Neale, J., Grant, E., Nathubhai, A., Smith, K. M., James, D. I., & Bryant, H. E. (2018). Radiosensitization with an inhibitor of poly(ADP-ribose) glycohydrolase: A comparison with the PARP1/2/3 inhibitor olaparib. *DNA Repair (Amst)*, *61*, 25-36. doi:10.1016/j.dnarep.2017.11.004
- Gupte, R., Liu, Z., & Kraus, W. L. (2017). PARPs and ADP-ribosylation: recent advances linking molecular functions to biological outcomes. *Genes Dev*, *31*(2), 101-126. doi:10.1101/gad.291518.116

- Hegi, M. E., Diserens, A. C., Gorlia, T., Hamou, M. F., de Tribolet, N., Weller, M., . . . Stupp, R. (2005). MGMT gene silencing and benefit from temozolomide in glioblastoma. *N Engl J Med*, 352(10), 997-1003. doi:10.1056/NEJMoa043331
- Jackson, S. P., & Bartek, J. (2009). The DNA-damage response in human biology and disease. *Nature*, 461(7267), 1071-1078. doi:10.1038/nature08467
- Jain, K. K. (2018). A Critical Overview of Targeted Therapies for Glioblastoma. *Front Oncol*, 8, 419. doi:10.3389/fonc.2018.00419
- James, D. I., Smith, K. M., Jordan, A. M., Fairweather, E. E., Griffiths, L. A., Hamilton, N. S., . . . Ogilvie, D. J. (2016). First-in-Class Chemical Probes against Poly(ADP-ribose) Glycohydrolase (PARG) Inhibit DNA Repair with Differential Pharmacology to Olaparib. *ACS Chem Biol*, 11(11), 3179-3190. doi:10.1021/acscchembio.6b00609
- Kaina, B., Christmann, M., Naumann, S., & Roos, W. P. (2007). MGMT: key node in the battle against genotoxicity, carcinogenicity and apoptosis induced by alkylating agents. *DNA Repair (Amst)*, 6(8), 1079-1099. doi:10.1016/j.dnarep.2007.03.008
- Lee, Y. R., Chen, M., & Pandolfi, P. P. (2018). The functions and regulation of the PTEN tumour suppressor: new modes and prospects. *Nat Rev Mol Cell Biol*, 19(9), 547-562. doi:10.1038/s41580-018-0015-0
- Lord, C. J., & Ashworth, A. (2017). PARP inhibitors: Synthetic lethality in the clinic. *Science*, 355(6330), 1152-1158. doi:10.1126/science.aam7344
- Louis, D. N., Perry, A., Reifenberger, G., von Deimling, A., Figarella-Branger, D., Cavenee, W. K., . . . Ellison, D. W. (2016). The 2016 World Health Organization Classification of Tumors of the Central Nervous System: a summary. *Acta Neuropathol*, 131(6), 803-820. doi:10.1007/s00401-016-1545-1
- Mahaney, B. L., Meek, K., & Lees-Miller, S. P. (2009). Repair of ionizing radiation-induced DNA double-strand breaks by non-homologous end-joining. *Biochem J*, 417(3), 639-650. doi:10.1042/BJ20080413
- McCabe, N., Turner, N. C., Lord, C. J., Kluzek, K., Bialkowska, A., Swift, S., . . . Ashworth, A. (2006). Deficiency in the repair of DNA damage by homologous recombination and sensitivity to poly(ADP-ribose) polymerase inhibition. *Cancer Res*, 66(16), 8109-8115. doi:10.1158/0008-5472.CAN-06-0140
- Montano, N., D'Alessandris, Q. G., Izzo, A., Fernandez, E., & Pallini, R. (2016). Biomarkers for glioblastoma multiforme: status quo. *J Clin Transl Res*, 2(1), 3-10.
- Murai, J., & Pommier, Y. (2016). Classification of PARP Inhibitors Based on PARP Trapping and Catalytic Inhibition, and Rationale for Combinations with Topoisomerase I Inhibitors and Alkylating Agents. In N. J. Curtin & R. A. Sharma (Eds.), *PARP Inhibitors for Cancer Therapy* (Vol. 83, pp. 261-274): Springer.
- Murai, J., Zhang, Y., Morris, J., Ji, J., Takeda, S., Doroshow, J. H., & Pommier, Y. (2014). Rationale for poly(ADP-ribose) polymerase (PARP) inhibitors in combination therapy with camptothecins or temozolomide based on PARP trapping versus catalytic inhibition. *J Pharmacol Exp Ther*, 349(3), 408-416. doi:10.1124/jpet.113.210146
- Nayak, L., Lee, E. Q., & Wen, P. Y. (2012). Epidemiology of brain metastases. *Curr Oncol Rep*, 14(1), 48-54. doi:10.1007/s11912-011-0203-y
- Omuro, A., & DeAngelis, L. M. (2013). Glioblastoma and other malignant gliomas: a clinical review. *JAMA*, 310(17), 1842-1850. doi:10.1001/jama.2013.280319
- Ostrom, Q. T., Bauchet, L., Davis, F. G., Deltour, I., Fisher, J. L., Langer, C. E., . . . Barnholtz-Sloan, J. S. (2014). The epidemiology of glioma in adults: a "state of the science" review. *Neuro Oncol*, 16(7), 896-913. doi:10.1093/neuonc/nou087
- Ostrom, Q. T., Gittleman, H., Fulop, J., Liu, M., Blanda, R., Kromer, C., . . . Barnholtz-Sloan, J. S. (2015). CBTRUS Statistical Report: Primary Brain and Central Nervous System Tumors

- Diagnosed in the United States in 2008-2012. *Neuro Oncol*, 17 Suppl 4, iv1-iv62. doi:10.1093/neuonc/nov189
- Pitroda, S. P., Pashtan, I. M., Logan, H. L., Budke, B., Darga, T. E., Weichselbaum, R. R., & Connell, P. P. (2014). DNA repair pathway gene expression score correlates with repair proficiency and tumor sensitivity to chemotherapy. *Sci Transl Med*, 6(229), 229ra242. doi:10.1126/scitranslmed.3008291
- Pommier, Y., O'Connor, M. J., & de Bono, J. (2016). Laying a trap to kill cancer cells: PARP inhibitors and their mechanisms of action. *Sci Transl Med*, 8(362), 362ps317. doi:10.1126/scitranslmed.aaf9246
- Scott, C. L., Swisher, E. M., & Kaufmann, S. H. (2015). Poly (ADP-ribose) polymerase inhibitors: recent advances and future development. *J Clin Oncol*, 33(12), 1397-1406. doi:10.1200/JCO.2014.58.8848
- Slade, D., Dunstan, M. S., Barkauskaite, E., Weston, R., Lafite, P., Dixon, N., . . . Ahel, I. (2011). The structure and catalytic mechanism of a poly(ADP-ribose) glycohydrolase. *Nature*, 477(7366), 616-620. doi:10.1038/nature10404
- Stupp, R., Mason, W. P., van den Bent, M. J., Weller, M., Fisher, B., Taphoorn, M. J., . . . National Cancer Institute of Canada Clinical Trials, G. (2005). Radiotherapy plus concomitant and adjuvant temozolomide for glioblastoma. *N Engl J Med*, 352(10), 987-996. doi:10.1056/NEJMoa043330
- Thompson, E. L., Yeo, J. E., Lee, E. A., Kan, Y., Raghunandan, M., Wiek, C., . . . Sobeck, A. (2017). FANCI and FANCD2 have common as well as independent functions during the cellular replication stress response. *Nucleic Acids Res*, 45(20), 11837-11857. doi:10.1093/nar/gkx847
- Turner, N., Tutt, A., & Ashworth, A. (2004). Hallmarks of 'BRCAness' in sporadic cancers. *Nat Rev Cancer*, 4(10), 814-819. doi:10.1038/nrc1457
- Zhang, J. (2013). The role of BRCA1 in homologous recombination repair in response to replication stress: significance in tumorigenesis and cancer therapy. *Cell Biosci*, 3(1), 11. doi:10.1186/2045-3701-3-11
- Zhao, S., Lin, Y., Xu, W., Jiang, W., Zha, Z., Wang, P., . . . Xiong, Y. (2009). Glioma-derived mutations in IDH1 dominantly inhibit IDH1 catalytic activity and induce HIF-1alpha. *Science*, 324(5924), 261-265. doi:10.1126/science.1170944

Table 1: List of primary antibodies.

Name of Protein	Dilution	Reference	Manufacturer	Technique
β -actin	1/50,000	A1978	Sigma-Aldrich	western blot
mIDH1/2	1/1,000	MABC1103	Millipore	
MGMT	1/2,000	2739	Cell signaling	
PAR	1/1,000	ALX-804-220	Enzo	
PARG	1/500	MABS61	Millipore	
PARP1	1/2,000	9532	Cell signaling	
PTEN	1/1,000	Ab32199	Abcam	
53BP1	1/500	NB100-904	Novus	
γ H2AX	1/700	ab2893	Abcam	
BRCA1	1/100	MA1-137	Invitrogen	
FANCD2	1/350	NB100-182	Novus	
Ku80	1/100	NBP1-56408	Novus	
Rad51	1/100	sc-398587	Santa Cruz	
CD133	1/500	D4W4N	Cell Signaling	immunohistochemistry
CD163	1/1600	HPA046404	Sigma-Aldrich	
GFAP	1/100	GA5	Cell Signaling	
MBP	1/400	D8X4Q	Cell Signaling	
NG2	1/25	HPA002951	Sigma-Aldrich	
PAR	1/1,000	ALX-804-220	Enzo	
PARG	1/10	PA5-14158	ThermoFisher	
PARP1	1/25	E102	Abcam	

Figure Legends:

Figure 1: Brain tumor incidence from 2008-2012 demonstrates GBM prevalence. Data acquired by the Centers for Disease Control and Prevention (CDC).

Figure 2: PARP-1 and PARG recruitment facilitates DNA damage repair. Different repair pathways are activated following DNA double-strand break (DSB), single-strand break (SSB) and base damage (*e.g.*, alkylated base). Major factors involved in DSB repair are indicated in green. PARP-1 and PARG participate in the represented pathways by interacting with or modifying target proteins and PARP-1 itself, using nicotinamide adenine dinucleotide (NAD⁺) as a substrate and release of nicotinamide (NAM). NAD⁺ biosynthesis can be achieved via salvage pathway from preformed substrates including NAM in presence of adenosine triphosphate (ATP) and phosphoribosyl diphosphate (PRPP). This reaction leads to the release of adenosine monophosphate (AMP) and pyrophosphate (PP_i) (orange box*). Abbreviations: Base excision repair (BER), mismatch repair (MMR), non-homologous end joining (NHEJ), nucleotide excision repair (NER), homologous recombination (HR).

Figure 3: Synthetic lethality leads to selective cell death. Two cells, biologically distinct by the presence (right panel) or absence (left panel) of a pre-existing “Gene A” defect (*e.g.*, BRCA1/2 mutation) are viable. Upon “Gene B” disruption (*e.g.*, PARP-1 inhibition), only the cell with the pre-existing “Gene A” mutation (right panel) faces lethal consequences, based on the concept of synthetic lethality.

Figure 4: PARPi and PARGi induce G2 arrest in GBM cells. GBM cells were treated with PARPi (veliparib or olaparib) and PARGi PDD00017273 at IC₅₀ for 24 hours. Cells were fixed and stained with propidium iodide before cell cycle analysis by flow cytometry. DNA quantity was measured to place the cells into 5 categories (Sub-G1, G1, S, G2, and Polyploidy). A) Cell distribution in function of the relative DNA quantity, which represent the phases of the cell cycle was plotted for one representative experiment. B) The average percentage of cells observed in each phase of the cell cycle was plotted in function of the cell line and treatment. Error bars correspond to standard deviation. C) The difference in percentage between treated and non-treated groups in G2 phase was represented for each treatment. Digitonin, doxorubicin, and temozolomide were used as positive controls. Data are representative of two biological replicates.

Figure 5: PARPi and PARGi do not induce apoptosis or necrosis in GBM cells. GBM cells were treated with PARPi (veliparib or olaparib) and PARGi PDD00017273 at IC₅₀ for 24 hours. Following annexin V and propidium iodide (PI) staining, apoptosis and necrosis activation was analysis by flow cytometry. The average percentage of cells observed as apoptotic/necrotic (annexin V⁺, PI⁺; black), apoptotic (annexin V⁺; medium gray), or living (annexin V⁻, PI⁻; light gray), was plotted against the corresponding cell line and treatment. Digitonin was used as positive control. Error bars represent standard deviation. Data are representative of two biological replicates.

Figure 6: PARPi and PARGi generate DNA damage in PTEN-wild type (LN-229) GBM cells. After 24 hours treatment at IC₅₀ with either PARPi (veliparib or olaparib) or PARGi PDD00017273, GBM cells were fixed and immunofluorescence-stained with γ H2AX. Nuclei were stained with DAPI. As a positive control, cells were treated with doxorubicin and representative images are presented (left panel). At least 100 cells displaying either ≤ 1 γ H2AX focus (black), 2-5 γ H2AX foci (medium gray)

or ≥ 6 γ H2AX foci (light gray) were counted per condition, per experiment. Average percentage (%) of cells in each category is plotted against the corresponding cell line and treatment group. Error bars correspond to standard deviation, and statistical significance has been assessed by ANOVA testing. Data are representative of three biological replicates. **** P<0.0001.

Figure 7: PARPi and PARGi activate NHEJ in PTEN-wildtype (LN-229) GBM cells. After 24 hours treatment at IC₅₀ with either PARPi (veliparib or olaparib) or PARGi PDD00017273, GBM cells were fixed and immunofluorescence-stained for 53BP1. Nuclei were stained with DAPI. As a positive control, cells were treated with doxorubicin and representative images are presented (left panel). At least 100 cells displaying either ≤ 1 53BP1 focus (black), 2-5 53BP1 foci (medium gray) or ≥ 6 53BP1 foci (light gray) were counted per condition, per experiment. Average percentage (%) of cells in each category was plotted against the corresponding cell line and treatment group. Error bars correspond to standard deviation, and statistical significance has been assessed by ANOVA testing. Data are representative of three biological replicates. **** P<0.0001; ** P \geq 0.0021.

Figure 8: PARPi and PARGi are associated with NHEJ completion defect in PTEN-wildtype (LN-229) and PTEN-mutant (U-87MG and U-118MG) GBM cells. After 24 hours treatment at IC₅₀ with either PARPi (veliparib or olaparib) or PARGi PDD00017273, GBM cells were fixed and immunofluorescence-stained for Ku80. Nuclei were stained with DAPI. As a positive control, cells were treated with doxorubicin and representative images were presented (left panel). Nuclear signal intensity of Ku80 was assessed by analyzing at least 100 cells. The ratio of Ku80 signal in the treatment group to the Not Treated group was plotted against the corresponding cell line and treatment group. Error bars correspond to standard deviation, and statistical significance has been assessed by ANOVA testing. Data are representative of three biological replicates. **** P<0.0001; ** P \geq 0.0021.

Figure 9: BRCA1 foci is not observed in GBM cells. After 24 hours treatment at IC₅₀ with either PARPi (veliparib or olaparib) or PARGi PDD00017273, GBM cells were fixed and immunofluorescence-stained for BRCA1. As a positive control, cells were treated with etoposide and representative images were presented. Nuclei were stained with DAPI. The Ku80, RAD51, and γ H2AX/53BP1/FANCD2 protocols were attempted, with no observation of BRCA1 foci formation using these methods.

Figure 10: PARPi and PARGi activate HR in PTEN-wild type (LN-229) and PTEN-mutant (U-87MG and U-118MG) GBM cells. After 24 hours treatment at IC₅₀ with either PARPi (veliparib or olaparib) or PARGi PDD00017273, GBM cells have been fixed and immunofluorescence-stained for RAD51. Nuclei were stained with DAPI. As a positive control, cells were treated with etoposide and representative images are presented (left panel). RAD51 foci number was assessed by counting at least 100 cells per condition, per experiment. Number of foci per cell was plotted against the corresponding cell line and treatment group on a box plot chart where the average, median (x), minimum, maximum, and first and third quartiles are indicated. Outliers are depicted by dots beyond the interquartile range (IQR). Statistical significance has been assessed by ANOVA testing. Data are representative of three biological replicates.

Figure 11: PARPi and PARGi are not associated with replicative stress in GBM cells. After 24 hours treatment at IC₅₀ with either PARPi (veliparib or olaparib) or PARGi PDD00017273, GBM cells were fixed and immunofluorescence-stained for FANCD2. Nuclei were stained with DAPI. As a

positive control, cells were treated with hydroxyurea and representative images were presented (left panel). FANCD2 foci were examined in at least 100 cells and categorized as negative (black) or positive (medium gray). Average percentage (%) of cells in each category was plotted against the corresponding cell line and treatment group. Error bars correspond to standard deviation, and statistical significance has been assessed by ANOVA testing. Data are representative of three biological replicates. **** $P < 0.0001$; ** $P \geq 0.0021$.

Figure 12: PAR, PARP-1 and PARG are differentially expressed in brain tumors. All proteins were extracted from 49 solid tissue samples (normal, malignant and benign). After migration on SDS-PAGE and transfer onto a nitrocellulose membrane, proteins of interest were revealed by western blot.

Figure 13: PAR, PARP-1 and PARG are over-expressed in GBM tissue section. Factors of interest, including specific cellular markers (i.e., CD133, CD163, GFAP, MBP and NG2) were sequentially immunostained on tissue section from normal and GBM-diagnosed patients.

Figure 14: PARPi and PARGi differently affect the DNA damage response in PTEN-wildtype and PTEN-mutant GBM cell lines. γ H2AX, 53BP1, Ku80, RAD51, and FANCD2 signals were assessed and summarized by PTEN status, and inhibitor treatment (PARPi versus PARGi). Text size indicates foci formation response as compared to NT (small=NT; medium>NT; large>>NT).

Figure 1.

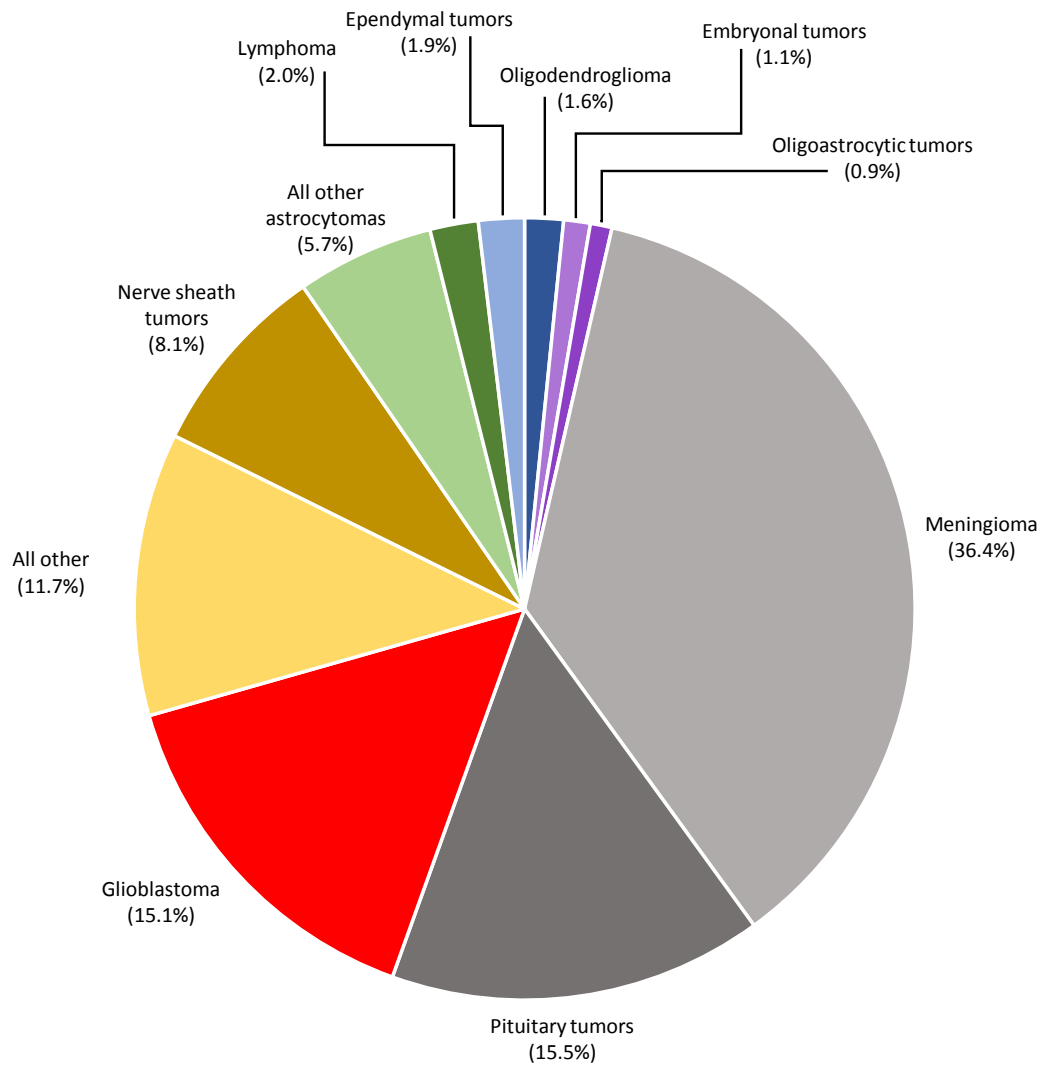


Figure 2.

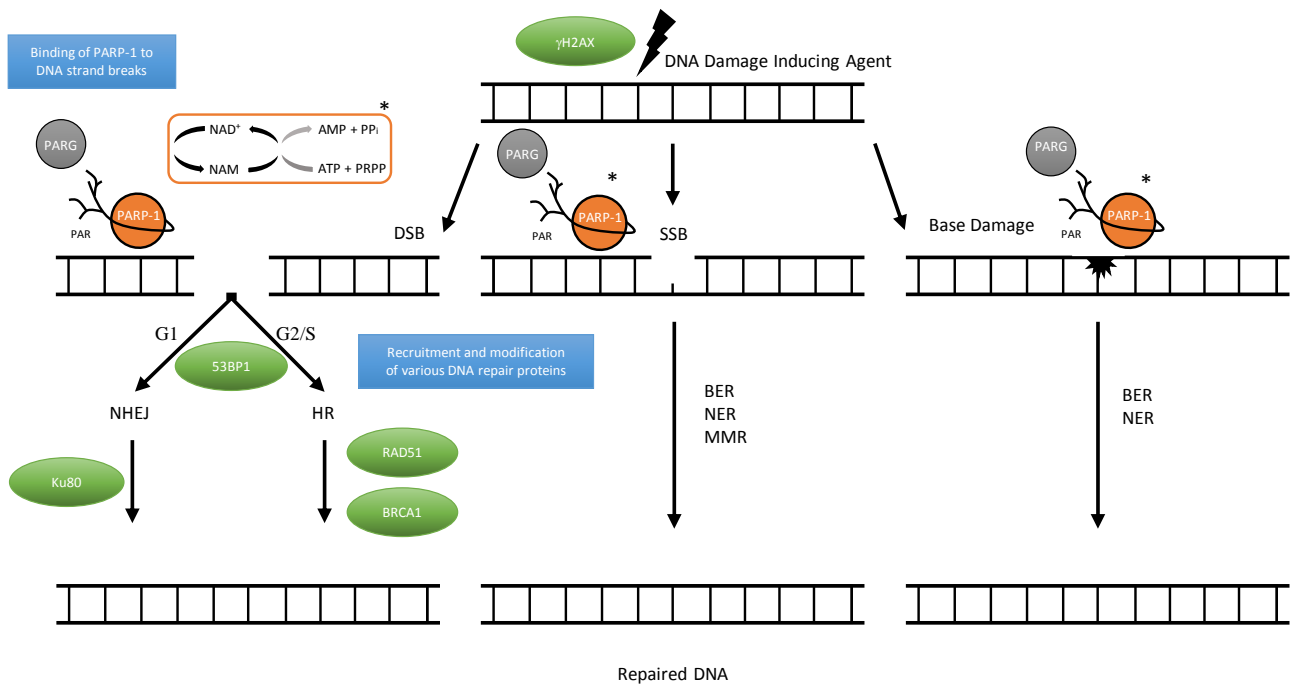


Figure 3.

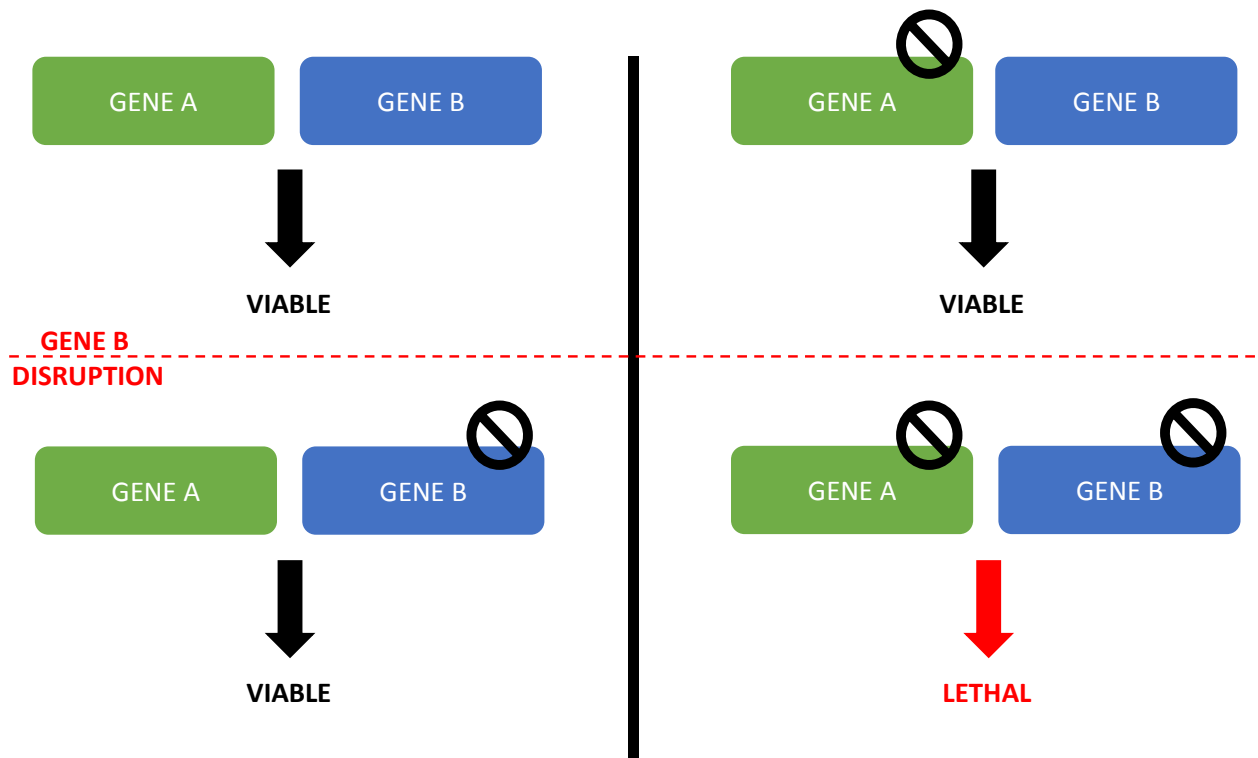
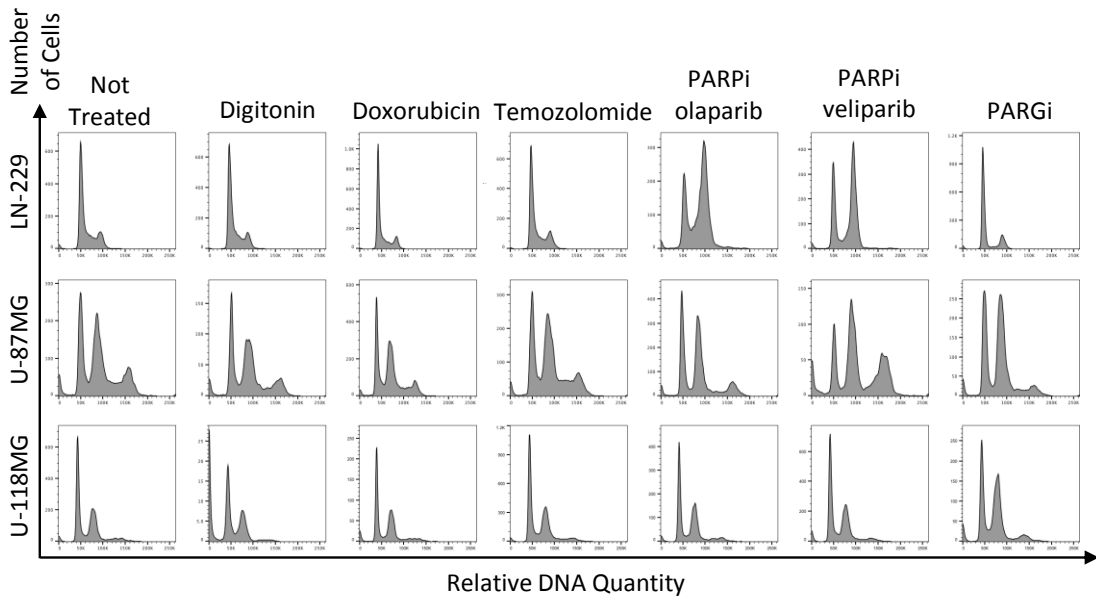
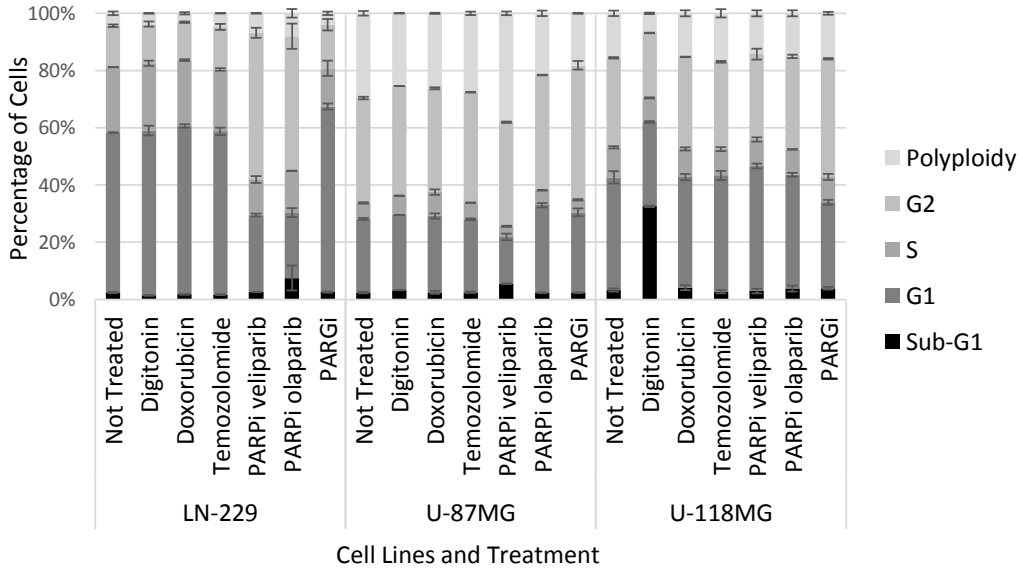


Figure 4.

A.



B.



C.

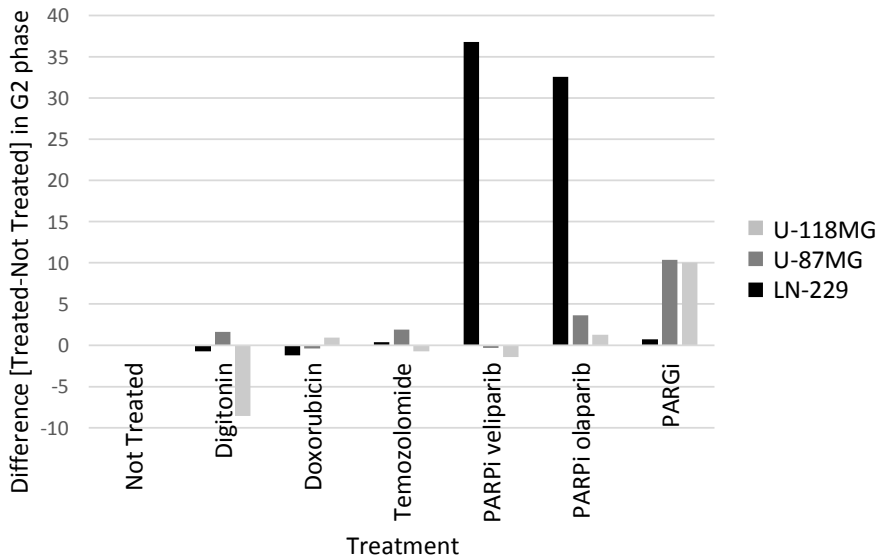


Figure 5.

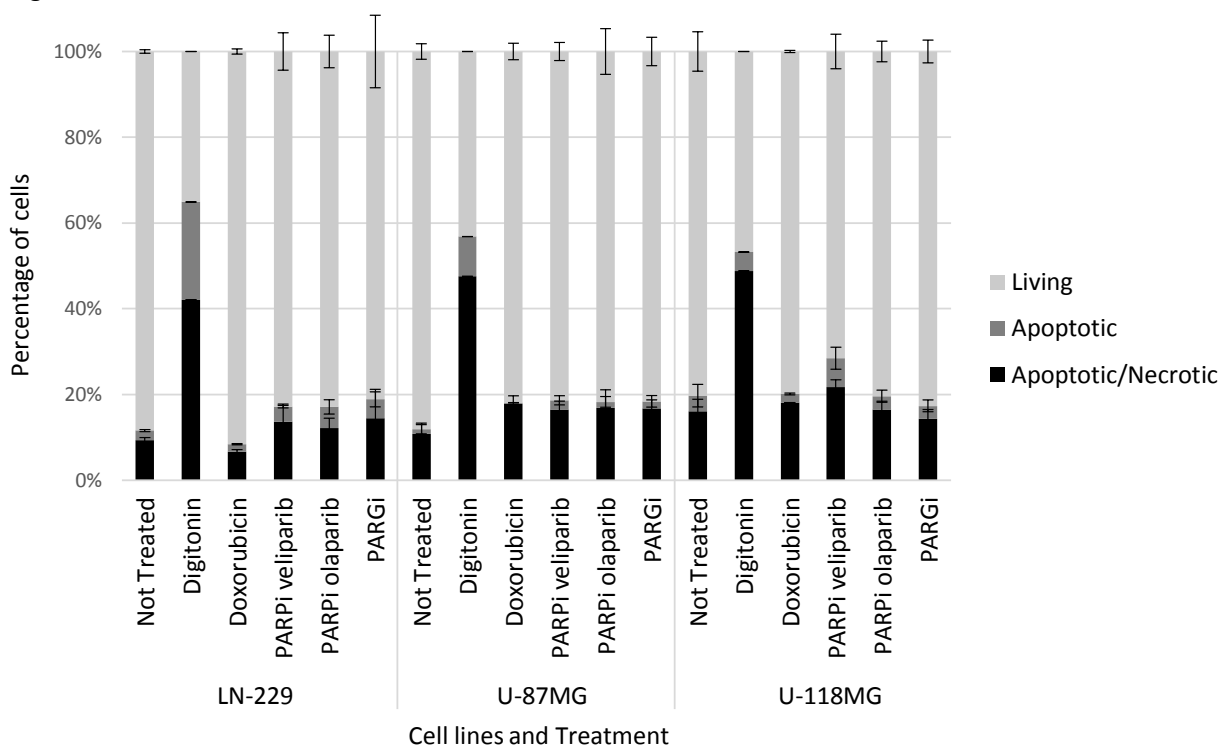


Figure 6.

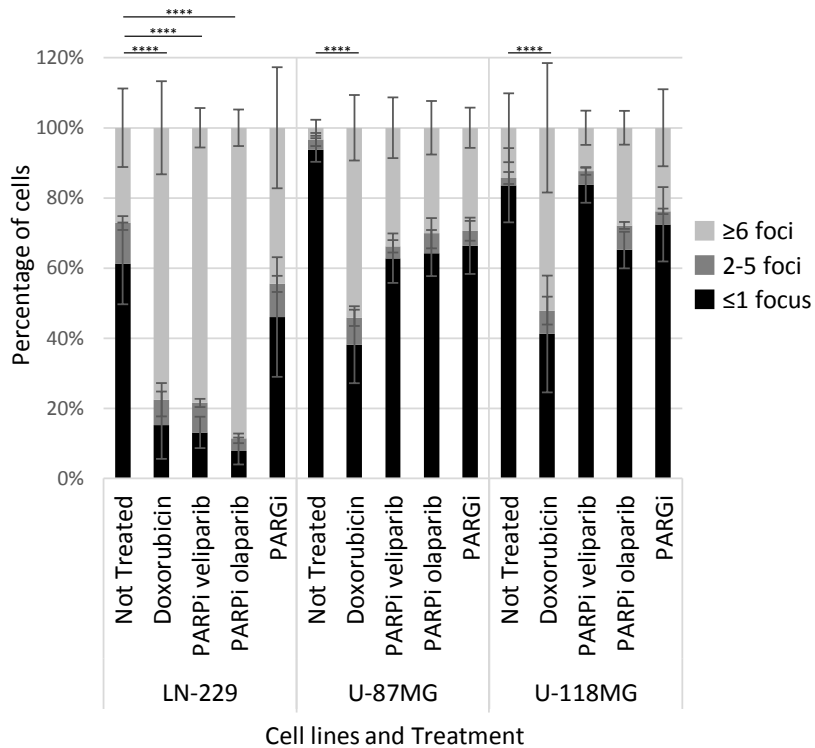
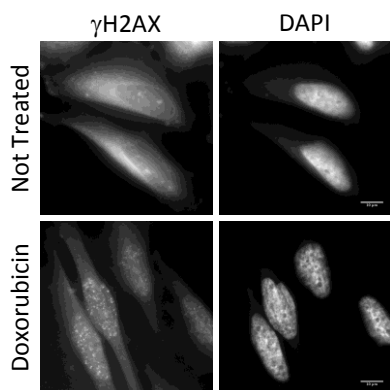


Figure 7.

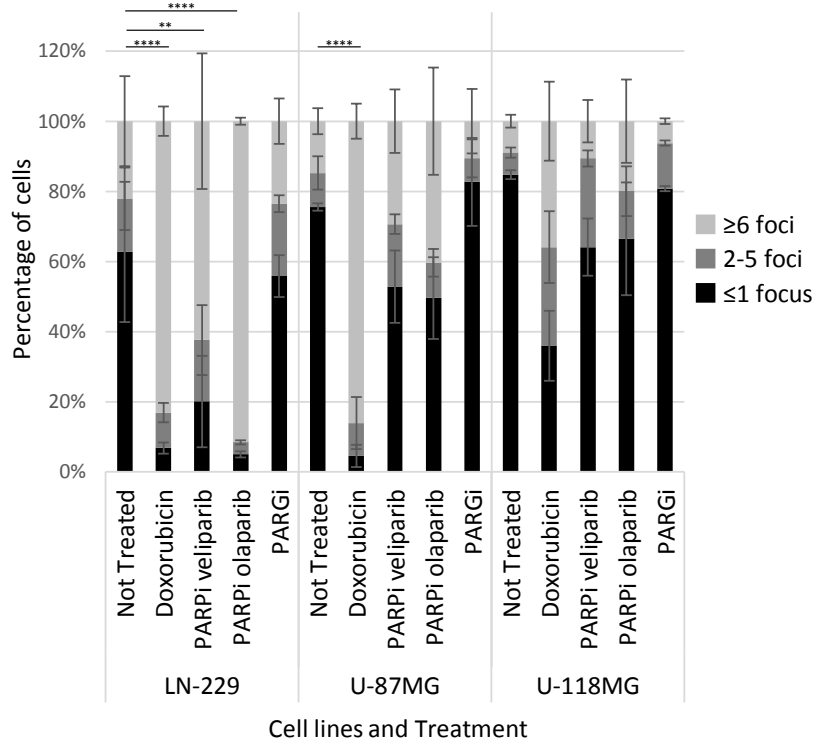
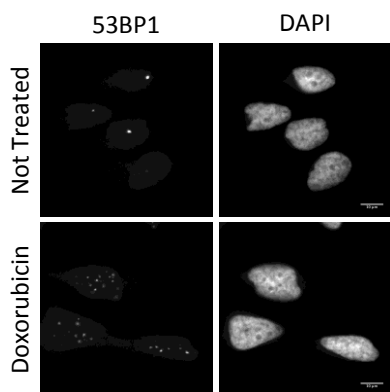


Figure 8.

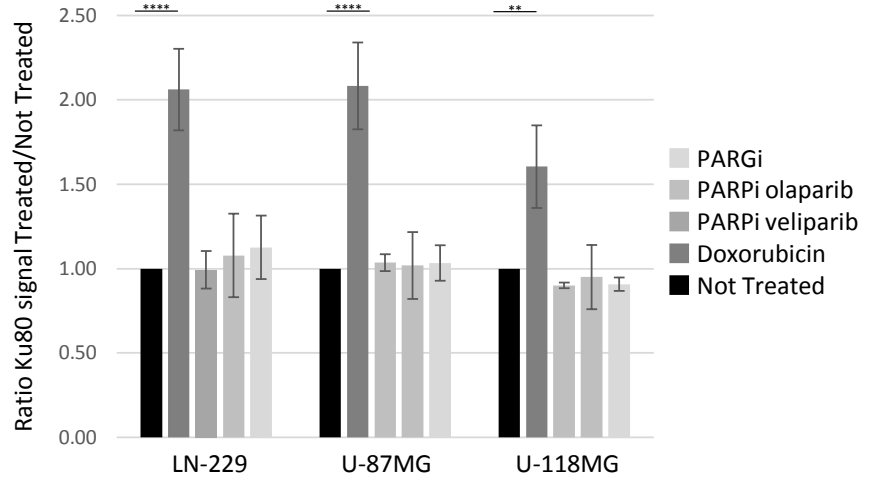
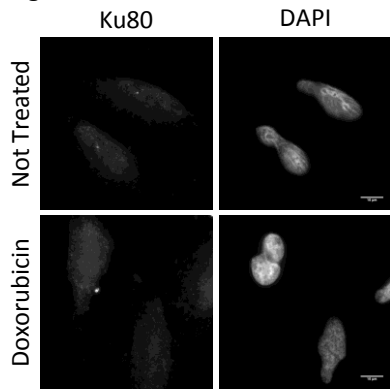


Figure 9.

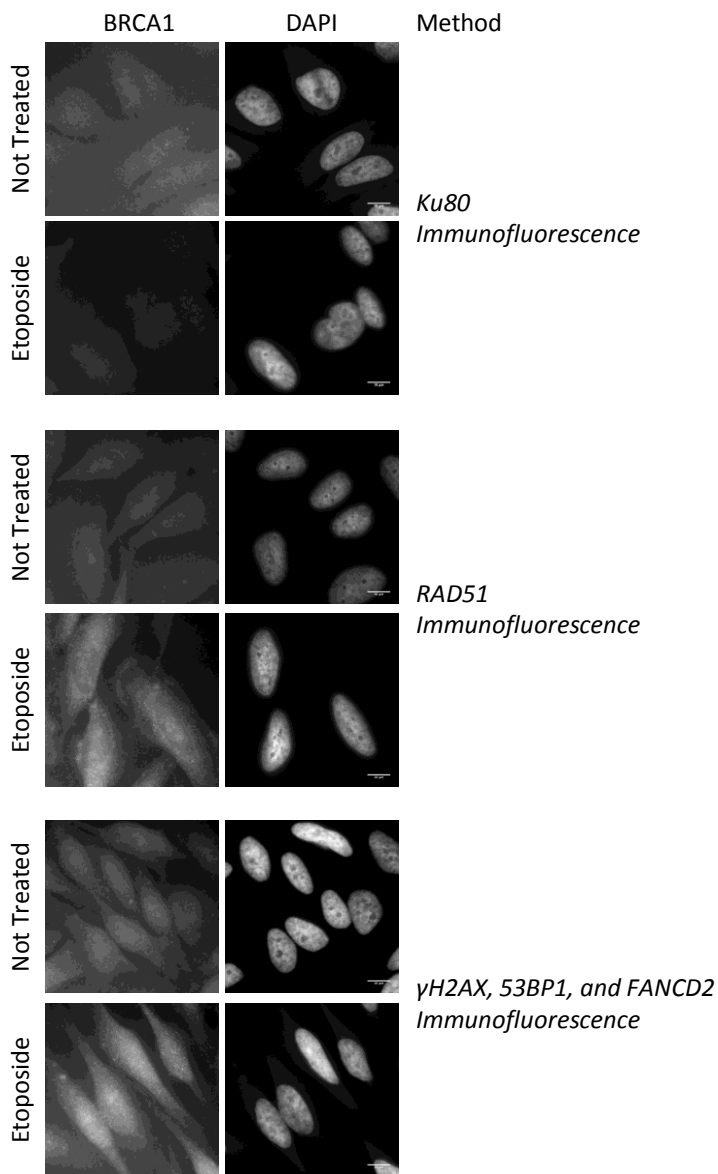


Figure 10.

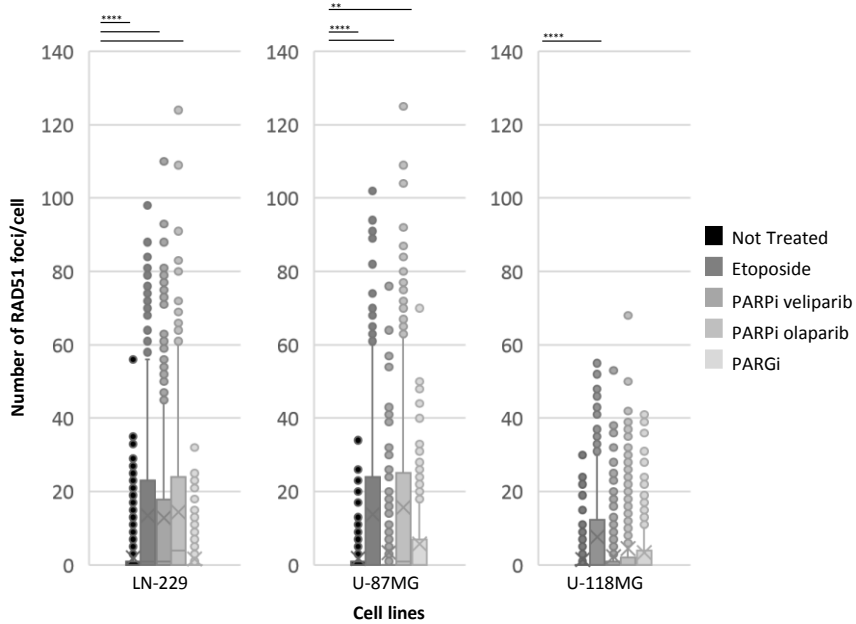
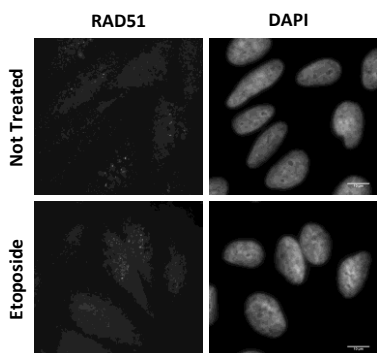


Figure 11.

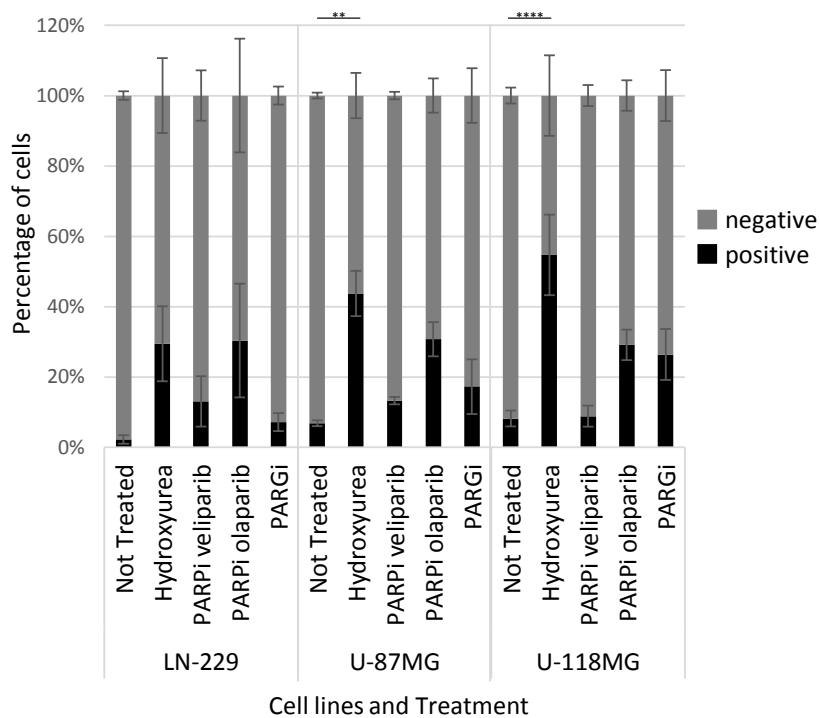
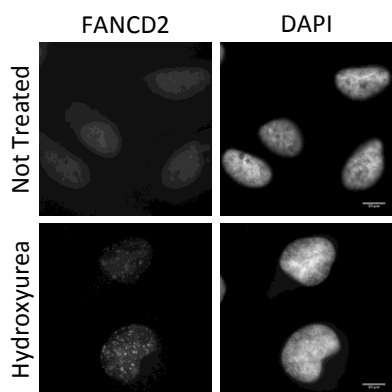


Figure 12.

	Tissue
N	Normal Tissue
G	Glioblastoma
AA	Anaplastic Astrocytoma
OD	Oligodendroglioma II/III
OA	Oligoastrocytoma II/III
MT	Brain Metastasis
MG	Meningioma

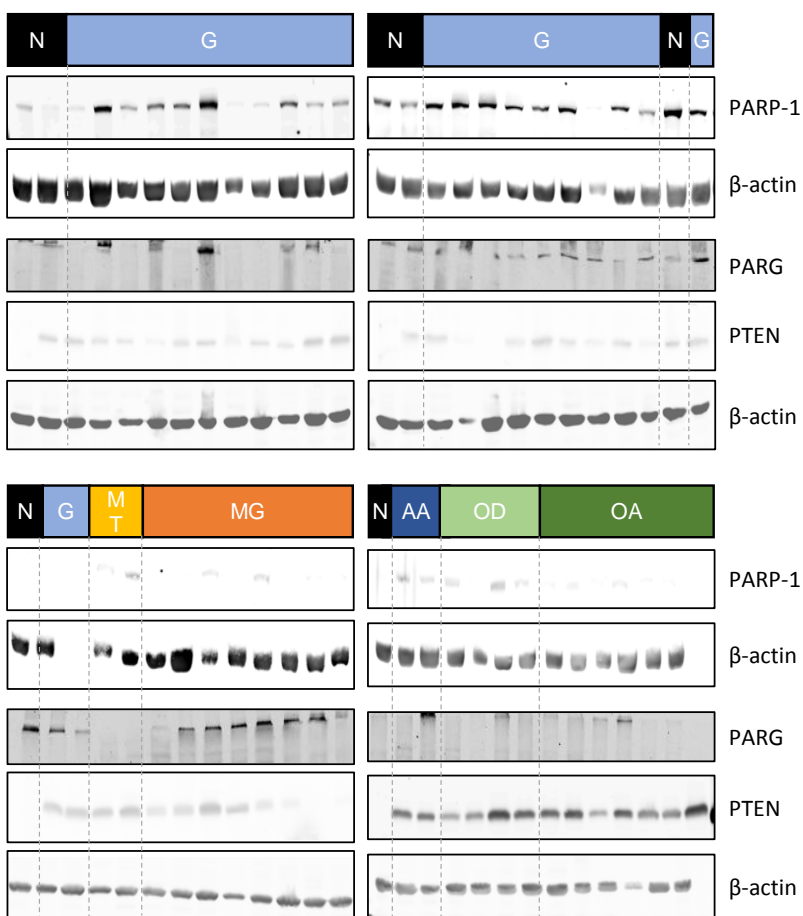


Figure 13.

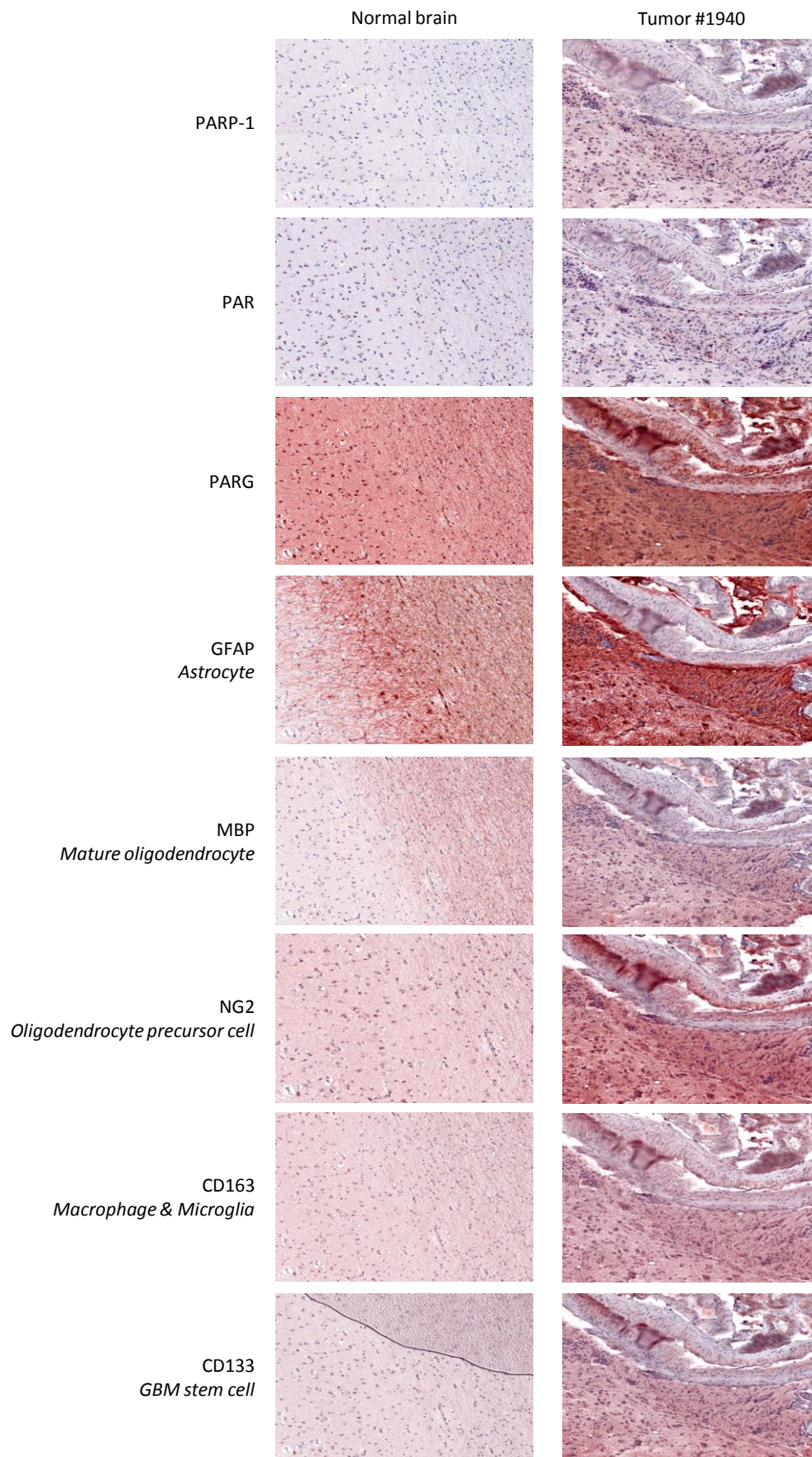


Figure 14.

		PTEN-wildtype		PTEN-mutant	
		PARPi	PARGi	PARPi	PARGi
DNA Damage Signaling		γH2AX	γH2AX	γH2AX	γH2AX
NHEJ	Initiation	53BP1	53BP1	53BP1	53BP1
	Completion	Ku80	Ku80	Ku80	Ku80
HR		RAD51	RAD51	RAD51	RAD51
Replication Stress		FANCD2	FANCD2	FANCD2	FANCD2

Supplemental Tables:

		Sub-G1		G1		S		G2		Polyploidy	
		Average	Std dev	Average	Std dev	Average	Std dev	Average	Std dev	Average	Std dev
LN-229	Not Treated	2.5	0.2	55.9	0.1	22.9	0.0	14.5	0.5	4.4	0.7
	Digitonin	1.5	0.1	57.6	1.7	23.5	0.9	13.7	0.9	3.8	0.2
	Doxorubicin	1.9	0.2	58.8	0.6	23.0	0.3	13.3	0.3	3.1	0.4
	Temozolomide	1.8	0.2	57.0	1.3	21.7	0.5	14.9	1.1	4.8	0.0
	PARPi veliparib	2.7	0.1	26.9	0.5	12.4	1.2	51.3	1.8	6.8	0.1
	PARPi olaparib	7.6	4.4	22.9	1.6	14.6	0.0	47.0	4.4	8.0	1.5
	PARGi	2.6	0.2	64.9	1.1	13.4	2.7	15.2	2.0	4.0	0.6
U-87MG	Not Treated	2.5	0.3	25.8	0.4	5.6	0.3	36.7	0.4	29.6	0.8
	Digitonin	3.3	0.0	26.3	0.0	6.7	0.0	38.3	0.0	25.4	0.0
	Doxorubicin	2.5	0.5	26.7	0.9	8.4	0.9	36.3	0.4	26.2	0.2
	Temozolomide	2.6	0.3	25.5	0.3	5.8	0.0	38.6	0.1	27.6	0.6
	PARPi veliparib	5.6	0.0	16.4	1.2	3.7	0.2	36.4	0.3	38.1	0.7
	PARPi olaparib	2.4	0.1	30.6	0.8	5.2	0.0	40.3	0.1	21.6	0.9
	PARGi	2.5	0.1	28.1	1.4	4.4	0.3	47.0	1.5	18.2	0.2
U-118MG	Not Treated	3.4	0.6	39.4	2.2	10.5	0.4	31.3	0.3	15.6	1.0
	Digitonin	32.6	0.3	29.5	0.3	8.4	0.2	22.7	0.1	6.9	0.3
	Doxorubicin	4.2	0.8	38.7	1.1	9.9	0.6	32.2	0.1	15.3	1.1
	Temozolomide	2.8	0.6	40.6	1.6	9.2	0.7	30.5	0.3	17.0	1.5
	PARPi veliparib	3.0	0.8	43.7	0.9	9.3	0.8	29.8	1.9	14.3	1.1
	PARPi olaparib	3.9	1.1	39.8	0.6	8.9	0.0	32.5	0.6	15.1	1.1
	PARGi	4.0	0.5	30.1	0.9	8.9	1.1	41.3	0.3	15.9	0.5

Supplemental Table 1: Distribution of cells (average percentage and standard deviation) over the cell cycle in function of treatment.

Tukey's multiple comparisons test	Mean Diff.	95.00% CI of diff.	Adjusted P Value	Summary
<i>Sub-G1</i>				
Not Treated vs. Digitonin	1.0500	-5.164 to 7.264	0.9982	ns
Not Treated vs. Doxorubicin	0.6500	-5.564 to 6.864	0.9999	ns
Not Treated vs. Temozolomide	0.7500	-5.464 to 6.964	0.9997	ns
Not Treated vs. PARPi veliparib	-0.1500	-6.364 to 6.064	>0.9999	ns
Not Treated vs. PARPi olaparib	-5.0500	-11.26 to 1.164	0.1762	ns
Not Treated vs. PARGi	-0.1000	-6.314 to 6.114	>0.9999	ns
Digitonin vs. Doxorubicin	-0.4000	-6.614 to 5.814	>0.9999	ns
Digitonin vs. Temozolomide	-0.3000	-6.514 to 5.914	>0.9999	ns
Digitonin vs. PARPi veliparib	-1.2000	-7.414 to 5.014	0.9963	ns
Digitonin vs. PARPi olaparib	-6.1000	-12.31 to 0.1136	0.0571	ns
Digitonin vs. PARGi	-1.1500	-7.364 to 5.064	0.9971	ns
Doxorubicin vs. Temozolomide	0.1000	-6.114 to 6.314	>0.9999	ns
Doxorubicin vs. PARPi veliparib	-0.8000	-7.014 to 5.414	0.9996	ns
Doxorubicin vs. PARPi olaparib	-5.7000	-11.91 to 0.5136	0.0899	ns
Doxorubicin vs. PARGi	-0.7500	-6.964 to 5.464	0.9997	ns
Temozolomide vs. PARPi veliparib	-0.9000	-7.114 to 5.314	0.9993	ns
Temozolomide vs. PARPi olaparib	-5.8000	-12.01 to 0.4136	0.0805	ns
Temozolomide vs. PARGi	-0.8500	-7.064 to 5.364	0.9995	ns
PARPi veliparib vs. PARPi olaparib	-4.9000	-11.11 to 1.314	0.2032	ns
PARPi veliparib vs. PARGi	0.0500	-6.164 to 6.264	>0.9999	ns
PARPi olaparib vs. PARGi	4.9500	-1.264 to 11.16	0.1939	ns
<i>G1</i>				
Not Treated vs. Digitonin	-1.7500	-7.964 to 4.464	0.9732	ns
Not Treated vs. Doxorubicin	-2.9500	-9.164 to 3.264	0.7520	ns
Not Treated vs. Temozolomide	-1.1500	-7.364 to 5.064	0.9971	ns
Not Treated vs. PARPi veliparib	28.9500	22.74 to 35.16	<0.0001	****
Not Treated vs. PARPi olaparib	33.0000	26.79 to 39.21	<0.0001	****
Not Treated vs. PARGi	-9.0000	-15.21 to -2.786	0.0012	**
Digitonin vs. Doxorubicin	-1.2000	-7.414 to 5.014	0.9963	ns
Digitonin vs. Temozolomide	0.6000	-5.614 to 6.814	>0.9999	ns
Digitonin vs. PARPi veliparib	30.7000	24.49 to 36.91	<0.0001	****
Digitonin vs. PARPi olaparib	34.7500	28.54 to 40.96	<0.0001	****
Digitonin vs. PARGi	-7.2500	-13.46 to -1.036	0.0136	*
Doxorubicin vs. Temozolomide	1.8000	-4.414 to 8.014	0.9692	ns
Doxorubicin vs. PARPi veliparib	31.9000	25.69 to 38.11	<0.0001	****
Doxorubicin vs. PARPi olaparib	35.9500	29.74 to 42.16	<0.0001	****
Doxorubicin vs. PARGi	-6.0500	-12.26 to 0.1636	0.0606	ns
Temozolomide vs. PARPi veliparib	30.1000	23.89 to 36.31	<0.0001	****
Temozolomide vs. PARPi olaparib	34.1500	27.94 to 40.36	<0.0001	****
Temozolomide vs. PARGi	-7.8500	-14.06 to -1.636	0.0061	**
PARPi veliparib vs. PARPi olaparib	4.0500	-2.164 to 10.26	0.4106	ns
PARPi veliparib vs. PARGi	-37.9500	-44.16 to -31.74	<0.0001	****
PARPi olaparib vs. PARGi	-42.0000	-48.21 to -35.79	<0.0001	****
<i>S</i>				
Not Treated vs. Digitonin	-0.6500	-6.864 to 5.564	0.9999	ns
Not Treated vs. Doxorubicin	-0.1500	-6.364 to 6.064	>0.9999	ns
Not Treated vs. Temozolomide	1.2000	-5.014 to 7.414	0.9963	ns
Not Treated vs. PARPi veliparib	10.4500	4.236 to 16.66	0.0001	***
Not Treated vs. PARPi olaparib	8.2500	2.036 to 14.46	0.0035	**
Not Treated vs. PARGi	9.5000	3.286 to 15.71	0.0006	***
Digitonin vs. Doxorubicin	0.5000	-5.714 to 6.714	>0.9999	ns
Digitonin vs. Temozolomide	1.8500	-4.364 to 8.064	0.9649	ns
Digitonin vs. PARPi veliparib	11.1000	4.886 to 17.31	<0.0001	****
Digitonin vs. PARPi olaparib	8.9000	2.686 to 15.11	0.0014	**
Digitonin vs. PARGi	10.1500	3.936 to 16.36	0.0002	***
Doxorubicin vs. Temozolomide	1.3500	-4.864 to 7.564	0.9930	ns
Doxorubicin vs. PARPi veliparib	10.6000	4.386 to 16.81	0.0001	***
Doxorubicin vs. PARPi olaparib	8.4000	2.186 to 14.61	0.0028	**
Doxorubicin vs. PARGi	9.6500	3.436 to 15.86	0.0005	***
Temozolomide vs. PARPi veliparib	9.2500	3.036 to 15.46	0.0008	***
Temozolomide vs. PARPi olaparib	7.0500	0.8364 to 13.26	0.0177	*
Temozolomide vs. PARGi	8.3000	2.086 to 14.51	0.0032	**
PARPi veliparib vs. PARPi olaparib	-2.2000	-8.414 to 4.014	0.9218	ns
PARPi veliparib vs. PARGi	-0.9500	-7.164 to 5.264	0.9990	ns
PARPi olaparib vs. PARGi	1.2500	-4.964 to 7.464	0.9954	ns

<i>G2</i>				
Not Treated vs. Digitonin	0.7500	-5.464 to 6.964	0.9997	ns
Not Treated vs. Doxorubicin	1.2000	-5.014 to 7.414	0.9963	ns
Not Treated vs. Temozolomide	-0.4000	-6.614 to 5.814	>0.9999	ns
Not Treated vs. PARPi veliparib	-36.8000	-43.01 to -30.59	<0.0001	****
Not Treated vs. PARPi olaparib	-32.5500	-38.76 to -26.34	<0.0001	****
Not Treated vs. PARGi	-0.7500	-6.964 to 5.464	0.9997	ns
Digitonin vs. Doxorubicin	0.4500	-5.764 to 6.664	>0.9999	ns
Digitonin vs. Temozolomide	-1.1500	-7.364 to 5.064	0.9971	ns
Digitonin vs. PARPi veliparib	-37.5500	-43.76 to -31.34	<0.0001	****
Digitonin vs. PARPi olaparib	-33.3000	-39.51 to -27.09	<0.0001	****
Digitonin vs. PARGi	-1.5000	-7.714 to 4.714	0.9877	ns
Doxorubicin vs. Temozolomide	-1.6000	-7.814 to 4.614	0.9829	ns
Doxorubicin vs. PARPi veliparib	-38.0000	-44.21 to -31.79	<0.0001	****
Doxorubicin vs. PARPi olaparib	-33.7500	-39.96 to -27.54	<0.0001	****
Doxorubicin vs. PARGi	-1.9500	-8.164 to 4.264	0.9549	ns
Temozolomide vs. PARPi veliparib	-36.4000	-42.61 to -30.19	<0.0001	****
Temozolomide vs. PARPi olaparib	-32.1500	-38.36 to -25.94	<0.0001	****
Temozolomide vs. PARGi	-0.3500	-6.564 to 5.864	>0.9999	ns
PARPi veliparib vs. PARPi olaparib	4.2500	-1.964 to 10.46	0.3539	ns
PARPi veliparib vs. PARGi	36.0500	29.84 to 42.26	<0.0001	****
PARPi olaparib vs. PARGi	31.8000	25.59 to 38.01	<0.0001	****
<i>Polyploidy</i>				
Not Treated vs. Digitonin	0.6000	-5.614 to 6.814	>0.9999	ns
Not Treated vs. Doxorubicin	1.2500	-4.964 to 7.464	0.9954	ns
Not Treated vs. Temozolomide	-0.4000	-6.614 to 5.814	>0.9999	ns
Not Treated vs. PARPi veliparib	-2.4500	-8.664 to 3.764	0.8765	ns
Not Treated vs. PARPi olaparib	-3.6500	-9.864 to 2.564	0.5338	ns
Not Treated vs. PARGi	0.3500	-5.864 to 6.564	>0.9999	ns
Digitonin vs. Doxorubicin	0.6500	-5.564 to 6.864	0.9999	ns
Digitonin vs. Temozolomide	-1.0000	-7.214 to 5.214	0.9986	ns
Digitonin vs. PARPi veliparib	-3.0500	-9.264 to 3.164	0.7228	ns
Digitonin vs. PARPi olaparib	-4.2500	-10.46 to 1.964	0.3539	ns
Digitonin vs. PARGi	-0.2500	-6.464 to 5.964	>0.9999	ns
Doxorubicin vs. Temozolomide	-1.6500	-7.864 to 4.564	0.9800	ns
Doxorubicin vs. PARPi veliparib	-3.7000	-9.914 to 2.514	0.5179	ns
Doxorubicin vs. PARPi olaparib	-4.9000	-11.11 to 1.314	0.2032	ns
Doxorubicin vs. PARGi	-0.9000	-7.114 to 5.314	0.9993	ns
Temozolomide vs. PARPi veliparib	-2.0500	-8.264 to 4.164	0.9431	ns
Temozolomide vs. PARPi olaparib	-3.2500	-9.464 to 2.964	0.6615	ns
Temozolomide vs. PARGi	0.7500	-5.464 to 6.964	0.9997	ns
PARPi veliparib vs. PARPi olaparib	-1.2000	-7.414 to 5.014	0.9963	ns
PARPi veliparib vs. PARGi	2.8000	-3.414 to 9.014	0.7936	ns
PARPi olaparib vs. PARGi	4.0000	-2.214 to 10.21	0.4253	ns

Supplemental Table 2: 2-way ANOVA test of cell cycle analysis of LN-229 cells by flow cytometry.
ns: non significant, *: ≥ 0.0332 , **: ≥ 0.0021 , ***: ≥ 0.0002 ****: < 0.0001

U-87MG

Tukey's multiple comparisons test	Mean Diff.	95.00% CI of diff.	Adjusted P Value	Summary
<i>Sub-G1</i>				
Not Treated vs. Digitonin	-0.8500	-4.194 to 2.494	0.9829	ns
Not Treated vs. Doxorubicin	-0.0500	-2.781 to 2.681	>0.9999	ns
Not Treated vs. Temozolomide	-0.1000	-2.831 to 2.631	>0.9999	ns
Not Treated vs. PARPi veliparib	-3.1000	-5.831 to -0.3693	0.0181	*
Not Treated vs. PARPi olaparib	0.0500	-2.681 to 2.781	>0.9999	ns
Not Treated vs. PARGi	0.0000	-2.731 to 2.731	>0.9999	ns
Digitonin vs. Doxorubicin	0.8000	-2.544 to 4.144	0.9875	ns
Digitonin vs. Temozolomide	0.7500	-2.594 to 4.094	0.9911	ns
Digitonin vs. PARPi veliparib	-2.2500	-5.594 to 1.094	0.3653	ns
Digitonin vs. PARPi olaparib	0.9000	-2.444 to 4.244	0.9772	ns
Digitonin vs. PARGi	0.8500	-2.494 to 4.194	0.9829	ns
Doxorubicin vs. Temozolomide	-0.0500	-2.781 to 2.681	>0.9999	ns
Doxorubicin vs. PARPi veliparib	-3.0500	-5.781 to -0.3193	0.0209	*
Doxorubicin vs. PARPi olaparib	0.1000	-2.631 to 2.831	>0.9999	ns
Doxorubicin vs. PARGi	0.0500	-2.681 to 2.781	>0.9999	ns
Temozolomide vs. PARPi veliparib	-3.0000	-5.731 to -0.2693	0.0240	*
Temozolomide vs. PARPi olaparib	0.1500	-2.581 to 2.881	>0.9999	ns
Temozolomide vs. PARGi	0.1000	-2.631 to 2.831	>0.9999	ns
PARPi veliparib vs. PARPi olaparib	3.1500	0.4193 to 5.881	0.0157	*
PARPi veliparib vs. PARGi	3.1000	0.3693 to 5.831	0.0181	*
PARPi olaparib vs. PARGi	-0.0500	-2.781 to 2.681	>0.9999	ns
<i>G1</i>				
Not Treated vs. Digitonin	-0.5500	-3.894 to 2.794	0.9984	ns
Not Treated vs. Doxorubicin	-0.9500	-3.681 to 1.781	0.9237	ns
Not Treated vs. Temozolomide	0.2500	-2.481 to 2.981	>0.9999	ns
Not Treated vs. PARPi veliparib	9.4000	6.669 to 12.13	<0.0001	****
Not Treated vs. PARPi olaparib	-4.8000	-7.531 to -2.069	<0.0001	****
Not Treated vs. PARGi	-2.3000	-5.031 to 0.4307	0.1444	ns
Digitonin vs. Doxorubicin	-0.4000	-3.744 to 2.944	0.9997	ns
Digitonin vs. Temozolomide	0.8000	-2.544 to 4.144	0.9875	ns
Digitonin vs. PARPi veliparib	9.9500	6.606 to 13.29	<0.0001	****
Digitonin vs. PARPi olaparib	-4.2500	-7.594 to -0.9056	0.0061	**
Digitonin vs. PARGi	-1.7500	-5.094 to 1.594	0.6514	ns
Doxorubicin vs. Temozolomide	1.2000	-1.531 to 3.931	0.8041	ns
Doxorubicin vs. PARPi veliparib	10.3500	7.619 to 13.08	<0.0001	****
Doxorubicin vs. PARPi olaparib	-3.8500	-6.581 to -1.119	0.0019	**
Doxorubicin vs. PARGi	-1.3500	-4.081 to 1.381	0.7071	ns
Temozolomide vs. PARPi veliparib	9.1500	6.419 to 11.88	<0.0001	****
Temozolomide vs. PARPi olaparib	-5.0500	-7.781 to -2.319	<0.0001	****
Temozolomide vs. PARGi	-2.5500	-5.281 to 0.1807	0.0795	ns
PARPi veliparib vs. PARPi olaparib	-14.2000	-16.93 to -11.47	<0.0001	****
PARPi veliparib vs. PARGi	-11.7000	-14.43 to -8.969	<0.0001	****
PARPi olaparib vs. PARGi	2.5000	-0.2307 to 5.231	0.0900	ns
<i>S</i>				
Not Treated vs. Digitonin	-1.1500	-4.494 to 2.194	0.9276	ns
Not Treated vs. Doxorubicin	-2.8000	-5.531 to -0.06930	0.0416	*
Not Treated vs. Temozolomide	-0.2500	-2.981 to 2.481	>0.9999	ns
Not Treated vs. PARPi veliparib	1.8500	-0.8807 to 4.581	0.3573	ns
Not Treated vs. PARPi olaparib	0.3500	-2.381 to 3.081	0.9996	ns
Not Treated vs. PARGi	1.2000	-1.531 to 3.931	0.8041	ns
Digitonin vs. Doxorubicin	-1.6500	-4.994 to 1.694	0.7090	ns
Digitonin vs. Temozolomide	0.9000	-2.444 to 4.244	0.9772	ns
Digitonin vs. PARPi veliparib	3.0000	-0.3444 to 6.344	0.1018	ns
Digitonin vs. PARPi olaparib	1.5000	-1.844 to 4.844	0.7892	ns
Digitonin vs. PARGi	2.3500	-0.9944 to 5.694	0.3161	ns
Doxorubicin vs. Temozolomide	2.5500	-0.1807 to 5.281	0.0795	ns
Doxorubicin vs. PARPi veliparib	4.6500	1.919 to 7.381	0.0002	***
Doxorubicin vs. PARPi olaparib	3.1500	0.4193 to 5.881	0.0157	*

Doxorubicin vs. PARGi	4.0000	1.269 to 6.731	0.0012	**
Temozolomide vs. PARPi veliparib	2.1000	-0.6307 to 4.831	0.2224	ns
Temozolomide vs. PARPi olaparib	0.6000	-2.131 to 3.331	0.9920	ns
Temozolomide vs. PARGi	1.4500	-1.281 to 4.181	0.6362	ns
PARPi veliparib vs. PARPi olaparib	-1.5000	-4.231 to 1.231	0.5999	ns
PARPi veliparib vs. PARGi	-0.6500	-3.381 to 2.081	0.9878	ns
PARPi olaparib vs. PARGi	0.8500	-1.881 to 3.581	0.9540	ns
G2				
Not Treated vs. Digitonin	-1.6500	-4.994 to 1.694	0.7090	ns
Not Treated vs. Doxorubicin	0.4000	-2.331 to 3.131	0.9991	ns
Not Treated vs. Temozolomide	-1.9000	-4.631 to 0.8307	0.3271	ns
Not Treated vs. PARPi veliparib	0.3000	-2.431 to 3.031	0.9998	ns
Not Treated vs. PARPi olaparib	-3.6500	-6.381 to -0.9193	0.0035	**
Not Treated vs. PARGi	-10.3500	-13.08 to -7.619	<0.0001	****
Digitonin vs. Doxorubicin	2.0500	-1.294 to 5.394	0.4744	ns
Digitonin vs. Temozolomide	-0.2500	-3.594 to 3.094	>0.9999	ns
Digitonin vs. PARPi veliparib	1.9500	-1.394 to 5.294	0.5327	ns
Digitonin vs. PARPi olaparib	-2.0000	-5.344 to 1.344	0.5034	ns
Digitonin vs. PARGi	-8.7000	-12.04 to -5.356	<0.0001	****
Doxorubicin vs. Temozolomide	-2.3000	-5.031 to 0.4307	0.1444	ns
Doxorubicin vs. PARPi veliparib	-0.1000	-2.831 to 2.631	>0.9999	ns
Doxorubicin vs. PARPi olaparib	-4.0500	-6.781 to -1.319	0.0010	**
Doxorubicin vs. PARGi	-10.7500	-13.48 to -8.019	<0.0001	****
Temozolomide vs. PARPi veliparib	2.2000	-0.5307 to 4.931	0.1802	ns
Temozolomide vs. PARPi olaparib	-1.7500	-4.481 to 0.9807	0.4220	ns
Temozolomide vs. PARGi	-8.4500	-11.18 to -5.719	<0.0001	****
PARPi veliparib vs. PARPi olaparib	-3.9500	-6.681 to -1.219	0.0014	**
PARPi veliparib vs. PARGi	-10.6500	-13.38 to -7.919	<0.0001	****
PARPi olaparib vs. PARGi	-6.7000	-9.431 to -3.969	<0.0001	****
Polyploidy				
Not Treated vs. Digitonin	4.2000	0.8556 to 7.544	0.0069	**
Not Treated vs. Doxorubicin	3.4000	0.6693 to 6.131	0.0075	**
Not Treated vs. Temozolomide	2.0000	-0.7307 to 4.731	0.2714	ns
Not Treated vs. PARPi veliparib	-8.4500	-11.18 to -5.719	<0.0001	****
Not Treated vs. PARPi olaparib	8.0500	5.319 to 10.78	<0.0001	****
Not Treated vs. PARGi	11.4500	8.719 to 14.18	<0.0001	****
Digitonin vs. Doxorubicin	-0.8000	-4.144 to 2.544	0.9875	ns
Digitonin vs. Temozolomide	-2.2000	-5.544 to 1.144	0.3914	ns
Digitonin vs. PARPi veliparib	-12.6500	-15.99 to -9.306	<0.0001	****
Digitonin vs. PARPi olaparib	3.8500	0.5056 to 7.194	0.0160	*
Digitonin vs. PARGi	7.2500	3.906 to 10.59	<0.0001	****
Doxorubicin vs. Temozolomide	-1.4000	-4.131 to 1.331	0.6720	ns
Doxorubicin vs. PARPi veliparib	-11.8500	-14.58 to -9.119	<0.0001	****
Doxorubicin vs. PARPi olaparib	4.6500	1.919 to 7.381	0.0002	***
Doxorubicin vs. PARGi	8.0500	5.319 to 10.78	<0.0001	****
Temozolomide vs. PARPi veliparib	-10.4500	-13.18 to -7.719	<0.0001	****
Temozolomide vs. PARPi olaparib	6.0500	3.319 to 8.781	<0.0001	****
Temozolomide vs. PARGi	9.4500	6.719 to 12.18	<0.0001	****
PARPi veliparib vs. PARPi olaparib	16.5000	13.77 to 19.23	<0.0001	****
PARPi veliparib vs. PARGi	19.9000	17.17 to 22.63	<0.0001	****
PARPi olaparib vs. PARGi	3.4000	0.6693 to 6.131	0.0075	**

Supplemental Table 3: 2-way ANOVA test of cell cycle analysis of U-87MG cells by flow cytometry.
ns: non significant, *: ≥ 0.0332 , **: ≥ 0.0021 , ***: ≥ 0.0002 ****: < 0.0001

U-118MG

Tukey's multiple comparisons test	Mean Diff.	95.00% CI of diff.	Adjusted P Value	Summary
<i>Sub-G1</i>				
Not Treated vs. Digitonin	-29.2000	-33.10 to -25.30	<0.0001	****
Not Treated vs. Doxorubicin	-0.8000	-4.695 to 3.095	0.9948	ns
Not Treated vs. Temozolomide	0.6000	-3.295 to 4.495	0.9989	ns
Not Treated vs. PARPi veliparib	0.3500	-3.545 to 4.245	>0.9999	ns
Not Treated vs. PARPi olaparib	-0.5000	-4.395 to 3.395	0.9996	ns
Not Treated vs. PARGi	-0.6000	-4.495 to 3.295	0.9989	ns
Digitonin vs. Doxorubicin	28.4000	24.50 to 32.30	<0.0001	****
Digitonin vs. Temozolomide	29.8000	25.90 to 33.70	<0.0001	****
Digitonin vs. PARPi veliparib	29.5500	25.65 to 33.45	<0.0001	****
Digitonin vs. PARPi olaparib	28.7000	24.80 to 32.60	<0.0001	****
Digitonin vs. PARGi	28.6000	24.70 to 32.50	<0.0001	****
Doxorubicin vs. Temozolomide	1.4000	-2.495 to 5.295	0.9165	ns
Doxorubicin vs. PARPi veliparib	1.1500	-2.745 to 5.045	0.9663	ns
Doxorubicin vs. PARPi olaparib	0.3000	-3.595 to 4.195	>0.9999	ns
Doxorubicin vs. PARGi	0.2000	-3.695 to 4.095	>0.9999	ns
Temozolomide vs. PARPi veliparib	-0.2500	-4.145 to 3.645	>0.9999	ns
Temozolomide vs. PARPi olaparib	-1.1000	-4.995 to 2.795	0.9729	ns
Temozolomide vs. PARGi	-1.2000	-5.095 to 2.695	0.9586	ns
PARPi veliparib vs. PARPi olaparib	-0.8500	-4.745 to 3.045	0.9928	ns
PARPi veliparib vs. PARGi	-0.9500	-4.845 to 2.945	0.9871	ns
PARPi olaparib vs. PARGi	-0.1000	-3.995 to 3.795	>0.9999	ns
<i>G1</i>				
Not Treated vs. Digitonin	9.8500	5.955 to 13.75	<0.0001	****
Not Treated vs. Doxorubicin	0.6500	-3.245 to 4.545	0.9983	ns
Not Treated vs. Temozolomide	-1.2500	-5.145 to 2.645	0.9499	ns
Not Treated vs. PARPi veliparib	-4.3000	-8.195 to -0.4047	0.0226	*
Not Treated vs. PARPi olaparib	-0.4000	-4.295 to 3.495	0.9999	ns
Not Treated vs. PARGi	9.3000	5.405 to 13.20	<0.0001	****
Digitonin vs. Doxorubicin	-9.2000	-13.10 to -5.305	<0.0001	****
Digitonin vs. Temozolomide	-11.1000	-15.00 to -7.205	<0.0001	****
Digitonin vs. PARPi veliparib	-14.1500	-18.05 to -10.25	<0.0001	****
Digitonin vs. PARPi olaparib	-10.2500	-14.15 to -6.355	<0.0001	****
Digitonin vs. PARGi	-0.5500	-4.445 to 3.345	0.9994	ns
Doxorubicin vs. Temozolomide	-1.9000	-5.795 to 1.995	0.7285	ns
Doxorubicin vs. PARPi veliparib	-4.9500	-8.845 to -1.055	0.0057	**
Doxorubicin vs. PARPi olaparib	-1.0500	-4.945 to 2.845	0.9785	ns
Doxorubicin vs. PARGi	8.6500	4.755 to 12.55	<0.0001	****
Temozolomide vs. PARPi veliparib	-3.0500	-6.945 to 0.8453	0.2099	ns
Temozolomide vs. PARPi olaparib	0.8500	-3.045 to 4.745	0.9928	ns
Temozolomide vs. PARGi	10.5500	6.655 to 14.45	<0.0001	****
PARPi veliparib vs. PARPi olaparib	3.9000	0.004656 to 7.795	0.0496	*
PARPi veliparib vs. PARGi	13.6000	9.705 to 17.50	<0.0001	****
PARPi olaparib vs. PARGi	9.7000	5.805 to 13.60	<0.0001	****
<i>S</i>				
Not Treated vs. Digitonin	2.1000	-1.795 to 5.995	0.6299	ns
Not Treated vs. Doxorubicin	0.6500	-3.245 to 4.545	0.9983	ns
Not Treated vs. Temozolomide	1.3000	-2.595 to 5.195	0.9400	ns
Not Treated vs. PARPi veliparib	1.2500	-2.645 to 5.145	0.9499	ns
Not Treated vs. PARPi olaparib	1.6500	-2.245 to 5.545	0.8361	ns
Not Treated vs. PARGi	1.6500	-2.245 to 5.545	0.8361	ns
Digitonin vs. Doxorubicin	-1.4500	-5.345 to 2.445	0.9029	ns
Digitonin vs. Temozolomide	-0.8000	-4.695 to 3.095	0.9948	ns
Digitonin vs. PARPi veliparib	-0.8500	-4.745 to 3.045	0.9928	ns
Digitonin vs. PARPi olaparib	-0.4500	-4.345 to 3.445	0.9998	ns
Digitonin vs. PARGi	-0.4500	-4.345 to 3.445	0.9998	ns
Doxorubicin vs. Temozolomide	0.6500	-3.245 to 4.545	0.9983	ns
Doxorubicin vs. PARPi veliparib	0.6000	-3.295 to 4.495	0.9989	ns
Doxorubicin vs. PARPi olaparib	1.0000	-2.895 to 4.895	0.9832	ns

Doxorubicin vs. PARGi	1.0000	-2.895 to 4.895	0.9832	ns
Temozolomide vs. PARPi veliparib	-0.0500	-3.945 to 3.845	>0.9999	ns
Temozolomide vs. PARPi olaparib	0.3500	-3.545 to 4.245	>0.9999	ns
Temozolomide vs. PARGi	0.3500	-3.545 to 4.245	>0.9999	ns
PARPi veliparib vs. PARPi olaparib	0.4000	-3.495 to 4.295	0.9999	ns
PARPi veliparib vs. PARGi	0.4000	-3.495 to 4.295	0.9999	ns
PARPi olaparib vs. PARGi	0.0000	-3.895 to 3.895	>0.9999	ns
G2				
Not Treated vs. Digitonin	8.5500	4.655 to 12.45	<0.0001	****
Not Treated vs. Doxorubicin	-0.9500	-4.845 to 2.945	0.9871	ns
Not Treated vs. Temozolomide	0.7500	-3.145 to 4.645	0.9963	ns
Not Treated vs. PARPi veliparib	1.4500	-2.445 to 5.345	0.9029	ns
Not Treated vs. PARPi olaparib	-1.2500	-5.145 to 2.645	0.9499	ns
Not Treated vs. PARGi	-10.0000	-13.90 to -6.105	<0.0001	****
Digitonin vs. Doxorubicin	-9.5000	-13.40 to -5.605	<0.0001	****
Digitonin vs. Temozolomide	-7.8000	-11.70 to -3.905	<0.0001	****
Digitonin vs. PARPi veliparib	-7.1000	-11.00 to -3.205	<0.0001	****
Digitonin vs. PARPi olaparib	-9.8000	-13.70 to -5.905	<0.0001	****
Digitonin vs. PARGi	-18.5500	-22.45 to -14.65	<0.0001	****
Doxorubicin vs. Temozolomide	1.7000	-2.195 to 5.595	0.8165	ns
Doxorubicin vs. PARPi veliparib	2.4000	-1.495 to 6.295	0.4776	ns
Doxorubicin vs. PARPi olaparib	-0.3000	-4.195 to 3.595	>0.9999	ns
Doxorubicin vs. PARGi	-9.0500	-12.95 to -5.155	<0.0001	****
Temozolomide vs. PARPi veliparib	0.7000	-3.195 to 4.595	0.9975	ns
Temozolomide vs. PARPi olaparib	-2.0000	-5.895 to 1.895	0.6801	ns
Temozolomide vs. PARGi	-10.7500	-14.65 to -6.855	<0.0001	****
PARPi veliparib vs. PARPi olaparib	-2.7000	-6.595 to 1.195	0.3386	ns
PARPi veliparib vs. PARGi	-11.4500	-15.35 to -7.555	<0.0001	****
PARPi olaparib vs. PARGi	-8.7500	-12.65 to -4.855	<0.0001	****
Polyploidy				
Not Treated vs. Digitonin	8.7000	4.805 to 12.60	<0.0001	****
Not Treated vs. Doxorubicin	0.3000	-3.595 to 4.195	>0.9999	ns
Not Treated vs. Temozolomide	-1.4000	-5.295 to 2.495	0.9165	ns
Not Treated vs. PARPi veliparib	1.3000	-2.595 to 5.195	0.9400	ns
Not Treated vs. PARPi olaparib	0.5000	-3.395 to 4.395	0.9996	ns
Not Treated vs. PARGi	-0.3500	-4.245 to 3.545	>0.9999	ns
Digitonin vs. Doxorubicin	-8.4000	-12.30 to -4.505	<0.0001	****
Digitonin vs. Temozolomide	-10.1000	-14.00 to -6.205	<0.0001	****
Digitonin vs. PARPi veliparib	-7.4000	-11.30 to -3.505	<0.0001	****
Digitonin vs. PARPi olaparib	-8.2000	-12.10 to -4.305	<0.0001	****
Digitonin vs. PARGi	-9.0500	-12.95 to -5.155	<0.0001	****
Doxorubicin vs. Temozolomide	-1.7000	-5.595 to 2.195	0.8165	ns
Doxorubicin vs. PARPi veliparib	1.0000	-2.895 to 4.895	0.9832	ns
Doxorubicin vs. PARPi olaparib	0.2000	-3.695 to 4.095	>0.9999	ns
Doxorubicin vs. PARGi	-0.6500	-4.545 to 3.245	0.9983	ns
Temozolomide vs. PARPi veliparib	2.7000	-1.195 to 6.595	0.3386	ns
Temozolomide vs. PARPi olaparib	1.9000	-1.995 to 5.795	0.7285	ns
Temozolomide vs. PARGi	1.0500	-2.845 to 4.945	0.9785	ns
PARPi veliparib vs. PARPi olaparib	-0.8000	-4.695 to 3.095	0.9948	ns
PARPi veliparib vs. PARGi	-1.6500	-5.545 to 2.245	0.8361	ns
PARPi olaparib vs. PARGi	-0.8500	-4.745 to 3.045	0.9928	ns

Supplemental Table 4: 2-way ANOVA test of cell cycle analysis of U-118MG cells by flow cytometry.

ns: non significant, *: ≥ 0.0332 , **: ≥ 0.0021 , ***: ≥ 0.0002 ****: < 0.0001

Tukey's multiple comparisons test	Mean Diff.	95.00% CI of diff.	Adjusted P Value	Summary
LN-229				
<i>Apoptotic/Necrotic</i>				
Not Treated vs. PARPi veliparib	-4.2970	-14.95 to 6.353	0.6852	ns
Not Treated vs. PARPi olaparib	-2.7800	-13.43 to 7.870	0.8881	ns
Not Treated vs. PARGi	-5.0570	-15.71 to 5.593	0.5658	ns
PARPi veliparib vs. PARPi olaparib	1.5170	-9.133 to 12.17	0.9790	ns
PARPi veliparib vs. PARGi	-0.7600	-11.41 to 9.890	0.9972	ns
PARPi olaparib vs. PARGi	-2.2770	-12.93 to 8.373	0.9342	ns
<i>Apoptotic</i>				
Not Treated vs. PARPi veliparib	-1.2730	-11.92 to 9.377	0.9873	ns
Not Treated vs. PARPi olaparib	-2.7530	-13.40 to 7.897	0.8909	ns
Not Treated vs. PARGi	-2.2270	-12.88 to 8.423	0.9381	ns
PARPi veliparib vs. PARPi olaparib	-1.4800	-12.13 to 9.170	0.9804	ns
PARPi veliparib vs. PARGi	-0.9533	-11.60 to 9.697	0.9946	ns
PARPi olaparib vs. PARGi	0.5267	-10.12 to 11.18	0.9991	ns
<i>Leaving</i>				
Not Treated vs. PARPi veliparib	5.5700	-5.080 to 16.22	0.4862	ns
Not Treated vs. PARPi olaparib	5.5330	-5.117 to 16.18	0.4918	ns
Not Treated vs. PARGi	7.2870	-3.363 to 17.94	0.2598	ns
PARPi veliparib vs. PARPi olaparib	-0.0367	-10.69 to 10.61	>0.9999	ns
PARPi veliparib vs. PARGi	1.7170	-8.933 to 12.37	0.9700	ns
PARPi olaparib vs. PARGi	1.7530	-8.897 to 12.40	0.9682	ns
U-87MG				
<i>Apoptotic/Necrotic</i>				
Not Treated vs. PARPi veliparib	-5.7570	-13.11 to 1.593	0.1631	ns
Not Treated vs. PARPi olaparib	-6.0830	-13.43 to 1.266	0.1302	ns
Not Treated vs. PARGi	-5.9930	-13.34 to 1.356	0.1387	ns
PARPi veliparib vs. PARPi olaparib	-0.3267	-7.676 to 7.023	0.9993	ns
PARPi veliparib vs. PARGi	-0.2367	-7.586 to 7.113	0.9997	ns
PARPi olaparib vs. PARGi	0.0900	-7.260 to 7.440	>0.9999	ns
<i>Apoptotic</i>				
Not Treated vs. PARPi veliparib	-0.9867	-8.336 to 6.363	0.9822	ns
Not Treated vs. PARPi olaparib	-0.2933	-7.643 to 7.056	0.9995	ns
Not Treated vs. PARGi	-0.5233	-7.873 to 6.826	0.9972	ns
PARPi veliparib vs. PARPi olaparib	0.6933	-6.656 to 8.043	0.9937	ns
PARPi veliparib vs. PARGi	0.4633	-6.886 to 7.813	0.9981	ns
PARPi olaparib vs. PARGi	-0.2300	-7.580 to 7.120	0.9998	ns
<i>Leaving</i>				
Not Treated vs. PARPi veliparib	6.7470	-0.6031 to 14.10	0.0801	ns
Not Treated vs. PARPi olaparib	6.3770	-0.9731 to 13.73	0.1055	ns
Not Treated vs. PARGi	6.5130	-0.8364 to 13.86	0.0954	ns
PARPi veliparib vs. PARPi olaparib	-0.3700	-7.720 to 6.980	0.9990	ns
PARPi veliparib vs. PARGi	-0.2333	-7.583 to 7.116	0.9998	ns
PARPi olaparib vs. PARGi	0.1367	-7.213 to 7.486	>0.9999	ns
U-118MG				
<i>Apoptotic/Necrotic</i>				
Not Treated vs. PARPi veliparib	-5.6930	-13.12 to 1.730	0.1767	ns
Not Treated vs. PARPi olaparib	-0.4967	-7.920 to 6.926	0.9977	ns
Not Treated vs. PARGi	1.6600	-5.763 to 9.083	0.9257	ns
PARPi veliparib vs. PARPi olaparib	5.1970	-2.226 to 12.62	0.2420	ns
PARPi veliparib vs. PARGi	7.3530	-0.06964 to 14.78	0.0528	ns
PARPi olaparib vs. PARGi	2.1570	-5.266 to 9.580	0.8530	ns
<i>Apoptotic</i>				
Not Treated vs. PARPi veliparib	-3.0500	-10.47 to 4.373	0.6730	ns
Not Treated vs. PARPi olaparib	0.6133	-6.810 to 8.036	0.9957	ns

Not Treated vs. PARGi	0.7133	-6.710 to 8.136	0.9933	ns
PARPi veliparib vs. PARPi olaparib	3.6630	-3.760 to 11.09	0.5346	ns
PARPi veliparib vs. PARGi	3.7630	-3.660 to 11.19	0.5123	ns
PARPi olaparib vs. PARGi	0.1000	-7.323 to 7.523	>0.9999	ns
<i>Leaving</i>				
Not Treated vs. PARPi veliparib	8.7400	1.317 to 16.16	0.0168	*
Not Treated vs. PARPi olaparib	-0.1167	-7.540 to 7.306	>0.9999	ns
Not Treated vs. PARGi	-2.3730	-9.796 to 5.050	0.8141	ns
PARPi veliparib vs. PARPi olaparib	-8.8570	-16.28 to -1.434	0.0152	*
PARPi veliparib vs. PARGi	-11.1100	-18.54 to -3.690	0.0020	**
PARPi olaparib vs. PARGi	-2.2570	-9.680 to 5.166	0.8356	ns

Supplemental Table 5: 2-way ANOVA test of cell death analysis by flow cytometry.

ns: non significant, *: ≥ 0.0332 , **: ≥ 0.0021

<= 1 focus				
	Mean Diff	95.00% CI of diff	Adjusted P Value	Summary
LN-229; <= 1 focus:Not Treated vs. U-87MG; <= 1 focus:Not Treated	-32.3400	-61.32 to -3.373	0.0104	*
LN-229; <= 1 focus:Not Treated vs. U-118MG; <= 1 focus:Not Treated	-22.3000	-53.59 to 8.993	0.6576	ns
LN-229; <= 1 focus:Doxorubicin vs. U-87MG; <= 1 focus:Doxorubicin	-26.8500	-60.31 to 6.601	0.3761	ns
LN-229; <= 1 focus:Doxorubicin vs. U-118MG; <= 1 focus:Doxorubicin	-29.9100	-63.36 to 3.545	0.1666	ns
LN-229; <= 1 focus:PARPi veliparib vs. U-87MG; <= 1 focus:PARPi veliparib	-49.7000	-83.15 to -16.24	<0.0001	****
LN-229; <= 1 focus:PARPi veliparib vs. U-118MG; <= 1 focus:PARPi veliparib	-70.5800	-104.0 to -37.13	<0.0001	****
LN-229; <= 1 focus:PARPi olaparib vs. U-87MG; <= 1 focus:PARPi olaparib	-56.4600	-89.92 to -23.01	<0.0001	****
LN-229; <= 1 focus:PARPi olaparib vs. U-118MG; 2-5 foci:PARPi olaparib	0.7800	-32.67 to 34.23	>0.9999	ns
LN-229; <= 1 focus:PARGi vs. U-87MG; <= 1 focus:PARGi	-20.3100	-51.61 to 10.98	0.8344	ns
LN-229; <= 1 focus:PARGi vs. U-118MG; <= 1 focus:PARGi	-26.4500	-57.75 to 4.839	0.2645	ns
LN-229; <= 1 focus:Not Treated vs. LN-229; <= 1 focus:Doxorubicin	50.0500	18.75 to 81.34	<0.0001	****
LN-229; <= 1 focus:Not Treated vs. LN-229; <= 1 focus:PARPi veliparib	48.2100	16.92 to 79.50	<0.0001	****
LN-229; <= 1 focus:Not Treated vs. LN-229; <= 1 focus:PARPi olaparib	53.5100	22.22 to 84.80	<0.0001	****
LN-229; <= 1 focus:Not Treated vs. LN-229; <= 1 focus:PARGi	15.3000	-13.68 to 44.27	0.9869	ns
LN-229; <= 1 focus:Doxorubicin vs. LN-229; <= 1 focus:PARPi veliparib	-1.8370	-35.29 to 31.62	>0.9999	ns
LN-229; <= 1 focus:Doxorubicin vs. LN-229; <= 1 focus:PARPi olaparib	3.4630	-29.99 to 36.92	>0.9999	ns
LN-229; <= 1 focus:Doxorubicin vs. LN-229; <= 1 focus:PARGi	-34.7500	-66.04 to -3.458	0.0113	*
LN-229; <= 1 focus:PARPi veliparib vs. LN-229; <= 1 focus:PARPi olaparib	5.2990	-28.15 to 38.75	>0.9999	ns
LN-229; <= 1 focus:PARPi veliparib vs. LN-229; <= 1 focus:PARGi	-32.9100	-64.21 to -1.621	0.0256	*
LN-229; <= 1 focus:PARPi olaparib vs. LN-229; <= 1 focus:PARGi	-38.2100	-69.51 to -6.921	0.0021	**
U-87MG; <= 1 focus:Not Treated vs. U-118MG; <= 1 focus:Not Treated	10.0400	-21.25 to 41.34	>0.9999	ns
U-87MG; <= 1 focus:Doxorubicin vs. U-118MG; <= 1 focus:Doxorubicin	-3.0560	-36.51 to 30.40	>0.9999	ns
U-87MG; <= 1 focus:PARPi veliparib vs. U-118MG; <= 1 focus:PARPi veliparib	-20.8900	-54.34 to 12.57	0.8865	ns
U-87MG; <= 1 focus:PARPi olaparib vs. U-118MG; <= 1 focus:PARPi olaparib	-0.8527	-34.31 to 32.60	>0.9999	ns
U-87MG; <= 1 focus:PARGi vs. U-118MG; <= 1 focus:PARGi	-6.1400	-39.59 to 27.31	>0.9999	ns
U-87MG; <= 1 focus:Not Treated vs. U-87MG; <= 1 focus:Doxorubicin	55.5400	24.25 to 86.83	<0.0001	****
U-87MG; <= 1 focus:Not Treated vs. U-87MG; <= 1 focus:PARPi veliparib	30.8600	-0.4342 to 62.15	0.0593	ns
U-87MG; <= 1 focus:Not Treated vs. U-87MG; <= 1 focus:PARPi olaparib	29.3900	-1.901 to 60.69	0.1027	ns
U-87MG; <= 1 focus:Not Treated vs. U-87MG; <= 1 focus:PARGi	27.3300	-3.967 to 58.62	0.2045	ns
U-87MG; <= 1 focus:Doxorubicin vs. U-87MG; <= 1 focus:PARPi veliparib	-24.6800	-58.13 to 8.774	0.5775	ns
U-87MG; <= 1 focus:Doxorubicin vs. U-87MG; <= 1 focus:PARPi olaparib	-26.1500	-59.60 to 7.307	0.4387	ns
U-87MG; <= 1 focus:Doxorubicin vs. U-87MG; <= 1 focus:PARGi	-28.2100	-61.67 to 5.241	0.2693	ns
U-87MG; <= 1 focus:PARPi veliparib vs. U-87MG; <= 1 focus:PARPi olaparib	-1.4660	-34.92 to 31.99	>0.9999	ns
U-87MG; <= 1 focus:PARPi veliparib vs. U-87MG; <= 1 focus:PARGi	-3.5330	-36.99 to 29.92	>0.9999	ns
U-87MG; <= 1 focus:PARPi olaparib vs. U-87MG; <= 1 focus:PARGi	-2.0660	-35.52 to 31.39	>0.9999	ns
U-118MG; <= 1 focus:Not Treated vs. U-118MG; <= 1 focus:Doxorubicin	42.4400	8.985 to 75.89	0.0010	***
U-118MG; <= 1 focus:Not Treated vs. U-118MG; <= 1 focus:PARPi veliparib	-0.0737	-33.53 to 33.38	>0.9999	ns
U-118MG; <= 1 focus:Not Treated vs. U-118MG; <= 1 focus:PARPi olaparib	18.5000	-14.96 to 51.95	0.9741	ns
U-118MG; <= 1 focus:Not Treated vs. U-118MG; <= 1 focus:PARGi	11.1400	-22.31 to 44.60	>0.9999	ns
U-118MG; <= 1 focus:Doxorubicin vs. U-118MG; <= 1 focus:PARPi veliparib	-42.5100	-75.97 to -9.059	0.0010	***
U-118MG; <= 1 focus:Doxorubicin vs. U-118MG; <= 1 focus:PARPi olaparib	-23.9400	-57.40 to 9.510	0.6478	ns
U-118MG; <= 1 focus:Doxorubicin vs. U-118MG; <= 1 focus:PARGi	-31.3000	-64.75 to 2.157	0.1071	ns
U-118MG; <= 1 focus:PARPi veliparib vs. U-118MG; <= 1 focus:PARPi olaparib	18.5700	-14.88 to 52.02	0.9726	ns
U-118MG; <= 1 focus:PARPi veliparib vs. U-118MG; <= 1 focus:PARGi	11.2200	-22.24 to 44.67	>0.9999	ns
U-118MG; <= 1 focus:PARPi olaparib vs. U-118MG; <= 1 focus:PARGi	-7.3530	-40.81 to 26.10	>0.9999	ns

2-5 foci				
LN-229; 2-5 foci:Not Treated vs. U-87MG; 2-5 foci:Not Treated	8.5230	-20.45 to 37.50	>0.9999	ns
LN-229; 2-5 foci:Not Treated vs. U-118MG; 2-5 foci:Not Treated	9.4580	-21.83 to 40.75	>0.9999	ns
LN-229; 2-5 foci:Doxorubicin vs. U-87MG; 2-5 foci:Doxorubicin	-0.4077	-33.86 to 33.05	>0.9999	ns
LN-229; 2-5 foci:Doxorubicin vs. U-118MG; 2-5 foci:Doxorubicin	0.5880	-32.87 to 34.04	>0.9999	ns
LN-229; 2-5 foci:PARPi veliparib vs. U-87MG; 2-5 foci:PARPi veliparib	5.0180	-28.44 to 38.47	>0.9999	ns
LN-229; 2-5 foci:PARPi veliparib vs. U-118MG; 2-5 foci:PARPi veliparib	4.5140	-28.94 to 37.97	>0.9999	ns
LN-229; 2-5 foci:PARPi olaparib vs. U-87MG; 2-5 foci:PARPi olaparib	-2.0520	-35.51 to 31.40	>0.9999	ns
LN-229; 2-5 foci:PARPi olaparib vs. U-118MG; 2-5 foci:PARPi olaparib	-3.4180	-36.87 to 30.04	>0.9999	ns
LN-229; 2-5 foci:PARGi vs. U-87MG; 2-5 foci:PARGi	5.1720	-26.12 to 36.46	>0.9999	ns
LN-229; 2-5 foci:PARGi vs. U-118MG; 2-5 foci:PARGi	5.7610	-25.53 to 37.05	>0.9999	ns
LN-229; 2-5 foci:Not Treated vs. LN-229; 2-5 foci:Doxorubicin	4.2520	-27.04 to 35.55	>0.9999	ns
LN-229; 2-5 foci:Not Treated vs. LN-229; 2-5 foci:PARPi veliparib	3.1020	-28.19 to 34.40	>0.9999	ns
LN-229; 2-5 foci:Not Treated vs. LN-229; 2-5 foci:PARPi olaparib	7.9080	-23.38 to 39.20	>0.9999	ns

LN-229; 2-5 foci:Not Treated vs. LN-229; 2-5 foci:PARGi	2.0610	-26.91 to 31.03	>0.9999	ns
LN-229; 2-5 foci:Doxorubicin vs. LN-229; 2-5 foci:PARPi veliparib	-1.1500	-34.60 to 32.30	>0.9999	ns
LN-229; 2-5 foci:Doxorubicin vs. LN-229; 2-5 foci:PARPi olaparib	3.6560	-29.80 to 37.11	>0.9999	ns
LN-229; 2-5 foci:Doxorubicin vs. LN-229; 2-5 foci:PARGi	-2.1910	-33.48 to 29.10	>0.9999	ns
LN-229; 2-5 foci:PARPi veliparib vs. LN-229; 2-5 foci:PARPi olaparib	4.8060	-28.65 to 38.26	>0.9999	ns
LN-229; 2-5 foci:PARPi veliparib vs. LN-229; 2-5 foci:PARGi	-1.0410	-32.33 to 30.25	>0.9999	ns
LN-229; 2-5 foci:PARPi olaparib vs. LN-229; 2-5 foci:PARGi	-5.8470	-37.14 to 25.45	>0.9999	ns
U-87MG; 2-5 foci:Not Treated vs. U-118MG; 2-5 foci:Not Treated	0.9347	-30.36 to 32.23	>0.9999	ns
U-87MG; 2-5 foci:Doxorubicin vs. U-118MG; 2-5 foci:Doxorubicin	0.9957	-32.46 to 34.45	>0.9999	ns
U-87MG; 2-5 foci:PARPi veliparib vs. U-118MG; 2-5 foci:PARPi veliparib	-0.5037	-33.96 to 32.95	>0.9999	ns
U-87MG; 2-5 foci:PARPi olaparib vs. U-118MG; 2-5 foci:PARPi olaparib	-1.3660	-34.82 to 32.09	>0.9999	ns
U-87MG; 2-5 foci:PARGi vs. U-118MG; 2-5 foci:PARGi	0.5893	-32.86 to 34.04	>0.9999	ns
U-87MG; 2-5 foci:Not Treated vs. U-87MG; 2-5 foci:Doxorubicin	-4.6790	-35.97 to 26.61	>0.9999	ns
U-87MG; 2-5 foci:Not Treated vs. U-87MG; 2-5 foci:PARPi veliparib	-0.4033	-31.70 to 30.89	>0.9999	ns
U-87MG; 2-5 foci:Not Treated vs. U-87MG; 2-5 foci:PARPi olaparib	-2.6680	-33.96 to 28.63	>0.9999	ns
U-87MG; 2-5 foci:Not Treated vs. U-87MG; 2-5 foci:PARGi	-1.2900	-32.58 to 30.00	>0.9999	ns
U-87MG; 2-5 foci:Doxorubicin vs. U-87MG; 2-5 foci:PARPi veliparib	4.2760	-29.18 to 37.73	>0.9999	ns
U-87MG; 2-5 foci:Doxorubicin vs. U-87MG; 2-5 foci:PARPi olaparib	2.0110	-31.44 to 35.46	>0.9999	ns
U-87MG; 2-5 foci:Doxorubicin vs. U-87MG; 2-5 foci:PARGi	3.3890	-30.06 to 36.84	>0.9999	ns
U-87MG; 2-5 foci:PARPi veliparib vs. U-87MG; 2-5 foci:PARPi olaparib	-2.2640	-35.72 to 31.19	>0.9999	ns
U-87MG; 2-5 foci:PARPi veliparib vs. U-87MG; 2-5 foci:PARGi	-0.8870	-34.34 to 32.57	>0.9999	ns
U-87MG; 2-5 foci:PARPi olaparib vs. U-87MG; 2-5 foci:PARGi	1.3770	-32.08 to 34.83	>0.9999	ns
U-118MG; 2-5 foci:Not Treated vs. U-118MG; 2-5 foci:Doxorubicin	-4.6180	-38.07 to 28.84	>0.9999	ns
U-118MG; 2-5 foci:Not Treated vs. U-118MG; 2-5 foci:PARPi veliparib	-1.8420	-35.30 to 31.61	>0.9999	ns
U-118MG; 2-5 foci:Not Treated vs. U-118MG; 2-5 foci:PARPi olaparib	-4.9680	-38.42 to 28.49	>0.9999	ns
U-118MG; 2-5 foci:Not Treated vs. U-118MG; 2-5 foci:PARGi	-1.6360	-35.09 to 31.82	>0.9999	ns
U-118MG; 2-5 foci:Doxorubicin vs. U-118MG; 2-5 foci:PARPi veliparib	2.7760	-30.68 to 36.23	>0.9999	ns
U-118MG; 2-5 foci:Doxorubicin vs. U-118MG; 2-5 foci:PARPi olaparib	-0.3500	-33.80 to 33.10	>0.9999	ns
U-118MG; 2-5 foci:Doxorubicin vs. U-118MG; 2-5 foci:PARGi	2.9820	-30.47 to 36.44	>0.9999	ns
U-118MG; 2-5 foci:PARPi veliparib vs. U-118MG; 2-5 foci:PARPi olaparib	-3.1260	-36.58 to 30.33	>0.9999	ns
U-118MG; 2-5 foci:PARPi veliparib vs. U-118MG; 2-5 foci:PARGi	0.2060	-33.25 to 33.66	>0.9999	ns
U-118MG; 2-5 foci:PARPi olaparib vs. U-118MG; 2-5 foci:PARGi	3.3320	-30.12 to 36.79	>0.9999	ns
>6 foci				
LN-229; >6 foci:Not Treated vs. U-87MG; >6 foci:Not Treated	23.8200	-5.151 to 52.79	0.3223	ns
LN-229; >6 foci:Not Treated vs. U-118MG; >6 foci:Not Treated	12.8400	-18.45 to 44.14	0.9999	ns
LN-229; >6 foci:Doxorubicin vs. U-87MG; >6 foci:Doxorubicin	23.3700	-10.09 to 56.82	0.7012	ns
LN-229; >6 foci:Doxorubicin vs. U-118MG; >6 foci:Doxorubicin	25.4200	-8.029 to 58.88	0.5061	ns
LN-229; >6 foci:PARPi veliparib vs. U-87MG; >6 foci:PARPi veliparib	44.6800	11.23 to 78.13	0.0003	***
LN-229; >6 foci:PARPi veliparib vs. U-118MG; >6 foci:PARPi veliparib	66.0700	32.62 to 99.52	<0.0001	****
LN-229; >6 foci:PARPi olaparib vs. U-87MG; >6 foci:PARPi olaparib	58.5100	25.06 to 91.97	<0.0001	****
LN-229; >6 foci:PARPi olaparib vs. U-118MG; >6 foci:PARPi olaparib	60.7300	27.28 to 94.19	<0.0001	****
LN-229; >6 foci:PARGi vs. U-87MG; >6 foci:PARGi	15.1400	-16.15 to 46.44	0.9970	ns
LN-229; >6 foci:PARGi vs. U-118MG; >6 foci:PARGi	20.6900	-10.60 to 51.99	0.8050	ns
LN-229; >6 foci:Not Treated vs. LN-229; >6 foci:Doxorubicin	-50.4000	-81.70 to -19.11	<0.0001	****
LN-229; >6 foci:Not Treated vs. LN-229; >6 foci:PARPi veliparib	-51.3100	-82.61 to -20.02	<0.0001	****
LN-229; >6 foci:Not Treated vs. LN-229; >6 foci:PARPi olaparib	-61.4200	-92.71 to -30.13	<0.0001	****
LN-229; >6 foci:Not Treated vs. LN-229; >6 foci:PARGi	-17.3600	-46.33 to 11.61	0.9276	ns
LN-229; >6 foci:Doxorubicin vs. LN-229; >6 foci:PARPi veliparib	-0.9100	-34.36 to 32.54	>0.9999	ns
LN-229; >6 foci:Doxorubicin vs. LN-229; >6 foci:PARPi olaparib	-11.0100	-44.47 to 22.44	>0.9999	ns
LN-229; >6 foci:Doxorubicin vs. LN-229; >6 foci:PARGi	33.0500	1.753 to 64.34	0.0242	*
LN-229; >6 foci:PARPi veliparib vs. LN-229; >6 foci:PARPi olaparib	-10.1000	-43.56 to 23.35	>0.9999	ns
LN-229; >6 foci:PARPi veliparib vs. LN-229; >6 foci:PARGi	33.9600	2.663 to 65.25	0.0162	*
LN-229; >6 foci:PARPi olaparib vs. LN-229; >6 foci:PARGi	44.0600	12.77 to 75.35	<0.0001	****
U-87MG; >6 foci:Not Treated vs. U-118MG; >6 foci:Not Treated	-10.9800	-42.27 to 20.31	>0.9999	ns
U-87MG; >6 foci:Doxorubicin vs. U-118MG; >6 foci:Doxorubicin	2.0590	-31.39 to 35.51	>0.9999	ns
U-87MG; >6 foci:PARPi veliparib vs. U-118MG; >6 foci:PARPi veliparib	21.3900	-12.06 to 54.85	0.8562	ns
U-87MG; >6 foci:PARPi olaparib vs. U-118MG; >6 foci:PARPi olaparib	2.2190	-31.23 to 35.67	>0.9999	ns
U-87MG; >6 foci:PARGi vs. U-118MG; >6 foci:PARGi	5.5510	-27.90 to 39.00	>0.9999	ns
U-87MG; >6 foci:Not Treated vs. U-87MG; >6 foci:Doxorubicin	-50.8600	-82.15 to -19.57	<0.0001	****
U-87MG; >6 foci:Not Treated vs. U-87MG; >6 foci:PARPi veliparib	-30.4600	-61.75 to 0.8373	0.0693	ns
U-87MG; >6 foci:Not Treated vs. U-87MG; >6 foci:PARPi olaparib	-26.7300	-58.02 to 4.568	0.2448	ns
U-87MG; >6 foci:Not Treated vs. U-87MG; >6 foci:PARGi	-26.0400	-57.33 to 5.257	0.2970	ns

U-87MG; >6 foci:Doxorubicin vs. U-87MG; >6 foci:PARPi veliparib	20.4000	-13.05 to 53.86	0.9115	ns
U-87MG; >6 foci:Doxorubicin vs. U-87MG; >6 foci:PARPi olaparib	24.1300	-9.320 to 57.59	0.6298	ns
U-87MG; >6 foci:Doxorubicin vs. U-87MG; >6 foci:PARGi	24.8200	-8.631 to 58.28	0.5638	ns
U-87MG; >6 foci:PARPi veliparib vs. U-87MG; >6 foci:PARPi olaparib	3.7300	-29.72 to 37.18	>0.9999	ns
U-87MG; >6 foci:PARPi veliparib vs. U-87MG; >6 foci:PARGi	4.4190	-29.03 to 37.87	>0.9999	ns
U-87MG; >6 foci:PARPi olaparib vs. U-87MG; >6 foci:PARGi	0.6890	-32.76 to 34.14	>0.9999	ns
U-118MG; >6 foci:Not Treated vs. U-118MG; >6 foci:Doxorubicin	-37.8200	-71.27 to -4.368	0.0085	**
U-118MG; >6 foci:Not Treated vs. U-118MG; >6 foci:PARPi veliparib	1.9150	-31.54 to 35.37	>0.9999	ns
U-118MG; >6 foci:Not Treated vs. U-118MG; >6 foci:PARPi olaparib	-13.5300	-46.98 to 19.93	>0.9999	ns
U-118MG; >6 foci:Not Treated vs. U-118MG; >6 foci:PARGi	-9.5070	-42.96 to 23.95	>0.9999	ns
U-118MG; >6 foci:Doxorubicin vs. U-118MG; >6 foci:PARPi veliparib	39.7400	6.283 to 73.19	0.0036	**
U-118MG; >6 foci:Doxorubicin vs. U-118MG; >6 foci:PARPi olaparib	24.2900	-9.160 to 57.75	0.6146	ns
U-118MG; >6 foci:Doxorubicin vs. U-118MG; >6 foci:PARGi	28.3100	-5.139 to 61.77	0.2622	ns
U-118MG; >6 foci:PARPi veliparib vs. U-118MG; >6 foci:PARPi olaparib	-15.4400	-48.90 to 18.01	0.9988	ns
U-118MG; >6 foci:PARPi veliparib vs. U-118MG; >6 foci:PARGi	-11.4200	-44.88 to 22.03	>0.9999	ns
U-118MG; >6 foci:PARPi olaparib vs. U-118MG; >6 foci:PARGi	4.0200	-29.43 to 37.47	>0.9999	ns

Supplemental Table 6: 2-way ANOVA test of γ H2AX foci.

ns: non significant, *: ≥ 0.0332 , **: ≥ 0.0021 , ***: ≥ 0.0002 ****: < 0.0001

<= 1 focus

	Mean Diff.	95.00% CI of diff.	Adjusted P Value	Summary
LN-229; <= 1 focus:Not Treated vs. U-87MG; <= 1 focus:Not Treated	-12.8100	-47.88 to 22.26	>0.9999	ns
LN-229; <= 1 focus:Not Treated vs. U-118MG; <= 1 focus:Not Treated	-22.0400	-57.11 to 13.03	0.8734	ns
LN-229; <= 1 focus:Doxorubicin vs. U-87MG; <= 1 focus:Doxorubicin	2.2330	-32.84 to 37.30	>0.9999	ns
LN-229; <= 1 focus:Doxorubicin vs. U-118MG; <= 1 focus:Doxorubicin	-29.1800	-64.25 to 5.889	0.2930	ns
LN-229; <= 1 focus:PARPi veliparib vs. U-87MG; <= 1 focus:PARPi veliparib	-32.7700	-67.84 to 2.299	0.1076	ns
LN-229; <= 1 focus:PARPi veliparib vs. U-118MG; <= 1 focus:PARPi veliparib	-53.2500	-88.32 to -18.18	<0.0001	****
LN-229; <= 1 focus:PARPi olaparib vs. U-87MG; <= 1 focus:PARPi olaparib	-44.5800	-79.65 to -9.514	0.0010	**
LN-229; <= 1 focus:PARPi olaparib vs. U-118MG; <= 1 focus:PARPi olaparib	-61.4900	-96.56 to -26.42	<0.0001	****
LN-229; <= 1 focus:PARGi vs. U-87MG; <= 1 focus:PARGi	-26.8700	-61.94 to 8.202	0.4804	ns
LN-229; <= 1 focus:PARGi vs. U-118MG; <= 1 focus:PARGi	-24.9500	-60.02 to 10.12	0.6535	ns
LN-229; <= 1 focus:Not Treated vs. LN-229; <= 1 focus:Doxorubicin	55.9500	20.88 to 91.02	<0.0001	****
LN-229; <= 1 focus:Not Treated vs. LN-229; <= 1 focus:PARPi veliparib	42.6800	7.611 to 77.75	0.0024	**
LN-229; <= 1 focus:Not Treated vs. LN-229; <= 1 focus:PARPi olaparib	57.7500	22.68 to 92.82	<0.0001	****
LN-229; <= 1 focus:Not Treated vs. LN-229; <= 1 focus:PARGi	6.8970	-28.17 to 41.97	>0.9999	ns
LN-229; <= 1 focus:Doxorubicin vs. LN-229; <= 1 focus:PARPi veliparib	-13.2700	-48.34 to 21.80	>0.9999	ns
LN-229; <= 1 focus:Doxorubicin vs. LN-229; <= 1 focus:PARPi olaparib	1.8030	-33.27 to 36.87	>0.9999	ns
LN-229; <= 1 focus:Doxorubicin vs. LN-229; <= 1 focus:PARGi	-49.0500	-84.12 to -13.98	0.0001	***
LN-229; <= 1 focus:PARPi veliparib vs. LN-229; <= 1 focus:PARPi olaparib	15.0700	-20.00 to 50.14	0.9997	ns
LN-229; <= 1 focus:PARPi veliparib vs. LN-229; <= 1 focus:PARGi	-35.7800	-70.85 to -0.7144	0.0387	*
LN-229; <= 1 focus:PARPi olaparib vs. LN-229; <= 1 focus:PARGi	-50.8500	-85.92 to -15.78	<0.0001	****
U-87MG; <= 1 focus:Not Treated vs. U-118MG; <= 1 focus:Not Treated	-9.2270	-44.30 to 25.84	>0.9999	ns
U-87MG; <= 1 focus:Doxorubicin vs. U-118MG; <= 1 focus:Doxorubicin	-31.4100	-66.48 to 3.656	0.1620	ns
U-87MG; <= 1 focus:PARPi veliparib vs. U-118MG; <= 1 focus:PARPi veliparib	-20.4800	-55.55 to 14.59	0.9433	ns
U-87MG; <= 1 focus:PARPi olaparib vs. U-118MG; <= 1 focus:PARPi olaparib	-16.9100	-51.98 to 18.16	0.9968	ns
U-87MG; <= 1 focus:PARGi vs. U-118MG; <= 1 focus:PARGi	1.9130	-33.16 to 36.98	>0.9999	ns
U-87MG; <= 1 focus:Not Treated vs. U-87MG; <= 1 focus:Doxorubicin	70.9900	35.92 to 106.1	<0.0001	****
U-87MG; <= 1 focus:Not Treated vs. U-87MG; <= 1 focus:PARPi veliparib	22.7200	-12.35 to 57.79	0.8312	ns
U-87MG; <= 1 focus:Not Treated vs. U-87MG; <= 1 focus:PARPi olaparib	25.9800	-9.092 to 61.05	0.5608	ns
U-87MG; <= 1 focus:Not Treated vs. U-87MG; <= 1 focus:PARGi	-7.1600	-42.23 to 27.91	>0.9999	ns
U-87MG; <= 1 focus:Doxorubicin vs. U-87MG; <= 1 focus:PARPi veliparib	-48.2700	-83.34 to -13.20	0.0002	***
U-87MG; <= 1 focus:Doxorubicin vs. U-87MG; <= 1 focus:PARPi olaparib	-45.0100	-80.08 to -9.944	0.0008	***
U-87MG; <= 1 focus:Doxorubicin vs. U-87MG; <= 1 focus:PARGi	-78.1500	-113.2 to -43.08	<0.0001	****
U-87MG; <= 1 focus:PARPi veliparib vs. U-87MG; <= 1 focus:PARPi olaparib	3.2570	-31.81 to 38.33	>0.9999	ns
U-87MG; <= 1 focus:PARPi veliparib vs. U-87MG; <= 1 focus:PARGi	-29.8800	-64.95 to 5.189	0.2461	ns
U-87MG; <= 1 focus:PARPi olaparib vs. U-87MG; <= 1 focus:PARGi	-33.1400	-68.21 to 1.932	0.0958	ns
U-118MG; <= 1 focus:Not Treated vs. U-118MG; <= 1 focus:Doxorubicin	48.8000	13.73 to 83.87	0.0001	***
U-118MG; <= 1 focus:Not Treated vs. U-118MG; <= 1 focus:PARPi veliparib	11.4700	-23.60 to 46.54	>0.9999	ns
U-118MG; <= 1 focus:Not Treated vs. U-118MG; <= 1 focus:PARPi olaparib	18.3000	-16.77 to 53.37	0.9880	ns
U-118MG; <= 1 focus:Not Treated vs. U-118MG; <= 1 focus:PARGi	3.9800	-31.09 to 39.05	>0.9999	ns
U-118MG; <= 1 focus:Doxorubicin vs. U-118MG; <= 1 focus:PARPi veliparib	-37.3400	-72.41 to -2.268	0.0217	*
U-118MG; <= 1 focus:Doxorubicin vs. U-118MG; <= 1 focus:PARPi olaparib	-30.5100	-65.58 to 4.562	0.2087	ns
U-118MG; <= 1 focus:Doxorubicin vs. U-118MG; <= 1 focus:PARGi	-44.8200	-79.89 to -9.754	0.0009	***
U-118MG; <= 1 focus:PARPi veliparib vs. U-118MG; <= 1 focus:PARPi olaparib	6.8300	-28.24 to 41.90	>0.9999	ns
U-118MG; <= 1 focus:PARPi veliparib vs. U-118MG; <= 1 focus:PARGi	-7.4870	-42.56 to 27.58	>0.9999	ns
U-118MG; <= 1 focus:PARPi olaparib vs. U-118MG; <= 1 focus:PARGi	-14.3200	-49.39 to 20.75	0.9999	ns
2-5 foci				
LN-229; 2-5 foci:Not Treated vs. U-87MG; 2-5 foci:Not Treated	5.4500	-29.62 to 40.52	>0.9999	ns
LN-229; 2-5 foci:Not Treated vs. U-118MG; 2-5 foci:Not Treated	8.8730	-26.20 to 43.94	>0.9999	ns
LN-229; 2-5 foci:Doxorubicin vs. U-87MG; 2-5 foci:Doxorubicin	0.7467	-34.32 to 35.82	>0.9999	ns
LN-229; 2-5 foci:Doxorubicin vs. U-118MG; 2-5 foci:Doxorubicin	-18.0300	-53.10 to 17.04	0.9905	ns
LN-229; 2-5 foci:PARPi veliparib vs. U-87MG; 2-5 foci:PARPi veliparib	-0.3067	-35.38 to 34.76	>0.9999	ns
LN-229; 2-5 foci:PARPi veliparib vs. U-118MG; 2-5 foci:PARPi veliparib	2.9800	-32.09 to 38.05	>0.9999	ns
LN-229; 2-5 foci:PARPi olaparib vs. U-87MG; 2-5 foci:PARPi olaparib	-6.6370	-41.71 to 28.43	>0.9999	ns
LN-229; 2-5 foci:PARPi olaparib vs. U-118MG; 2-5 foci:PARPi olaparib	-10.1400	-45.21 to 24.93	>0.9999	ns
LN-229; 2-5 foci:PARGi vs. U-87MG; 2-5 foci:PARGi	13.9300	-21.14 to 49.00	>0.9999	ns
LN-229; 2-5 foci:PARGi vs. U-118MG; 2-5 foci:PARGi	7.6400	-27.43 to 42.71	>0.9999	ns
LN-229; 2-5 foci:Not Treated vs. LN-229; 2-5 foci:Doxorubicin	5.0530	-30.02 to 40.12	>0.9999	ns
LN-229; 2-5 foci:Not Treated vs. LN-229; 2-5 foci:PARPi veliparib	-2.3770	-37.45 to 32.69	>0.9999	ns

LN-229; 2-5 foci:Not Treated vs. LN-229; 2-5 foci:PARPi olaparib	11.7300	-23.34 to 46.80	>0.9999	ns
LN-229; 2-5 foci:Not Treated vs. LN-229; 2-5 foci:PARGi	-5.4900	-40.56 to 29.58	>0.9999	ns
LN-229; 2-5 foci:Doxorubicin vs. LN-229; 2-5 foci:PARPi veliparib	-7.4300	-42.50 to 27.64	>0.9999	ns
LN-229; 2-5 foci:Doxorubicin vs. LN-229; 2-5 foci:PARPi olaparib	6.6770	-28.39 to 41.75	>0.9999	ns
LN-229; 2-5 foci:Doxorubicin vs. LN-229; 2-5 foci:PARGi	-10.5400	-45.61 to 24.53	>0.9999	ns
LN-229; 2-5 foci:PARPi veliparib vs. LN-229; 2-5 foci:PARPi olaparib	14.1100	-20.96 to 49.18	>0.9999	ns
LN-229; 2-5 foci:PARPi veliparib vs. LN-229; 2-5 foci:PARGi	-3.1130	-38.18 to 31.96	>0.9999	ns
LN-229; 2-5 foci:PARPi olaparib vs. LN-229; 2-5 foci:PARGi	-17.2200	-52.29 to 17.85	0.9956	ns
U-87MG; 2-5 foci:Not Treated vs. U-118MG; 2-5 foci:Not Treated	3.4230	-31.65 to 38.49	>0.9999	ns
U-87MG; 2-5 foci:Doxorubicin vs. U-118MG; 2-5 foci:Doxorubicin	-18.7800	-53.85 to 16.29	0.9822	ns
U-87MG; 2-5 foci:PARPi veliparib vs. U-118MG; 2-5 foci:PARPi veliparib	3.2870	-31.78 to 38.36	>0.9999	ns
U-87MG; 2-5 foci:PARPi olaparib vs. U-118MG; 2-5 foci:PARPi olaparib	-3.5070	-38.58 to 31.56	>0.9999	ns
U-87MG; 2-5 foci:PARGi vs. U-118MG; 2-5 foci:PARGi	-6.2870	-41.36 to 28.78	>0.9999	ns
U-87MG; 2-5 foci:Not Treated vs. U-87MG; 2-5 foci:Doxorubicin	0.3500	-34.72 to 35.42	>0.9999	ns
U-87MG; 2-5 foci:Not Treated vs. U-87MG; 2-5 foci:PARPi veliparib	-8.1330	-43.20 to 26.94	>0.9999	ns
U-87MG; 2-5 foci:Not Treated vs. U-87MG; 2-5 foci:PARPi olaparib	-0.3567	-35.43 to 34.71	>0.9999	ns
U-87MG; 2-5 foci:Not Treated vs. U-87MG; 2-5 foci:PARGi	2.9870	-32.08 to 38.06	>0.9999	ns
U-87MG; 2-5 foci:Doxorubicin vs. U-87MG; 2-5 foci:PARPi veliparib	-8.4830	-43.55 to 26.59	>0.9999	ns
U-87MG; 2-5 foci:Doxorubicin vs. U-87MG; 2-5 foci:PARPi olaparib	-0.7067	-35.78 to 34.36	>0.9999	ns
U-87MG; 2-5 foci:Doxorubicin vs. U-87MG; 2-5 foci:PARGi	2.6370	-32.43 to 37.71	>0.9999	ns
U-87MG; 2-5 foci:PARPi veliparib vs. U-87MG; 2-5 foci:PARPi olaparib	7.7770	-27.29 to 42.85	>0.9999	ns
U-87MG; 2-5 foci:PARPi veliparib vs. U-87MG; 2-5 foci:PARGi	11.1200	-23.95 to 46.19	>0.9999	ns
U-87MG; 2-5 foci:PARPi olaparib vs. U-87MG; 2-5 foci:PARGi	3.3430	-31.73 to 38.41	>0.9999	ns
U-118MG; 2-5 foci:Not Treated vs. U-118MG; 2-5 foci:Doxorubicin	-21.8500	-56.92 to 13.22	0.8835	ns
U-118MG; 2-5 foci:Not Treated vs. U-118MG; 2-5 foci:PARPi veliparib	-8.2700	-43.34 to 26.80	>0.9999	ns
U-118MG; 2-5 foci:Not Treated vs. U-118MG; 2-5 foci:PARPi olaparib	-7.2870	-42.36 to 27.78	>0.9999	ns
U-118MG; 2-5 foci:Not Treated vs. U-118MG; 2-5 foci:PARGi	-6.7230	-41.79 to 28.35	>0.9999	ns
U-118MG; 2-5 foci:Doxorubicin vs. U-118MG; 2-5 foci:PARPi veliparib	13.5800	-21.49 to 48.65	>0.9999	ns
U-118MG; 2-5 foci:Doxorubicin vs. U-118MG; 2-5 foci:PARPi olaparib	14.5700	-20.50 to 49.64	0.9998	ns
U-118MG; 2-5 foci:Doxorubicin vs. U-118MG; 2-5 foci:PARGi	15.1300	-19.94 to 50.20	0.9996	ns
U-118MG; 2-5 foci:PARPi veliparib vs. U-118MG; 2-5 foci:PARPi olaparib	0.9833	-34.09 to 36.05	>0.9999	ns
U-118MG; 2-5 foci:PARPi veliparib vs. U-118MG; 2-5 foci:PARGi	1.5470	-33.52 to 36.62	>0.9999	ns
U-118MG; 2-5 foci:PARPi olaparib vs. U-118MG; 2-5 foci:PARGi	0.5633	-34.51 to 35.63	>0.9999	ns
>6 foci				
LN-229; >6 foci:Not Treated vs. U-87MG; >6 foci:Not Treated	7.3670	-27.70 to 42.44	>0.9999	ns
LN-229; >6 foci:Not Treated vs. U-118MG; >6 foci:Not Treated	13.1700	-21.90 to 48.24	>0.9999	ns
LN-229; >6 foci:Doxorubicin vs. U-87MG; >6 foci:Doxorubicin	-2.9870	-38.06 to 32.08	>0.9999	ns
LN-229; >6 foci:Doxorubicin vs. U-118MG; >6 foci:Doxorubicin	47.2100	12.14 to 82.28	0.0003	***
LN-229; >6 foci:PARPi veliparib vs. U-87MG; >6 foci:PARPi veliparib	33.0800	-1.992 to 68.15	0.0977	ns
LN-229; >6 foci:PARPi veliparib vs. U-118MG; >6 foci:PARPi veliparib	50.2700	15.20 to 85.34	<0.0001	****
LN-229; >6 foci:PARPi olaparib vs. U-87MG; >6 foci:PARPi olaparib	51.2200	16.15 to 86.29	<0.0001	****
LN-229; >6 foci:PARPi olaparib vs. U-118MG; >6 foci:PARPi olaparib	71.6300	36.56 to 106.7	<0.0001	****
LN-229; >6 foci:PARGi vs. U-87MG; >6 foci:PARGi	12.9400	-22.13 to 48.01	>0.9999	ns
LN-229; >6 foci:PARGi vs. U-118MG; >6 foci:PARGi	17.3100	-17.76 to 52.38	0.9952	ns
LN-229; >6 foci:Not Treated vs. LN-229; >6 foci:Doxorubicin	-60.9900	-96.06 to -25.92	<0.0001	****
LN-229; >6 foci:Not Treated vs. LN-229; >6 foci:PARPi veliparib	-40.3000	-75.37 to -5.228	0.0066	**
LN-229; >6 foci:Not Treated vs. LN-229; >6 foci:PARPi olaparib	-69.4700	-104.5 to -34.40	<0.0001	****
LN-229; >6 foci:Not Treated vs. LN-229; >6 foci:PARGi	-1.4000	-36.47 to 33.67	>0.9999	ns
LN-229; >6 foci:Doxorubicin vs. LN-229; >6 foci:PARPi veliparib	20.6900	-14.38 to 55.76	0.9358	ns
LN-229; >6 foci:Doxorubicin vs. LN-229; >6 foci:PARPi olaparib	-8.4800	-43.55 to 26.59	>0.9999	ns
LN-229; >6 foci:Doxorubicin vs. LN-229; >6 foci:PARGi	59.5900	24.52 to 94.66	<0.0001	****
LN-229; >6 foci:PARPi veliparib vs. LN-229; >6 foci:PARPi olaparib	-29.1700	-64.24 to 5.896	0.2935	ns
LN-229; >6 foci:PARPi veliparib vs. LN-229; >6 foci:PARGi	38.9000	3.828 to 73.97	0.0117	*
LN-229; >6 foci:PARPi olaparib vs. LN-229; >6 foci:PARGi	68.0700	33.00 to 103.1	<0.0001	****
U-87MG; >6 foci:Not Treated vs. U-118MG; >6 foci:Not Treated	5.8000	-29.27 to 40.87	>0.9999	ns
U-87MG; >6 foci:Doxorubicin vs. U-118MG; >6 foci:Doxorubicin	50.1900	15.12 to 85.26	<0.0001	****
U-87MG; >6 foci:PARPi veliparib vs. U-118MG; >6 foci:PARPi veliparib	17.1900	-17.88 to 52.26	0.9957	ns
U-87MG; >6 foci:PARPi olaparib vs. U-118MG; >6 foci:PARPi olaparib	20.4100	-14.66 to 55.48	0.9456	ns
U-87MG; >6 foci:PARGi vs. U-118MG; >6 foci:PARGi	4.3700	-30.70 to 39.44	>0.9999	ns
U-87MG; >6 foci:Not Treated vs. U-87MG; >6 foci:Doxorubicin	-71.3400	-106.4 to -36.27	<0.0001	****
U-87MG; >6 foci:Not Treated vs. U-87MG; >6 foci:PARPi veliparib	-14.5900	-49.66 to 20.48	0.9998	ns
U-87MG; >6 foci:Not Treated vs. U-87MG; >6 foci:PARPi olaparib	-25.6200	-60.69 to 9.449	0.5934	ns

U-87MG; >6 foci:Not Treated vs. U-87MG; >6 foci:PARGi	4.1730	-30.90 to 39.24	>0.9999	ns
U-87MG; >6 foci:Doxorubicin vs. U-87MG; >6 foci:PARPi veliparib	56.7600	21.69 to 91.83	<0.0001	****
U-87MG; >6 foci:Doxorubicin vs. U-87MG; >6 foci:PARPi olaparib	45.7200	10.65 to 80.79	0.0006	***
U-87MG; >6 foci:Doxorubicin vs. U-87MG; >6 foci:PARGi	75.5200	40.45 to 110.6	<0.0001	****
U-87MG; >6 foci:PARPi veliparib vs. U-87MG; >6 foci:PARPi olaparib	-11.0300	-46.10 to 24.04	>0.9999	ns
U-87MG; >6 foci:PARPi veliparib vs. U-87MG; >6 foci:PARGi	18.7600	-16.31 to 53.83	0.9825	ns
U-87MG; >6 foci:PARPi olaparib vs. U-87MG; >6 foci:PARGi	29.7900	-5.276 to 64.86	0.2516	ns
U-118MG; >6 foci:Not Treated vs. U-118MG; >6 foci:Doxorubicin	-26.9500	-62.02 to 8.119	0.4730	ns
U-118MG; >6 foci:Not Treated vs. U-118MG; >6 foci:PARPi veliparib	-3.1930	-38.26 to 31.88	>0.9999	ns
U-118MG; >6 foci:Not Treated vs. U-118MG; >6 foci:PARPi olaparib	-11.0100	-46.08 to 24.06	>0.9999	ns
U-118MG; >6 foci:Not Treated vs. U-118MG; >6 foci:PARGi	2.7430	-32.33 to 37.81	>0.9999	ns
U-118MG; >6 foci:Doxorubicin vs. U-118MG; >6 foci:PARPi veliparib	23.7600	-11.31 to 58.83	0.7550	ns
U-118MG; >6 foci:Doxorubicin vs. U-118MG; >6 foci:PARPi olaparib	15.9400	-19.13 to 51.01	0.9990	ns
U-118MG; >6 foci:Doxorubicin vs. U-118MG; >6 foci:PARGi	29.6900	-5.376 to 64.76	0.2581	ns
U-118MG; >6 foci:PARPi veliparib vs. U-118MG; >6 foci:PARPi olaparib	-7.8170	-42.89 to 27.25	>0.9999	ns
U-118MG; >6 foci:PARPi veliparib vs. U-118MG; >6 foci:PARGi	5.9370	-29.13 to 41.01	>0.9999	ns
U-118MG; >6 foci:PARPi olaparib vs. U-118MG; >6 foci:PARGi	13.7500	-21.32 to 48.82	>0.9999	ns

Supplemental Table 7: 2-way ANOVA test of 53BP1 foci.

ns: non significant, *: ≥ 0.0332 , **: ≥ 0.0021 , ***: ≥ 0.0002 ****: < 0.0001

Tukey's multiple comparisons test	Mean Diff.	95.00% CI of diff.	Adjusted P Value	Summary
Not Treated:LN-229 vs. Not Treated:U-87MG	0.0000	-0.6012 to 0.6012	>0.9999	ns
Not Treated:LN-229 vs. Not Treated:U-118MG	0.0000	-0.6012 to 0.6012	>0.9999	ns
Not Treated:U-87MG vs. Not Treated:U-118MG	0.0000	-0.6012 to 0.6012	>0.9999	ns
Not Treated:LN-229 vs. Doxorubicin:LN-229	-1.0610	-1.662 to -0.4597	<0.0001	****
Not Treated:LN-229 vs. PARPi veliparib:LN-229	0.0070	-0.5941 to 0.6082	>0.9999	ns
Not Treated:LN-229 vs. PARPi olaparib:LN-229	-0.0781	-0.6793 to 0.5231	>0.9999	ns
Not Treated:LN-229 vs. PARGi:LN-229	-0.1261	-0.7272 to 0.4751	>0.9999	ns
Not Treated:U-87MG vs. Doxorubicin:U-87MG	-1.0830	-1.684 to -0.4816	<0.0001	****
Not Treated:U-87MG vs. PARPi veliparib:U-87MG	-0.0351	-0.6363 to 0.5661	>0.9999	ns
Not Treated:U-87MG vs. PARPi olaparib:U-87MG	-0.0182	-0.6194 to 0.5829	>0.9999	ns
Not Treated:U-87MG vs. PARGi:U-87MG	-0.0331	-0.6343 to 0.5680	>0.9999	ns
Not Treated:U-118MG vs. Doxorubicin:U-118MG	-0.6040	-1.205 to -0.002851	0.0480	*
Not Treated:U-118MG vs. PARPi veliparib:U-118MG	0.0995	-0.5017 to 0.7006	>0.9999	ns
Not Treated:U-118MG vs. PARPi olaparib:U-118MG	0.0504	-0.5507 to 0.6516	>0.9999	ns
Not Treated:U-118MG vs. PARGi:U-118MG	0.0925	-0.5797 to 0.7646	>0.9999	ns
Doxorubicin:LN-229 vs. Doxorubicin:U-87MG	-0.0219	-0.6231 to 0.5793	>0.9999	ns
Doxorubicin:LN-229 vs. Doxorubicin:U-118MG	0.4568	-0.1443 to 1.058	0.2964	ns
Doxorubicin:U-87MG vs. Doxorubicin:U-118MG	0.4787	-0.1224 to 1.080	0.2352	ns
Doxorubicin:LN-229 vs. PARPi veliparib:LN-229	1.0680	0.4667 to 1.669	<0.0001	****
Doxorubicin:LN-229 vs. PARPi olaparib:LN-229	0.9828	0.3816 to 1.584	0.0001	***
Doxorubicin:LN-229 vs. PARGi:LN-229	0.9348	0.3336 to 1.536	0.0003	***
Doxorubicin:U-87MG vs. PARPi veliparib:U-87MG	1.0480	0.4465 to 1.649	<0.0001	****
Doxorubicin:U-87MG vs. PARPi olaparib:U-87MG	1.0650	0.4634 to 1.666	<0.0001	****
Doxorubicin:U-87MG vs. PARGi:U-87MG	1.0500	0.4485 to 1.651	<0.0001	****
Doxorubicin:U-118MG vs. PARPi veliparib:U-118MG	0.7035	0.1023 to 1.305	0.0110	*
Doxorubicin:U-118MG vs. PARPi olaparib:U-118MG	0.6545	0.05328 to 1.256	0.0231	*
Doxorubicin:U-118MG vs. PARGi:U-118MG	0.6965	0.02434 to 1.369	0.0367	*
PARPi veliparib:LN-229 vs. PARPi veliparib:U-87MG	-0.0421	-0.6433 to 0.5590	>0.9999	ns
PARPi veliparib:LN-229 vs. PARPi veliparib:U-118MG	0.0924	-0.5087 to 0.6936	>0.9999	ns
PARPi veliparib:U-87MG vs. PARPi veliparib:U-118MG	0.1346	-0.4666 to 0.7357	>0.9999	ns
PARPi veliparib:LN-229 vs. PARPi olaparib:LN-229	-0.0851	-0.6863 to 0.5160	>0.9999	ns
PARPi veliparib:LN-229 vs. PARGi:LN-229	-0.1331	-0.7343 to 0.4681	>0.9999	ns
PARPi veliparib:U-87MG vs. PARPi olaparib:U-87MG	0.0169	-0.5843 to 0.6180	>0.9999	ns
PARPi veliparib:U-87MG vs. PARGi:U-87MG	0.0020	-0.5992 to 0.6031	>0.9999	ns
PARPi veliparib:U-118MG vs. PARPi olaparib:U-118MG	-0.0490	-0.6502 to 0.5521	>0.9999	ns
PARPi veliparib:U-118MG vs. PARGi:U-118MG	-0.0070	-0.6792 to 0.6651	>0.9999	ns
PARPi olaparib:LN-229 vs. PARPi olaparib:U-87MG	0.0599	-0.5413 to 0.6610	>0.9999	ns
PARPi olaparib:LN-229 vs. PARPi olaparib:U-118MG	0.1285	-0.4726 to 0.7297	>0.9999	ns
PARPi olaparib:U-87MG vs. PARPi olaparib:U-118MG	0.0687	-0.5325 to 0.6698	>0.9999	ns
PARPi olaparib:LN-229 vs. PARGi:LN-229	-0.0480	-0.6491 to 0.5532	>0.9999	ns
PARPi olaparib:U-87MG vs. PARGi:U-87MG	-0.0149	-0.6161 to 0.5863	>0.9999	ns
PARPi olaparib:U-118MG vs. PARGi:U-118MG	0.0420	-0.6301 to 0.7142	>0.9999	ns
PARGi:LN-229 vs. PARGi:U-87MG	0.0929	-0.5082 to 0.6941	>0.9999	ns
PARGi:LN-229 vs. PARGi:U-118MG	0.2185	-0.4536 to 0.8907	0.9951	ns
PARGi:U-87MG vs. PARGi:U-118MG	0.1256	-0.5466 to 0.7977	>0.9999	ns

Supplemental Table 8: 2-way ANOVA test of Ku80 signal.

ns: non significant

LN-229					
Nb Foci	Not-Treated	Etoposide	PARPi Veliparib	PARPi Olaparib	PARGi
min	0	0	0	0	0
max	56	99	110	124	32
median	0	1	1	4	0
mean	2	13	13	14	2

U-87MG					
Nb Foci	Not-Treated	Etoposide	PARPi Veliparib	PARPi Olaparib	PARGi
min	0	0	0	0	0
max	34	102	76	125	70
median	0	0	0	1	0
mean	2	14	3	16	6

U-118MG					
Nb Foci	Not-Treated	Etoposide	PARPi Veliparib	PARPi Olaparib	PARGi
min	0	0	0	0	0
max	30	56	53	68	41
median	0	0	0	0	0
mean	1	8	2	4	3

Supplemental Table 9: Analysis of RAD51 foci.

Tukey's multiple comparisons test	Mean Diff.	95.00% CI of diff.	Adjusted P Value	Summary
	1.776E-			
LN-229:Not Treated vs. U-87MG:Not Treated	15	-3.077 to 3.077	>0.9999	ns
LN-229:Not Treated vs. U-118MG:Not Treated	1	-2.104 to 4.104	0.999	ns
LN-229:Etoposide vs. U-87MG:Etoposide	-1	-4.241 to 2.241	0.9994	ns
LN-229:Etoposide vs. U-118MG:Etoposide	5	1.822 to 8.178	<0.0001	****
LN-229:PARPi veliparib vs. U-87MG:PARPi veliparib	10	6.430 to 13.57	<0.0001	****
LN-229:PARPi veliparib vs. U-118MG:PARPi veliparib	11	7.466 to 14.53	<0.0001	****
LN-229:PARPi olaparib vs. U-87MG:PARPi olaparib	-2	-5.249 to 1.249	0.7431	ns
LN-229:PARPi olaparib vs. U-118MG:PARPi olaparib	10	6.830 to 13.17	<0.0001	****
LN-229:PARGi vs. U-87MG:PARGi	-4	-7.269 to -0.7308	0.0031	**
LN-229:PARGi vs. U-118MG:PARGi	-1	-4.267 to 2.267	0.9994	ns
LN-229:Not Treated vs. LN-229:Etoposide	-11	-13.86 to -8.144	<0.0001	****
LN-229:Not Treated vs. LN-229:PARPi veliparib	-11	-14.05 to -7.948	<0.0001	****
LN-229:Not Treated vs. LN-229:PARPi olaparib	-12	-14.89 to -9.113	<0.0001	****
LN-229:Not Treated vs. LN-229:PARGi	0	-2.859 to 2.859	>0.9999	ns
LN-229:Etoposide vs. LN-229:PARPi veliparib	0	-3.165 to 3.165	>0.9999	ns
LN-229:Etoposide vs. LN-229:PARPi olaparib	-1	-4.006 to 2.006	0.9986	ns
LN-229:Etoposide vs. LN-229:PARGi	11	8.021 to 13.98	<0.0001	****
LN-229:PARPi veliparib vs. LN-229:PARPi olaparib	-1	-4.193 to 2.193	0.9993	ns
LN-229:PARPi veliparib vs. LN-229:PARGi	11	7.832 to 14.17	<0.0001	****
LN-229:PARPi olaparib vs. LN-229:PARGi	12	8.991 to 15.01	<0.0001	****
U-87MG:Not Treated vs. U-118MG:Not Treated	1	-2.413 to 4.413	0.9997	ns
U-87MG:Etoposide vs. U-118MG:Etoposide	6	2.572 to 9.428	<0.0001	****
U-87MG:PARPi veliparib vs. U-118MG:PARPi veliparib	1	-2.748 to 4.748	0.9999	ns
U-87MG:PARPi olaparib vs. U-118MG:PARPi olaparib	12	8.624 to 15.38	<0.0001	****
U-87MG:PARGi vs. U-118MG:PARGi	3	-0.5308 to 6.531	0.2045	ns
U-87MG:Not Treated vs. U-87MG:Etoposide	-12	-15.44 to -8.562	<0.0001	****
U-87MG:Not Treated vs. U-87MG:PARPi veliparib	-1	-4.591 to 2.591	0.9998	ns
U-87MG:Not Treated vs. U-87MG:PARPi olaparib	-14	-17.42 to -10.58	<0.0001	****
U-87MG:Not Treated vs. U-87MG:PARGi	-4	-7.462 to -0.5380	0.0078	**
U-87MG:Etoposide vs. U-87MG:PARPi veliparib	11	7.363 to 14.64	<0.0001	****
U-87MG:Etoposide vs. U-87MG:PARPi olaparib	-2	-5.468 to 1.468	0.8238	ns
U-87MG:Etoposide vs. U-87MG:PARGi	8	4.490 to 11.51	<0.0001	****
U-87MG:PARPi veliparib vs. U-87MG:PARPi olaparib	-13	-16.62 to -9.380	<0.0001	****
U-87MG:PARPi veliparib vs. U-87MG:PARGi	-3	-6.660 to 0.6598	0.2573	ns
U-87MG:PARPi olaparib vs. U-87MG:PARGi	10	6.508 to 13.49	<0.0001	****
U-118MG:Not Treated vs. U-118MG:Etoposide	-7	-10.40 to -3.597	<0.0001	****
U-118MG:Not Treated vs. U-118MG:PARPi veliparib	-1	-4.578 to 2.578	0.9998	ns
U-118MG:Not Treated vs. U-118MG:PARPi olaparib	-3	-6.369 to 0.3690	0.1455	ns
U-118MG:Not Treated vs. U-118MG:PARGi	-2	-5.483 to 1.483	0.8284	ns
U-118MG:Etoposide vs. U-118MG:PARPi veliparib	6	2.455 to 9.545	<0.0001	****
U-118MG:Etoposide vs. U-118MG:PARPi olaparib	4	0.6657 to 7.334	0.0043	**
U-118MG:Etoposide vs. U-118MG:PARGi	5	1.551 to 8.449	<0.0001	****
U-118MG:PARPi veliparib vs. U-118MG:PARPi olaparib	-2	-5.513 to 1.513	0.8374	ns
U-118MG:PARPi veliparib vs. U-118MG:PARGi	-1	-4.622 to 2.622	0.9998	ns
U-118MG:PARPi olaparib vs. U-118MG:PARGi	1	-2.416 to 4.416	0.9997	ns

Supplemental Table 10: 2-way ANOVA test of RAD51 foci.

ns: non significant, *: ≥ 0.0332 , **: ≥ 0.0021 , ***: ≥ 0.0002 ****: < 0.0001

Tukey's multiple comparisons test	Mean		Adjusted P	
	Diff.	95.00% CI of diff.	Value	Summary
LN-229 - no foci:Not Treated vs. U-87MG - no foci:Not Treated	4.617	-23.73 to 32.96	>0.9999	ns
LN-229 - no foci:Not Treated vs. U-118MG - no foci:Not Treated	5.97	-22.38 to 34.32	>0.9999	ns
LN-229 - no foci:Hydroxyurea vs. U-87MG - no foci:Hydroxyurea	14.3	-14.04 to 42.65	0.9707	ns
LN-229 - no foci:Hydroxyurea vs. U-118MG - no foci:Hydroxyurea	25.27	-3.072 to 53.62	0.1491	ns
LN-229 - no foci:PARPi veliparib vs. U-87MG - no foci:PARPi veliparib	0.22	-28.13 to 28.57	>0.9999	ns
LN-229 - no foci:PARPi veliparib vs. U-118MG - no foci:PARPi veliparib	-4.19	-32.54 to 24.16	>0.9999	ns
LN-229 - no foci:PARPi olaparib vs. U-87MG - no foci:PARPi olaparib	0.3833	-27.96 to 28.73	>0.9999	ns
LN-229 - no foci:PARPi olaparib vs. U-118MG - no foci:PARPi olaparib	-1.223	-29.57 to 27.12	>0.9999	ns
LN-229 - no foci:PARGi vs. U-87MG - no foci:PARGi	10.07	-18.27 to 38.42	0.9998	ns
LN-229 - no foci:PARGi vs. U-118MG - no foci:PARGi	19.22	-9.122 to 47.57	0.6501	ns
LN-229 - no foci:Not Treated vs. LN-229 - no foci:Hydroxyurea	27.2	-1.142 to 55.55	0.0767	ns
LN-229 - no foci:Not Treated vs. LN-229 - no foci:PARPi veliparib	10.82	-17.52 to 39.17	0.9994	ns
LN-229 - no foci:Not Treated vs. LN-229 - no foci:PARPi olaparib	28.11	-0.2323 to 56.46	0.0546	ns
LN-229 - no foci:Not Treated vs. LN-229 - no foci:PARGi	4.94	-23.41 to 33.29	>0.9999	ns
LN-229 - no foci:Hydroxyurea vs. LN-229 - no foci:PARPi veliparib	-16.38	-44.73 to 11.97	0.8863	ns
LN-229 - no foci:Hydroxyurea vs. LN-229 - no foci:PARPi olaparib	0.91	-27.44 to 29.26	>0.9999	ns
LN-229 - no foci:Hydroxyurea vs. LN-229 - no foci:PARGi	-22.26	-50.61 to 6.082	0.3532	ns
LN-229 - no foci:PARPi veliparib vs. LN-229 - no foci:PARPi olaparib	17.29	-11.06 to 45.64	0.824	ns
LN-229 - no foci:PARPi veliparib vs. LN-229 - no foci:PARGi	-5.883	-34.23 to 22.46	>0.9999	ns
LN-229 - no foci:PARPi olaparib vs. LN-229 - no foci:PARGi	-23.17	-51.52 to 5.172	0.2789	ns
U-87MG - no foci:Not Treated vs. U-118MG - no foci:Not Treated	1.353	-26.99 to 29.70	>0.9999	ns
U-87MG - no foci:Hydroxyurea vs. U-118MG - no foci:Hydroxyurea	10.97	-17.38 to 39.32	0.9993	ns
U-87MG - no foci:PARPi veliparib vs. U-118MG - no foci:PARPi veliparib	-4.41	-32.76 to 23.94	>0.9999	ns
U-87MG - no foci:PARPi olaparib vs. U-118MG - no foci:PARPi olaparib	-1.607	-29.95 to 26.74	>0.9999	ns
U-87MG - no foci:PARGi vs. U-118MG - no foci:PARGi	9.15	-19.20 to 37.50	>0.9999	ns
U-87MG - no foci:Not Treated vs. U-87MG - no foci:Hydroxyurea	36.89	8.544 to 65.24	0.0011	**
U-87MG - no foci:Not Treated vs. U-87MG - no foci:PARPi veliparib	6.427	-21.92 to 34.77	>0.9999	ns
U-87MG - no foci:Not Treated vs. U-87MG - no foci:PARPi olaparib	23.88	-4.466 to 52.23	0.2287	ns
U-87MG - no foci:Not Treated vs. U-87MG - no foci:PARGi	10.4	-17.95 to 38.74	0.9997	ns
U-87MG - no foci:Hydroxyurea vs. U-87MG - no foci:PARPi veliparib	-30.46	-58.81 to -2.118	0.0214	*
U-87MG - no foci:Hydroxyurea vs. U-87MG - no foci:PARPi olaparib	-13.01	-41.36 to 15.34	0.9909	ns
U-87MG - no foci:Hydroxyurea vs. U-87MG - no foci:PARGi	-26.49	-54.84 to 1.852	0.0988	ns
U-87MG - no foci:PARPi veliparib vs. U-87MG - no foci:PARPi olaparib	17.45	-10.89 to 45.80	0.8113	ns
U-87MG - no foci:PARPi veliparib vs. U-87MG - no foci:PARGi	3.97	-24.38 to 32.32	>0.9999	ns
U-87MG - no foci:PARPi olaparib vs. U-87MG - no foci:PARGi	-13.48	-41.83 to 14.86	0.9856	ns
U-118MG - no foci:Not Treated vs. U-118MG - no foci:Hydroxyurea	46.51	18.16 to 74.85	<0.0001	****
U-118MG - no foci:Not Treated vs. U-118MG - no foci:PARPi veliparib	0.6633	-27.68 to 29.01	>0.9999	ns
U-118MG - no foci:Not Treated vs. U-118MG - no foci:PARPi olaparib	20.92	-7.426 to 49.27	0.4789	ns
U-118MG - no foci:Not Treated vs. U-118MG - no foci:PARGi	18.19	-10.15 to 46.54	0.7484	ns
U-118MG - no foci:Hydroxyurea vs. U-118MG - no foci:PARPi veliparib	-45.84	-74.19 to -17.50	<0.0001	****
U-118MG - no foci:Hydroxyurea vs. U-118MG - no foci:PARPi olaparib	-25.59	-53.93 to 2.759	0.1345	ns
U-118MG - no foci:Hydroxyurea vs. U-118MG - no foci:PARGi	-28.31	-56.66 to 0.03227	0.0506	ns
U-118MG - no foci:PARPi veliparib vs. U-118MG - no foci:PARPi olaparib	20.26	-8.089 to 48.60	0.5456	ns
U-118MG - no foci:PARPi veliparib vs. U-118MG - no foci:PARGi	17.53	-10.82 to 45.88	0.8052	ns
U-118MG - no foci:PARPi olaparib vs. U-118MG - no foci:PARGi	-2.727	-31.07 to 25.62	>0.9999	ns

Supplemental Table 11: 2-way ANOVA test of FANCD2 foci.

ns: non significant, *: ≥ 0.0332 , **: ≥ 0.0021 , ***: ≥ 0.0002 ****: < 0.0001